The Hong Kong Polytechnic University
Department of Civil and Structural Engineering

# STUDY OF PHOTOCHEMICAL OZONE POLLUTION IN HONG KONG

A thesis submitted in partial fulfilment of
the requirements for the Degree of Doctor of Philosophy

by

So King Lung

June 2006

# CERTIFICATE OF ORGINALITY

I hereby declare that this thesis is my own work and that, to the best of my knowledge and belief, it reproduces no material previously published or written, nor material that has been accepted for the award of any other degree or diploma, except where due acknowledgement has been made in the text.

____________________________ (Signed)

So King Lung (Name of student)

# ABSTRACT

The Pearl River Delta (PRD) of China has experienced serious air pollution along with the astonishing economic and industrial developments in the past two decades. Large emissions of pollutants like respirable suspended particulates, sulphur dioxides ($SO_2$), nitrogen oxides ($NO_x$) and volatile organic compounds (VOC), coupled with the subtropical climate, have resulted in photochemical ozone ($O_3$) pollution and visibility degradation in the region, including Hong Kong (HK) which is situated in the southern part of the PRD.

Photochemical theory and overseas experience show that control of $O_3$ pollution is a very challenging undertaking because of the non-linear dependency of $O_3$ on its precursors, VOC and $NO_x$. Such $O_3$-$O_3$ precursors' relationship is often site specific and the $O_3$ migration strategy is effective only should there be an in-depth understanding of the sources, patterns, and formation of photochemical $O_3$ and its precursors, as well as their relationship in the region. However, as the information on the above aspects is very limited in the PRD (including HK), efforts to formulate an effective $O_3$ control strategy has been hindered.

This research is therefore aimed at filling our knowledge gap and improving our understanding of the spatio-temporal distribution of $O_3$ and $O_3$ precursors in HK, the roles of $O_3$ precursors in $O_3$ production, and the fast $O_3$ chemistry in the subtropical region. Measurement data from Environmental Protection Department (EPD) of HK and by researchers of the Hong Kong

Polytechnic University were analyzed using various statistical and modelling tools. The results are summarized in the following sections.

$O_3$ and regularly monitored gaseous air-quality data collected from June 1999 to May 2000 at three EPD's sites (rural, urban and suburban) were analyzed in order to obtain the information on the seasonal and spatial distribution of $O_3$ and the relationship with other gas pollutants. The highest average $O_3$ level was found at a rural site (Tap Mun) in northeastern HK which had increased levels of carbon monoxide (CO) and $SO_2$ (relative to $NO_x$) indicating frequent influences of regional air masses from the inland region. The lowest concentration of $O_3$ was found at the urban site (Tsuen Wan). The southwestern suburban site (Tung Chung) showed intermediate $O_3$ levels on average, and analysis of $CO/NO_x$ and $SO_2/NO_x$ ratios suggests this site was impacted by both local and regional pollution. Principal component analysis further elucidated that the $O_3$ variation in the northeastern rural area was largely determined by regional chemical and transport processes, while the $O_3$ variability in the southwestern suburban and urban sites were more influenced by local emissions. High $O_3$ episodes were also found to correlate with an enhanced ratio of $SO_2$ to $NO_x$, further suggesting the influence of regional emissions from the PRD. The results indicated that it is imperative to consider regional scale emissions and dynamic transport in managing $O_3$ pollution in HK.

VOC data collected by the EPD at the rural, urban and roadside sites from November 2000 to October 2001 and September 2002 to August 2003 were examined for their spatial distribution, seasonal variation, source-receptor relationships and photochemical reactivity. As expected, the roadside site showed the highest VOC level owing to the vehicular emissions and the rural site was characterized by the aged air mass with the lowest VOC level. Ratios of VOC with different photochemical reactivities indicated the mix of emission sources and increased atmospheric processing from urban to rural areas. Ratios of VOC to $NO_x$ were about 2-3 in the urban areas and 10 at the rural site, suggesting that the formation of $O_3$ in HK is generally sensitive to VOC. Among the VOC, toluene was the most abundant species on a carbon basis and also a leading contributor to $O_3$ production, especially in the urban areas. Isoprene, despite having a low mass concentration compared to other VOC, had a high reactivity value and was a key precursor contributing to $O_3$ formation especially in the rural area.

To further quantify the roles of $O_3$ precursors in the $O_3$ formation, an observation-based model (OBM) and measurement indicators method were employed using the data collected in autumn 2002 and summer 2004 at two suburban/rural sites in HK (Tai O) and the PRD (Wan Qing Sha), respectively. Photochemical $O_3$ production was calculated to be limited by VOC at both sites. Nitric oxide (NO) tended to suppress the $O_3$ formation, and CO was found to be negligible in the $O_3$ formation. Among different VOC, reactive aromatic compounds such as toluene and xylenes dominated the $O_3$ production in most cases, but naturally emitted isoprene could be important on warm days. This result is consistent with that from previous analysis of urban datasets. Model results revealed that $O_3$ formation at Tai O was most sensitive to stationary hydrocarbons but a stronger influence of mobile hydrocarbons was found at Wan Qing Sha. The results were in line with the corresponding emission patterns in HK and the PRD.

The OBM, which is a time-dependent photochemical model using the Carbon Bond (IV) mechanism, was used to infer the $O_3$ chemistry and elucidate the processes (*in-situ* production versus transport) that control the variation of $O_3$ at the sites. About half of the $O_3$ episodes at Tai O were indicative of an impact from long-range transport but the $O_3$ episodes at Wan Qing Sha were mainly attributable to local production. Photochemistry of two $O_3$ episodes was further investigated in detail. It shows that *in-situ* $O_3$ production accounted for most of the observed increase in $O_3$ concentrations at the PRD site (1-hour $O_3$ = 178 ppbv) indicating the importance of local sources, while for the case of HK (1-hour $O_3$ = 203 ppbv), local production accounted for only 50% suggesting the importance of transport of regional pollution in this case. In both cases, conversion of NO to $NO_2$ by $HO_2$ was the major reaction for photochemical $O_3$ production. The photochemical $O_3$ loss rate was dominated by the reaction between $NO_2$ and OH at Tai O while the reaction of $O_3$ and $HO_2$ was the major $O_3$ destruction pathway at Wan Qing Sha. The $O_3$ production efficiency and partition of reactive nitrogen compounds were also estimated with the calculated concentrations of $NO_2$, PAN, $HNO_3$ and measured values of NO and $NO_y$ during the two $O_3$ episodes. The results showed that three to four $O_3$ molecules were formed per $NO_x$

molecule oxidized while PAN and $HNO_3$ were the most significant reactive nitrogen compounds in the afternoon.

# TABLE OF CONTENTS

Page No.

List of Tables……………………………………………………………... viii

List of Figures…………………………………………………………….. xii

List of Equations………………………………………………………….. xix

Acknowledgments………………………………………………………… xxi

CHAPTER 1 INTRODUCTION………………………………… 1

1.1 Background of Ozone…………….……….... 3

1.2 Meteorological Influences on Ozone Formation……………………………….. 12

*1.2.1 Sunlight Intensity and Temperature…* 12

*1.2.2 Wind Speed and Wind Direction….…..* 13

*1.2.3 Atmospheric Mixing and Transport…* 14

1.3 Analysis of Ozone Episodes……………….. 15

1.4 Overseas Ozone Studies and their Comparison………………………………... 15

*1.4.1 Overseas Ozone Studies…….……..…* 16

(a) Western Countries…………... 16

(b) Eastern Countries…………… 18

(c) African Countries…………… 20

*1.4.2 Comparison of Ozone Levels around the World………………………………* 20
1.5 Ozone Studies in Hong Kong...................... 26
1.6 Overseas Studies on Volatile Organic Compounds and their Comparison………… 29
1.7 Volatile Organic Compounds Studies in Hong Kong………………………………… 33
1.8 Background of Reactive Nitrogen Compounds………………………………… 33
1.9 Objectives of this Thesis…………………... 36

CHAPTER 2 METHODOLOGY……………………………….. 38
2.1 Analyses of Spatial and Temporal Variation 38
2.2 Chemical Ratios Analysis…………………. 39
(a) Ratios of $SO_2/NO_x$ and $CO/NO_x$ for Different Emission Patterns………... 39
(b) $O_3+NO_2$ for Total Ozone Potential…. 40
(c) Ratio of $VOC/NO_x$ and $O_3/NO_y$ for $O_3$-$NO_x$-VOC chemistry……………. 40
(d) Ratios of Hydrocarbons for Ages of Air Mass……………………………. 41
2.3 Principal Component Analysis…………….. 42

2.4 Photochemical Reactivity of VOC on Ozone Formation………………………………….. 43
(a) OH Reactivity (Propene-Equivalent Concentration)……………………… 44
(b) Ozone-forming Potential (Maximum Incremental Reactivity)…………….. 45
2.5 Observation-based Model………………….. 46
(a) Emission- versus Observation-based Models……………………………… 46
(b) Background of the OBM…………… 47
(c) Relative Incremental Reactivity (RIR)………………………………... 50
(d) Sensitivity to ΔS……………………. 51
(e) Treatment of Entrainment, Mixing 53 Height and Deposition in the OBM....
(f) Applications of the OBM…………... 54

CHAPTER 3 DATA USED IN THIS THESIS AND EXPERIMENTAL DETAILS FOR DATA………. 56
3.1 Summary of Data Sets used in this Thesis… 56
3.2 Environment of Hong Kong and Pearl River Delta Region………………………… 56
3.3 Site Characteristics………………………… 59

*3.3.1 EPD's Stations…………………………* 59

*3.3.2 HKPU's Stations………………………* 62

3.4 Measurement Techniques………………….. 64

*3.4.1 Trace Gases……………………………* 64

*3.4.2 Volatile Organic Compounds………..* 67

*3.4.3 Meteorological Data…………………* 68

CHAPTER 4 GROUND-LEVEL OZONE STUDY IN HONG KONG DURING 1999/2000……………………… 69

4.1 Spatial Distribution of Ozone and Other Pollutants………………………………….. 70

4.2 Temporal Variation of Ozone……………… 71

4.3 Chemical Ratio Analysis…………………... 75

4.4 Principal Component Analysis…………….. 76

4.5 Analysis of Ozone Episodes……………….. 79

4.6 Chapter Summary………………………….. 86

CHAPTER 5 STUDY OF $C_3$ TO $C_{12}$ HYDROCARBONS IN HONG KONG DURING 2000/2001……………... 88

5.1 Spatial Distribution, Seasonal Variation and Inter-city Comparison of Non-methane Hydrocarbons……………………………… 89

5.2 Sources of Isoprene at Different Sites in

Hong Kong………………………………… 92

5.3 Photochemical Age and Evaluation of Emission Ratios……………………………. 103

5.4 Ratios of Total NMHC to $NO_x$ in Hong Kong……………………………………….. 107

5.5 Photochemical Reactivity and Ozone Formation…………………………………... 108

5.6 Chapter Summary………………………….. 114

CHAPTER 6 STUDY OF $C_1$ TO $C_8$ HYDROCARBONS IN HONG KONG DURING 2002/2003……………... 116

6.1 Overall Description: Spatial and Seasonal Patterns…………………………………….. 118

6.2 Atmospheric Processing of Air Masses Impacting Hong Kong……………………... 125

*6.2.1 VOC Ratios………………………………..* 125

*6.2.2 Hydrocarbons versus CO……………..* 127

*6.2.3 Relations to Ethyne / CO and Propane / Ethane……………………….* 130

6.3 Chapter Summary………………………….. 133

CHAPTER 7 ROLES OF HYDROCARBONS IN CONTROLLING OZONE FORMATION IN THE

PRD………………………………………………….. 134

7.1 Overview of Measurement Data and Techniques…………………………………. 135

7.2. Measurement Indicators for $O_3$-$NO_x$-VOC Sensitivity………………………………….. 139

7.3 Assessment of $O_3$-$NO_x$-VOC Chemistry from OBM Results…………………………. 142

7.4 The Relative Importance of VOC Species on Ozone Formation……………………….. 144

7.5 Diurnal Variation of Hydrocarbons……….. 151

7.6 Significance of Aromatic Hydrocarbons on Ozone Formation…………………………... 155

7.7 Sensitivity to ΔS in RIR Calculation………. 157

7.8 Chapter Summary………………………….. 159

CHAPTER 8 CHEMISTRY OF PHOTOCHEMICAL OZONE PRODUCTION OVER THE PRD………………... 161

8.1 *In-situ* Photochemical Production versus Long-range Transport contributing to High Ozone Levels over the PRD………… 162

8.2 Comparison of Ozone Production at Tai O and Wan Qing Sha…………………………. 166

*8.2.1 Time Series of Hourly Data…………..* 167

*8.2.2 Ozone Budget…………………………..* 172

*8.2.3 Diurnal Variations of OH Radicals…* 176

*8.2.4 Ozone Production Efficiency……….* 179

*8.2.5 Partition of Reactive Nitrogen Compounds…………………………….* 183

*8.2.6 Comparison of Observed and Calculated Ozone Changes…………..* 185

8.3 Chapter Summary………………………….. 188

CHAPTER 9 CONCLUSIONS AND RECOMMENDATIONS... 190

9.1 Summary of Major Findings……………….. 190

9.2 Significance of this Thesis…………………. 193

9.3 Suggestions for Further Work……………... 194

REFERENCES …………………………………………………….. 197

# LIST OF TABLES

Page No.

*Table 1.1* *Range of annual (January–December) hourly ozone concentrations (ppbv) at background sites around the world (CMDL, 2004)……………………………….* 23

*Table 1.2* *Range of annual (January–December) hourly median and maximum ozone concentrations (ppbv) at background stations in protected areas of the United States (CASTNet, 2004)……………………….* 24

*Table 1.3* *Range of annual (January–December) hourly median and maximum ozone concentrations (ppbv) at Canadian background stations (CAPMoN, 2003).* 25

*Table 1.4* *Comparison of selected hydrocarbons measured in Hong Kong (average of three urban sites) and in other cities (units are in ppbv unless otherwise specified).……………………………………………….* 31

*Table 2.1* *Carbon Number of Carbon-Bond Groups for Primary Species under CBM-IV.……………………….* 49

*Table 3.1* *Summary of data sets used in this thesis.…………….* 58

*Table 3.2* *Site information of six EPD's air quality monitoring stations.……………………………………………………* 61

*Table 4.1* *Annual averages of major air pollutants and respective chemical ratios at TM, TC and TW from June 1999 to May 2000……………………………….* 71

*Table 4.2* *Factor loadings of concentrations of the different air pollutants at TM, TC and TW (Varimax rotated factor pattern and strong factor loadings are in bold)……………………………………………………* 78

*Table 4.3* *Summary of* $O_3$ *episodes (hourly* $O_3$ *concentration > 122 ppbv) at TM, TC and TW from June 1999 to May 2000……………………………………………….* 81

*Table 4.4* *Averaged* $O_3$ *levels and* $SO_2/NO_x$ *during the 4 days of* $O_3$ *episode (LST 1300 to 1700)……………………* 83

*Table 5.1* *Comparison of selected NMHC measured in Hong Kong (roadside area) and other cities………………* 94

*Table 5.2* *Results of principal component analysis of 20 NMHC at the four sites (Only PCs with eigenvalue larger than 1 and loading larger than 0.4 are shown)……………………………………………………* 99

*Table 5.3* *Summary of the average ratios of total NMHC to* $NO_x$ *(*$NO_y$ *for HT) with standard deviations at the four sites…………………………………………………* 109

*Table 5.4* *Top 10 NMHC ranked according to mass concentration, PE and $O_3$ formation in MIR calculated from the annual averages of NMHC at the four sites…………………………………………..* 110

*Table 6.1* *Statistics (average and standard deviation (S.D.)) of trace gases and selected NMHC measured from September 2002 to August 2003 at the four sites (There were 62 canisters samples at each site and units are in pptv unless otherwise specified)……….* 119

*Table 6.2* *Comparison of the annual averages (from September 2002 to August 2003) of selected hydrocarbons in Central/Western analyzed by the GL and UCI……………………………………………..* 123

*Table 7.1* *Statistics of trace gases at Tai O (01 September to 30 November 2002) and Wan Qing Sha (19 April to 28 June 2004)…………………………………………* 137

*Table 7.2* *Mean and median of afternoon (LST 1500 to 1600) $NO_y$ and $O_3/NO_y$ at Tai O (01 September to 30 November 2002) and Wan Qing Sha (19 April to 28 June 2004)……………………………………………….* 140

*Table 7.3* *OBM-calculated relative incremental reactivities (RIRs) in %/% for CO, NO and THC and daily maximum 1-hour $O_3$ for 13 days at Tai O and Wan Qing Sha*……………………………………………. 143

*Table 7.4* *The apportionment among source categories (mobile, stationary and natural) for 46 $C_2$-$C_{10}$ hydrocarbons*……………………………………………. 147

*Table 7.5* *Emission inventory of VOC by sector for the year 2000*…………………………………………………. 150

*Table 8.1* *OBM-calculated OH peak values and the corresponding comparison between observed and calculated $O_3$ production for 13 days at Tai O and Wan Qing Sha*…………………………………………… 177

# LIST OF FIGURES

Page No.

*Figure 1.1* *Long term trend of $SO_2$, $NO_2$, $O_3$ and RSP measured at Central/Western from 1990 to 2004………………* 2

*Figure 1.2* *Ozone is generated in the lower atmosphere from the photochemical smog mechanism involving the oxidation of VOC with $NO_x$ acting as a catalyst in the presence of sunlight. Eventually the process is terminated when $NO_x$ oxidized to $NO_z$ and removed by deposition to soils, vegetation and surface waters of the VOC is exhausted………………………* 5

*Figure 1.3* *Ozone isopleth plot based on simulations of chemistry along air trajectories in Atlanta (Jeffries and Crouse, 1990). Each isopleth is 10 ppbv higher in $O_3$ as one moves upward and to the right………..* 9

*Figure 1.4* *Inter-city comparison of 1-hour maximum $O_3$ concentrations…………………………………………..* 22

*Figure 1.5* *EPD's Air Quality Monitoring Network of Hong Kong……………………………………………………….* 27

*Figure 1.6* *Schematic of $NO_y$ chemistry…………………………..* 35

*Figure 2.1* *Area-averaged RIR calculated from the multiple day analysis dataset in Atlanta for nitric oxide (NO), anthropogenic hydrocarbons (AHC), natural hydrocarbons (NHC), and carbon monoxide (CO) as functions of the percent change in precursor source………………………………………………….* 52

*Figure 3.1* *Location of six EPD's air quality monitoring stations, two HKPU's air quality monitoring stations and HKO's meteorological station……….* 57

*Figure 3.2* *Map of the PRD showing Tai O, Hok Tsui and Wan Qing Sha……………………………………………….* 62

*Figure 4.1* *Monthly averaged concentration of (a)* $O_3$*, (b) TOP (*$O_3$ + $NO_2$*) and (c) annual averaged diurnal* $O_3$ *variation measured at TM, TC and TW for June 1999 to May 2000……………………………………….* 74

*Figure 4.2* *Daily maximum 1-hour* $O_3$ *at (a) TM, (b) TC and (c) TW from June 1999 to May 2000……………………….* 80

*Figure 4.3* *Synoptic weather maps for 19 and 20 August 1999…* 84

*Figure 4.4* *Multiple pollutants variation at (a) TM, (b) TC and (c) TW on 19 and 20 August 1999……………………..* 85

*Figure 5.1* *Seasonal variations of alkanes, alkenes, aromatic hydrocarbons and their summations (total NMHC) at the four sites in HK: HT (rural); C/W (residential); TW (industrial) and MK (roadside). Winter: November 2000-February 2001; spring: March 2001-April 2001; summer: May 2001-August 2001; autumn: September 2001-October 2001……………………………………………………* 90

*Figure 5.2* *Daily variations of isoprene at the four sites: TW (industrial); C/W (residential); HT (rural); and MK (roadside)……………………….……………………….* 96

*Figure 5.3* *Scatter plots of monthly data from November 2000 to October 2001 for (a) m,p-xylene versus ethylbenzene and (b) butane versus propane at the four sites: HT (rural); C/W (residential); TW (industrial) and MK (roadside)……………………….* 105

*Figure 6.1* *Monthly averages of (a) toluene and (b) isoprene from September 2002 to August 2003 at the four sites in HK………………………………………………..* 124

*Figure 6.2* *Box plots of (a) propane / ethane and (b) ethene / ethane ratios from September 2002 to August 2003 at the four sites in HK. Whiskers indicate the minimum and maximum values and box indicates 25th – 75th percentile range with line for median….* 126

*Figure 6.3* *Scatter plots of CO with ethyne from September 2002 to August 2003 at the four sites in HK………..* 128

*Figure 6.4* *Scatter plots of CO with isoprene from September 2002 to August 2003 at the four sites in HK………..* 129

*Figure 6.5* *Scatter plots of* $O_3$*,* *CO,* $SO_2$ *and* $NO_2$ *with ethyne / CO at the rural TM………………………………………* 131

*Figure 6.6* *Scatter plots of* $O_3$*,* *CO,* $SO_2$ *and* $NO_2$ *with propane / ethane at the rural TM…………………………………* 132

*Figure 7.1* *Plots of* $O_3$ *versus* $NO_y$ *and* $O_3/NO_y$ *versus* $O_3$ *for afternoon data (LST 1500 to 1600) at Tai O (01 September to 30 November 2002) and at Wan Qing Sha (19 April to 28 June 2004).* $NO_x$*-sensitive regimes are represented by elliptic circles which are created in accordance with the 3-D simulations given by Sillman and He (2002)…………………….* 141

*Figure 7.2* *OBM-calculated daytime average RIRs for CO, NO, THC, SHC, MHC and NHC for (a) Tai O on 5 September 2002; (b) Tai O on 7 November 2002; (c) Wan Qing Sha on 17 May 2004; and (d) Wan Qing Sha on 24 May 2004……………………………* 146

*Figure 7.3* *Diurnal profiles of $O_3$ and THC (SHC, MHC and NHC) in terms of concentrations and PE for Tai O on (a)5 September 2002; (b) 7 November 2002;for Wan Qing Sha on (c)17 May 2004 and (d) 24 May 2004. ……………………………………………………....* 153

*Figure 7.4* *Comparison of average composition for NHC and sub-groups of AHC in (a) mass concentration at Tai O; (b) mass concentration at Wan Qing Sha; (c) PE at Tai O; and (d) PE at Wan Qing Sha.………………* 156

*Figure 7.5* *Variation of daytime average RIR as functions of the percent change in precursor group for AHC, NHC, CO and NO for (a) Tai O on September 2002; (b) Tai O on 7 November 2002; (c) Wan Qing Sha on 17 May 2004; and (d) Wan Qing Sha on 24 May 2004………………………………………………………* 158

*Figure 8.1* *Comparison of net $O_3$ photochemical production calculated by the OBM and the observed $O_3$ increment at Tai O on eight days……………………..* 164

*Figure 8.2* *Comparison of net $O_3$ photochemical production calculated by the OBM and the observed $O_3$ increment at Wan Qing Sha on five days…………….* 165

*Figure 8.3* *Diurnal measurement of $O_3$ (at Tai O, Tung Chung and Tap Mun), CO, $SO_2$, $NO_y$, their ratios ($NO/NO_y$ and $\Delta CO/\Delta NO_y$), PE of VOC and wind at Tai O on 7 November 2002………………………………………..* 169

*Figure 8.4* *Back trajectory for air mass arriving at Tai O on 7 November 2002…………………………………………* 170

*Figure 8.5* *Diurnal measurement of $O_3$, CO, $SO_2$, $NO_y$, their ratios ($NO/NO_y$ and $\Delta CO/\Delta NO_y$), PE of VOC and wind at Wan Qing Sha on 24 May 2004……………..* 171

*Figure 8.6* *Daytime average $O_3$ production (P) and destruction (D) rates at Tai O on 7 November 2002 and Wan Qing Sha on 24 May 2004 calculated by the OBM…* 175

*Figure 8.7* *Daytime diurnal cycle of hydroxyl (OH) radical concentration (molecules per* $cm^3$*) at Tai O on 7 November 2002 and Wan Qing Sha on 24 May 2004 calculated by the OBM…………………………..* 178

*Figure 8.8* *Ozone Production Efficiency at Tai O on 7 November 2002 estimated from the plot of measured* $O_3$ *versus calculated* $NO_z$ *for afternoon data (LST 1300 to 1700)……………………………….* 181

*Figure 8.9* *Ozone Production Efficiency at Wan Qing Sha on 24 May 2004 estimated from the plot of measured* $O_3$ *versus calculated* $NO_z$ *for afternoon data (LST 1300 to 1700)…………………………………………….* 182

*Figure 8.10* *Relative proportion of daytime average calculated* $NO_y$ *species (nitrogen oxides (*$NO_x$*), total inorganic nitrate (*$HNO_3$*+*$NO_3^-$*) and PAN) at Tai O on 7 November 2002 and Wan Qing Sha on 24 May 2004…………………………………………………………..* 184

*Figure 8.11* *Daytime diurnal cycles of observed and calculated* $O_3$ *production rates at Tai O on 7 November 2002..* 186

*Figure 8.12* *Daytime diurnal cycles of observed and calculated* $O_3$ *production rates at Wan Qing Sha on 24 May 2004…………………………………………………………..* 187

# LIST OF EQUATIONS

Page No.

*[Equation 1.1]* $NO_2 + h\nu \text{ (280-430nm)} \rightarrow NO + O$ 4

*[Equation 1.2]* $O + O_2 + M \rightarrow O_3 + M$ 4

*[Equation 1.3]* $NO + O_3 \rightarrow NO_2 + O_2$ 4

*[Equation 1.4]* $O_3 + h\nu \rightarrow O(^1D) + O_2$ 6

*[Equation 1.5]* $O(^1D) + H_2O \rightarrow 2OH$ 6

*[Equation 1.6]* $RH + OH \rightarrow R + H_2O$ 6

*[Equation 1.7]* $R + O_2 \rightarrow RO_2$ 6

*[Equation 1.8]* $RO_2 + NO \rightarrow NO_2 + RO$ 6

*[Equation 1.9]* $RO + O_2 \rightarrow R'CHO + HO_2$ 6

*[Equation 1.10]* $NO + HO_2 \rightarrow NO_2 + OH$ 6

*[Equation 1.11]* $RH + 2\ NO + O_2 \rightarrow R'CHO + 2\ NO_2 + H_2O$ 6

*[Equation 1.12]* $OH + NO_2 \rightarrow HNO_3$ 7

*[Equation 1.13]* $HO_2 + HO_2 \rightarrow H_2O_2 + O_2$ 7

*[Equation 1.14]* $RO_2 + HO_2 \rightarrow ROOH + O_2$ 7

*[Equation 1.15]* $RO_2 + NO \rightarrow RONO_2$ 7

*[Equation 1.16]* $CH_3C(O)O_2 + NO_2 \rightarrow CH_3C(O)O_2NO_2$ 7

*[Equation 2.1]* $\mathrm{PE(j) = Conc.(j)} \frac{k_{OH}(j)}{k_{OH}(C_3H_6)}$ 44

*[Equation 2.2]* $O_3$ formation (j) = Conc.(j) * MIR coefficient 45

*[Equation 2.3]* $\mathrm{IR}^{S}(X)=\frac{P^{S}_{O_3-NO}(X)-P^{S}_{O_3-NO}(X-\Delta X)}{\Delta S(X)}$ 50

*[Equation 2.4]* $\mathrm{RIR}^{S}(X)=\frac{\frac{P^{S}_{O_3-NO}(X)-P^{S}_{O_3-NO}(X-\Delta X)}{P^{S}_{O_3-NO}(X)}}{\frac{\Delta S(X)}{S(X)}}$ 51

*[Equation 2.5]* $(dc_i/dt)_{Deposition} = V_d * C_i / H(t) * 0.6$ 54

*[Equation 2.6]* $\frac{dO_3}{dt}=\frac{O_3(n+1)-O_3(n-1)}{2}$ 55

*[Equation 8.1]* $NO + CH_3O_2 \rightarrow NO_2 + CH_2O$ 172

*[Equation 8.2]* $O_3 + OH \rightarrow HO_2 + O_2$ 172

*[Equation 8.3]* $O_3 + HO_2 \rightarrow OH + 2O_2$ 172

# ACKNOWLEDGMENTS

I would like to sincerely thank Prof. T. Wang, my chief supervisor, for his guidance and support during my study. Through his supervision, I have learnt how to improve myself in the areas of data interpretation, logical thinking as well as scientific papers writing which are all very important to my career development. He also provided me with an invaluable opportunity to make a short-term attachment to the Georgia Institute of Technology (GIT) in May 2004, which could broaden my horizons in handling data analysis.

Sincere thanks are also directed to the following persons:

- Prof. S. C. Lee, my co-supervisor, for his guidance and advice to my study;
- Drs. H. Guo, A. J. Ding and T. F. Cheung of our research team, for their encouragement, support and helpful comments to my work;
- Joey Kwok, Steven Poon, Anson Wong, Benny Wu, W. S. Wu and other team members, for their support and effort in producing the data used in this study;
- Prof. W. L. Chameides and Dr. J. Zhang, for their hospitality during my short-term attachment at the GIT in May 2004; and
- Prof. D. R. Blake, Department of Chemistry, University of California-Irvine, for his analysis of our volatile organic compounds samples.

I am grateful to the Environmental Protection Department and Hong Kong Observatory of the Hong Kong Special Administrative Region (HKSAR) for providing their data to this study. I would also like to express my gratitude

to the Hong Kong Civic Exchange for its financial support of my attachment at the GIT.

It is my pleasure to acknowledge the Department Research Committee of the Hong Kong Polytechnic University for granting me the Hong Kong Polytechnic University Tuition Scholarship for Research Postgraduate Studies. Last but not least, I also acknowledge the financial support for my study from the Research Grants Council of the HKSAR (Project No. PolyU 0562/99E and PolyU 5059/00E).

# CHAPTER 1 INTRODUCTION

Hong Kong (HK) is currently facing the problem of deteriorating regional air quality which has been evidenced by the gradually declining visibility, and the frequent occurrence of respirable suspended particulates (RSP) as well as ozone ($O_3$) pollution episodes throughout HK. Compared to the street-level air quality problem which stems mainly from local vehicular emissions, our photochemical smog problem is more complicated and caused by both local and regional air pollution sources.

Photochemical smog is characterized by the formation of high concentrations of oxidants and aerosols in the atmosphere by chemical reactions involving nitrogen oxides ($NO_x$), carbon monoxides (CO) and reactive hydrocarbons in the presence of sunlight and warm temperature. $O_3$ is the most important photochemical oxidants and such secondary pollutant has an adverse impact on human health, agricultural crops and forests (NRC, 1991). In recent years, there is a trend of increasing ground-level $O_3$ concentration measured in HK. Figure 1.1 compares the long term trend of four different air pollutants which are based on their annual average concentrations recorded at a HK residential area (Central/Western) from 1990 to 2004. It is interesting to note that there is a steady rising trend of $O_3$ at this site during the period. By comparison, the annual averages of RSP, nitrogen dioxide ($NO_2$) and sulphur dioxide ($SO_2$) have remained quite steady over the past decade. Such findings reflect the increasing impact of $O_3$ pollution at this residential area. Elevated $O_3$ levels have also been observed at the upwind and downwind areas. The rising $O_3$ trend in HK indicates the $O_3$ pollution is increasingly serious. To address this problem effectively, we should first understand the causes and characteristics of our $O_3$ pollution which are the main objectives of this thesis.

*Figure 1.1 Long term trend of* $SO_2$*,* $NO_2$*,* $O_3$ *and RSP measured at Central/Western from 1990 to 2004.*

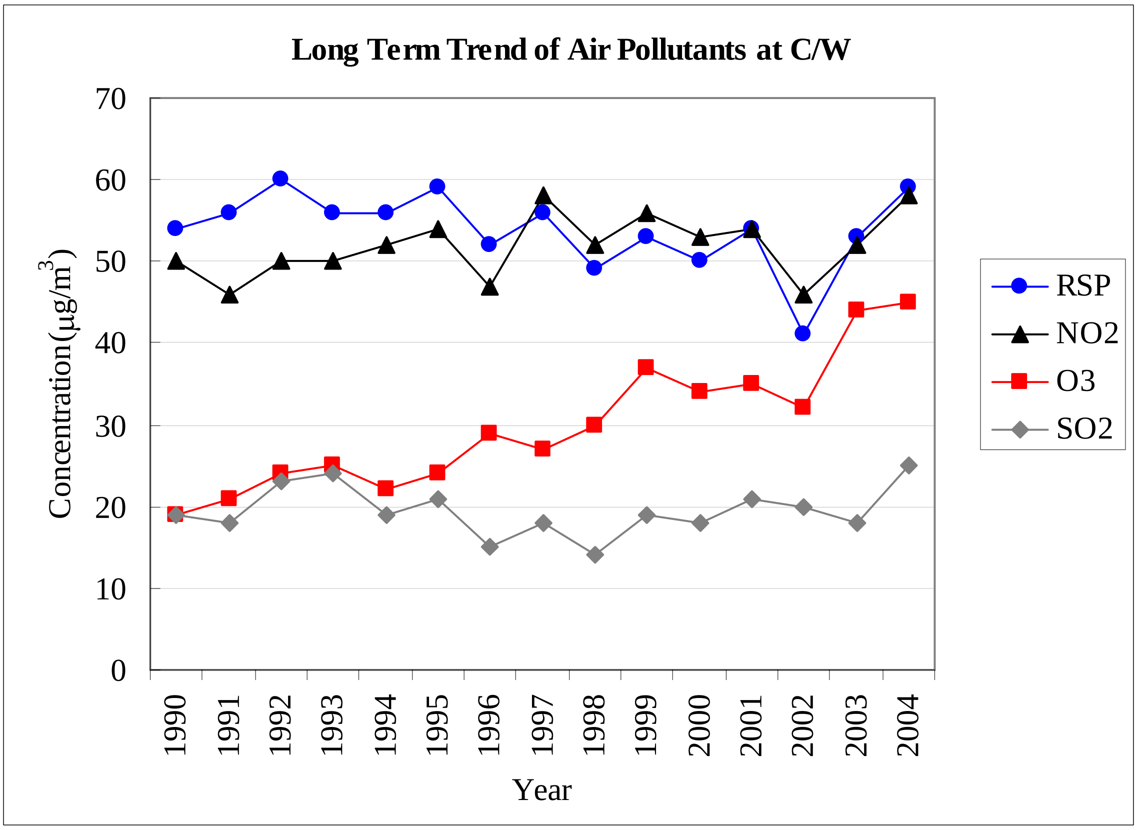

## 1.1 Background of Ozone

In the atmosphere, $O_3$ can have both beneficial and harmful effects to us depending upon its location. In the stratosphere, $O_3$ is beneficial to the environment because it provides a very efficient shield that blocks harmful UV radiation from reaching the ground and thus helps protect the life of all living things. In the troposphere, however, $O_3$ is a major gaseous pollutant present in photochemical smog. Such photochemical smog not only occurs in densely populated urban areas, it can also spread hundred of kilometres from the city centre to the surrounding rural areas under suitable meteorological conditions. $O_3$ can cause human health problems such as temporary decreases in lung capacity or inflammation of lung tissue (Folinsbee et al., 1988; Horvath and McKee, 1993). In addition, $O_3$ pollution can contribute to crop and tree damage (Skarby and Sellden, 1984; NRC, 1991). Moreover, $O_3$ plays an important role in the production of secondary particulates such as sulphates ($SO_4^{2-}$) and nitrates ($NO_3^-$) which contribute directly to visibility impairment (Lee and Sequeira, 2001; Wang, 2003).

Unlike other air pollutants such as $SO_2$ and carbon monoxide (CO) that are directly emitted, $O_3$ is produced via chemical reactions involving $NO_x$, volatile organic compounds (VOC) and sunlight. $NO_x$ is primarily emitted from fossil fuel combustion (mainly from power plants and vehicle exhaust in HK), whereas VOC are released from diverse sources including both man-made (e.g. vehicle exhaust, fuel evaporation and various industrial processes etc.) and natural origins (vegetation and trees). Because of their special roles on $O_3$ formation, $NO_x$ and VOC are commonly known as $O_3$ precursors (Seinfeld and Pandis, 1998).

The $O_3$ formation process begins with the breakdown of $NO_2$ by sunlight to form nitric oxide (NO) and free oxygen atom (O) *[Equation 1.1]*. The free oxygen atom left over from this reaction then combines with an oxygen molecule ($O_2$) to form an $O_3$ molecule *[Equation 1.2]*. Normally, the $O_3$ molecule would react again with NO to give $O_2$ and $NO_2$ *[Equation 1.3]*, hence establishing a formation/destruction cycle of $O_3$:

$NO_2 + h\nu$ (280-430nm) $\rightarrow NO + O$ ($NO_2$ photolysis) *[Equation 1.1]*

$O + O_2 + M \rightarrow O_3 + M$ (M is another third molecule, such as $N_2$ or $O_2$) *[Equation 1.2]*

$NO + O_3 \rightarrow NO_2 + O_2$ ($NO_2$ production) *[Equation 1.3]*

However, in the presence of VOC, the above-described cycle will be disrupted since the VOC can produce certain chemicals to accelerate the conversion rate of NO to $NO_2$. The role of VOC is to convert NO to $NO_2$ without using up $O_3$, so that there are not enough NO molecules to react with all the $O_3$ molecules, and $O_3$ accumulates. Figure 1.2 describes how the reactive nitrogen family participates in $O_3$ production (SOS, 1995). Reactions involving VOC and radical initiation, propagation as well as termination, compete with each other and play significant roles on $O_3$ formation and are discussed below (Seinfeld and Pandis, 1998).

*Figure 1.2* *Ozone is generated in the lower atmosphere from the photochemical smog mechanism involving the oxidation of VOC with* $NO_x$ *acting as a catalyst in the presence of sunlight. Eventually the process is terminated when* $NO_x$ *oxidized to* $NO_z$ *and removed by deposition to soils, vegetation and surface waters of the VOC is exhausted.*

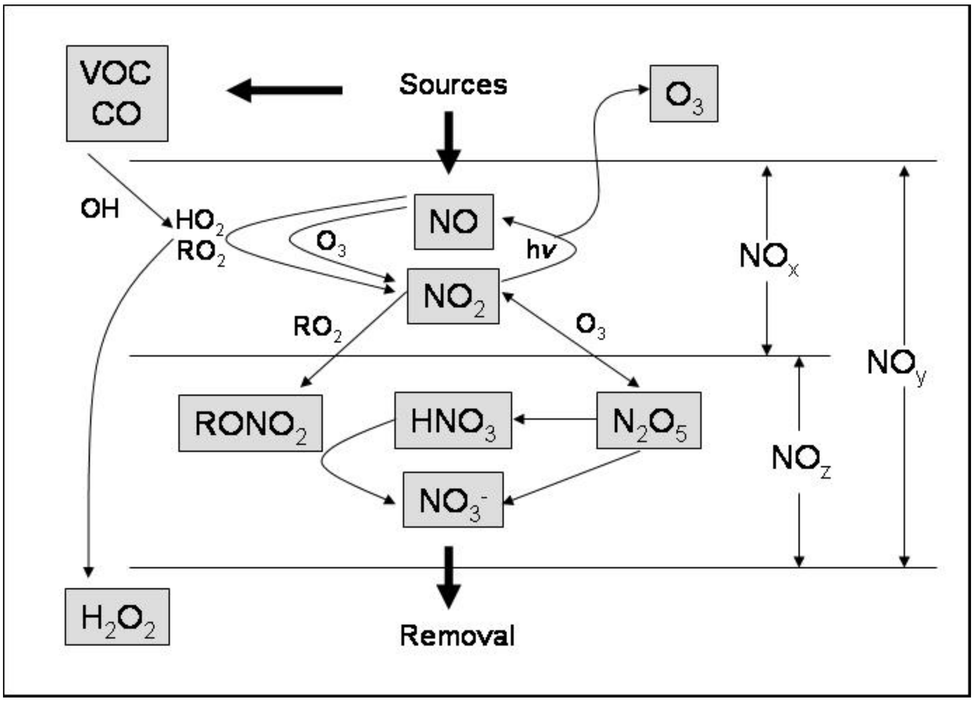

(Source: SOS 1995)

### *(a) Radical Initiation Reactions*

Radical initiation is a process which produces new hydroxyl (OH) radicals and the major OH production is attributed to the photochemical dissociation of $O_3$:

$O_3 + hv \rightarrow O(^1D) + O_2$ *[Equation 1.4]*

$O(^1D) + H_2O \rightarrow 2OH$ *[Equation 1.5]*

### *(b) Radical Propagation Reactions*

Radical propagation steps are where VOC (e.g. RH) are oxidized and NO-to-$NO_2$ conversions occur:

$RH + OH \rightarrow R + H_2O$ *[Equation 1.6]*

$R + O_2 \rightarrow RO_2$ *[Equation 1.7]*

$NO + RO_2 \rightarrow NO_2 + RO$ ($RO_2$ refers to organic peroxy radicals other than $CH_3O_2$) *[Equation 1.8]*

$RO + O_2 \rightarrow R'CHO + HO_2$ *[Equation 1.9]*

$NO + HO_2 \rightarrow NO_2 + OH$ *[Equation 1.10]*

Adding the above five reactions *[Equations 1.6 to 1.10]* and cancelling like terms, we see that the overall reaction is:

$RH + 2\,NO + O_2 \rightarrow R'CHO + 2\,NO_2 + H_2O$ *[Equation 1.11]*

where reaction *[Equation 1.10]* recreates an OH to perhaps begin another chain. As a result, NO is converted to $NO_2$ without using up $O_3$, leading the accumulation of $O_3$ level.

### (c) *Radical Termination Reactions*

Radical termination stops propagation because the reacting radical is incorporated into stable products. $NO_2$ reacts with OH, $HO_2$ and $RO_2$ as termination processes as they consume radicals. The most ubiquitous termination reaction (OH removal) is:

$OH + NO_2 \rightarrow HNO_3$ *[Equation 1.12]*

The reason why the above reaction *[Equation 1.12]* dominates termination is that radical propagation steps produce $NO_2$, thus making $NO_2$ available during the time that a large flux of radicals is also available. Other common termination reactions are:

$HO_2 + HO_2 \rightarrow H_2O_2 + O_2$ *[Equation 1.13]*

$RO_2 + HO_2 \rightarrow ROOH + O_2$ *[Equation 1.14]*

$RO_2 + NO \rightarrow RONO_2$ *[Equation 1.15]*

$CH_3C(O)O_2 + NO_2 \rightarrow CH_3C(O)O_2NO_2$ *[Equation 1.16]*

(i.e. peroxyacetyl nitrate, PAN)

As a result, $NO_2$ complicates the whole process because it can react with an OH radical to produce nitric acid and reduce the availability of OH radicals as shown in *[Equation 1.12]*. Therefore, the above equations suggest that in some situations adding $NO_2$ to the atmosphere will reduce the amount of $O_3$ formed. The net result of the chemical mechanism is VOC is oxidized to carbonyls and eventually to $CO_2$, whereas $NO_x$ is converted to other forms of reactive nitrogen compounds (products of $NO_x$ oxidation), $NO_z$ ($NO_z$ = $HNO_3$ + $NO_3^-$ + HONO + $HO_2NO_2$ + PAN + organic nitrate and aerosol nitrate, etc.). As such, $HNO_3$, $NO_3^-$ and PAN are often the most abundant components of $NO_z$ in the lower troposphere (Parrish et al., 1993).

The non-linear chemistry between $O_3$, $NO_x$ and VOC can be illustrated by an $O_3$ isopleth plot as shown in Figure 1.3 (Seinfeld, 1989; Chameides et al., 1992; Sillman et al., 1999). For this $O_3$-$NO_x$-VOC system, the formation of $O_3$ can either increase or decrease with increasing concentrations of $NO_x$ or VOC, depending on their relative abundance. While, in general, decreasing VOC emissions results in lower levels of $O_3$, decreasing $NO_x$ emissions may lead to either more or less $O_3$ depending on the initial amount of VOC and $NO_x$ emitted into the air (the VOC-to-$NO_x$ ratio to be exact). Luo et al. (2000) listed the factors that ultimately determine whether $O_3$ concentrations at a given locale are most sensitive to VOC or $NO_x$ emissions. These factors include:

(i) the VOC-to-$NO_x$ ratio of the emissions;

(ii) the reactivity of the VOC emissions;

(iii) the meteorological conditions, which control the rate of transport of pollutants from source regions to rural areas;

(iv) the degree to which the VOC and $NO_x$ emissions are spatially dispersed; and

(v) the presence of biogenic VOC emissions.

*Figure 1.3 Ozone isopleth plot based on simulations of chemistry along air trajectories in Atlanta (Jeffries and Crouse, 1990). Each isopleth is 10 ppbv higher in* $O_3$ *as one moves upward and to the right.*

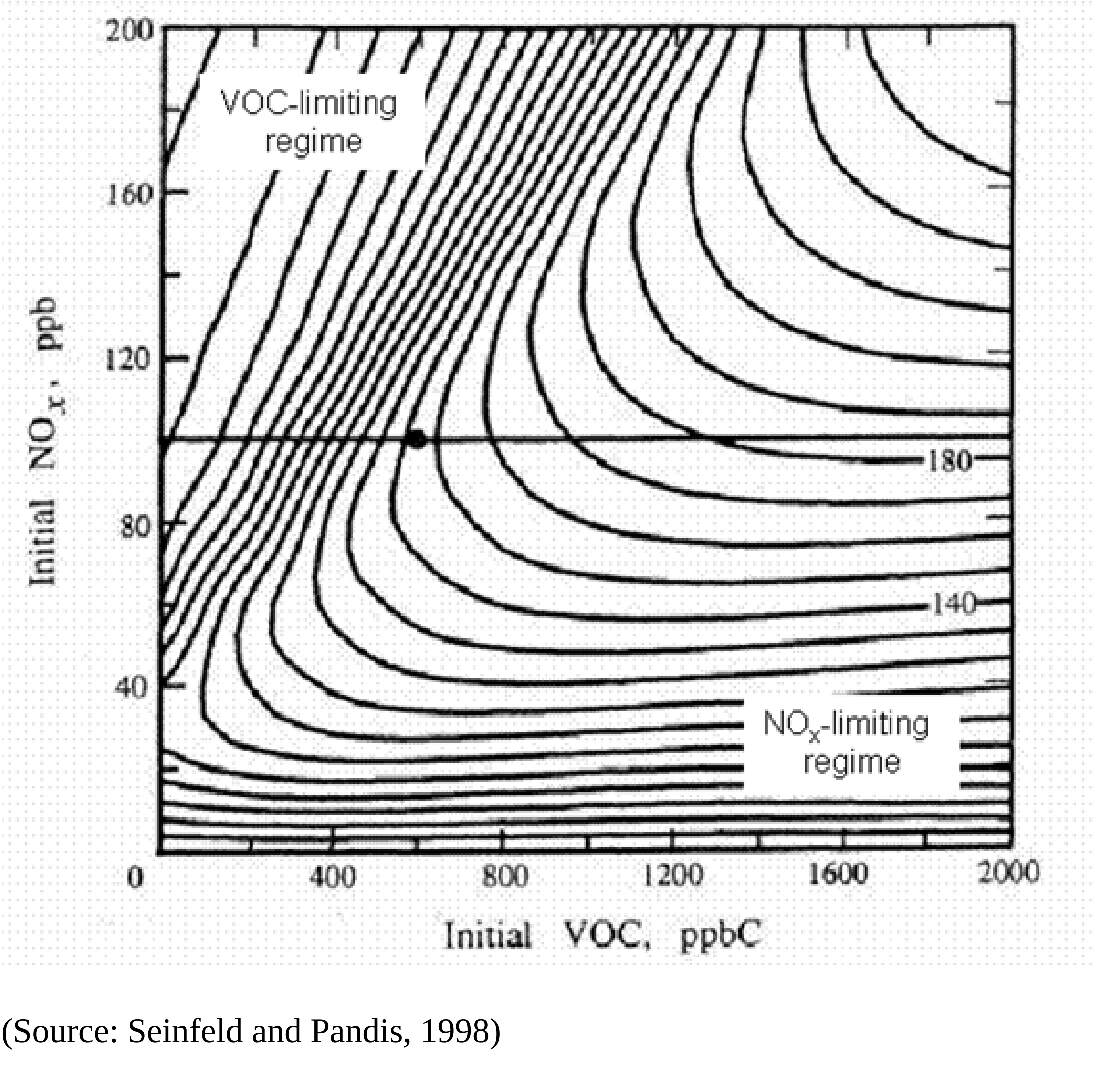

(Source: Seinfeld and Pandis, 1998)

In urban areas and in plumes immediately downwind of $NO_x$ sources, the $NO_x$ sources are greater than the odd hydrogen source. There is an excess of $NO_x$ and the VOC-to-$NO_x$ ratio is usually small (VOC-limiting). Increasing $NO_x$ will reduce peak $O_3$ concentrations because the reaction of $NO_2 + OH \rightarrow HNO_3$ *[Equation 1.12]* becomes dominant, which suppresses OH radicals and subsequently the peak $O_3$. In contrast, decreasing $NO_x$ emissions normally leads to a higher $O_3$ level. Increasing VOC, on the other hand, will increase $RO_2$ radicals, leading to a faster reaction of $NO + RO_2 \rightarrow NO_2 + RO$ *[Equation 1.8]* and faster $O_3$ production. Therefore, in this situation (low VOC-to-$NO_x$ ratio), $O_3$ formation in urban centres is largely limited by the availability of VOC.

In suburban and rural areas where the $NO_x$ source is less than the odd-hydrogen source, there is an excess of free radicals. Under the condition of a high VOC-to-$NO_x$ ratio ($NO_x$-limiting), increasing $NO_x$ will increase the rate of $NO + RO_2 \rightarrow NO_2 + RO$ *[Equation 1.8]* and lead to a faster production of $NO_2$ and then more $O_3$ will be formed. In this case, $O_3$ formation is more dependent on the amount of $NO_x$ than the levels of VOC and the $O_3$ production chemistry is under the $NO_x$–limiting regime.

Subject to the various supplies of $NO_x$ and VOC in promoting the $O_3$-producing reactions, the $O_3$ production rate and the division into $NO_x$-sensitive and VOC-sensitive photochemical regimes are linked to the abundance and sinks of odd hydrogen ($HO_x = OH + HO_2$) and odd nitrogen *[Equations 1.13 and 1.14]*, i.e. ratio of sources of odd hydrogen ($S_H$) to odd nitrogen ($S_N$) (Sillman, 1995; Sillman and He, 2002).

As discussed above, formation of $O_3$ in the $O_3$-$NO_x$-VOC system can either increase or decrease with increasing concentrations of $NO_x$ or VOC, depending on their relative abundance. An effective $O_3$ control program should be planned with the consideration of different factors including site characteristics, chemicals mix and meteorological conditions of the region concerned. Apart from the selection of $NO_x$ or VOC control, the control of different types (stationary versus mobile sources) of VOC may also provide different outcomes. For example, in sylvan cities, such as Atlanta, Georgia, large emissions of biogenic VOC from trees render pollution control strategies based on lowering anthropogenic VOC emissions relatively ineffective (Chameides et al., 1988). Another complication arises from the fact that, under some circumstances, lowering $NO_x$ emissions can actually lead to a temporary $O_3$ increase. For these reasons, determining the best pollution control strategy for a given area has proven to be a complex and challenging undertaking, requiring the application of sufficient measurement data and the appropriate air quality simulation model.

To summarize, controlling the overall $NO_x$ emission alone may sometimes produce undesirable results, particularly in areas already with low VOC-to-$NO_x$ ratio. It is therefore crucial to have accurate emission inventories of VOC and $NO_x$ for different types of regions before deciding on the most suitable control strategy for $O_3$ (i.e. to determine whether to control $NO_x$ or VOC, or both).

## 1.2 Meteorological Influences on Ozone Formation

Studies have shown that meteorological factors, such as sunlight, vertical mixing, temperature, wind, and cloud cover can strongly influence the chemical formation of $O_3$, transport of $O_3$ and the precursor pollutants, and evaporative emissions of VOC (NRC, 1991). In the case of $O_3$, its formation and accumulation near the ground level is known to vary closely with the day-to-day variations in meteorological conditions. The meteorological factors that are of the most concern are sunlight intensity, temperature, wind speed and atmospheric mixing and transport. In North America and Europe, high-$O_3$ conditions are often associated with slow-moving anticyclones (e.g. NRC, 1991). For examples, Vukovich et al. (1977) examined the $O_3$ concentrations associated with high pressure systems in the Eastern United States (US). St John and Chameides (1997) found that the highest $O_3$ concentrations in Atlanta, Georgia were associated with stagnant meteorological conditions and recirculation of Atlanta's plume.

### *1.2.1 Sunlight Intensity and Temperature*

Higher levels of $O_3$ are often observed on hot and sunny days for the following reasons:

(i) the rate of $O_3$ formation increases rapidly with sunlight intensity;

(ii) anthropogenic and natural emissions of VOC increase with ambient temperature (e.g. the release of VOC from petrol filling stations and certain plants can increase substantially with a slight rise of temperature); and

(iii) high pressure, stagnant atmospheric conditions that tends to limit pollutant dispersal are usually associated with high temperatures (Olszyna et al., 1997).

### *1.2.2 Wind Speed and Wind Direction*

Wind speed is the most important parameter in determining the amount of accumulation of $O_3$ and its precursors. In general, lower wind speed will lead to reduced ventilation and, hence, a greater chance for pollutants to accumulate in the atmosphere. In HK, a stagnant atmosphere (sometimes with temperature inversion) usually occurs under the following conditions:

(i) a high pressure system with abnormally high temperature is over the territory;

(ii) a number of weak pressure systems with slack pressure gradients are developed in the South China and western Pacific regions; and

(iii) the PRD region is under the influence of the outer circulation of a tropical cyclone near the Balintang Channel (southeast of HK).

Wind direction also plays a key role in controlling the formation of $O_3$ pollution as very different types of air pollutants / $O_3$ precursors would be brought to an area under different wind profiles. As the climate of HK is governed by the Asian monsoons, the prevailing synoptic winds are from the north and northeast in winter, east in spring and autumn, and southwest in summer. The southwesterly winds in summer bring in clean maritime air to HK. Coupled with the unstable weather conditions, it is not favourable for the photochemical production of $O_3$ and accumulation of air pollutants. In late autumn, however, the northeast monsoon can carry precursors-laden air from the Asian continent to HK which are conductive to the photochemical $O_3$ formation (Wang et al., 2001b).

Furthermore, land/sea breeze may dominate the local wind flow when the prevailing wind is weak. This makes possible the re-circulation of polluted air mass (enriched with $O_3$ and its precursors) in the coastal region of HK, again resulting in elevated levels of pollutants (Wang et al., 2003b; Ding et al., 2004).

### *1.2.3 Atmospheric Mixing and Transport*

$O_3$ episodes are not necessarily confined to urban downtown areas although the ambient levels of $O_3$ precursors are usually higher there. This is because $O_3$ or its precursors can be carried away from their emission sources by the wind to nearby suburban or rural areas. Furthermore, the levels of NO, which is a very effective scavenger of $O_3$, are usually much lower in suburban and rural areas. In such cases, reductions in VOC (and sometimes $NO_x$) emissions in the urban area could probably improve air quality in the suburban and rural areas as well (Sillman, 1999).

## 1.3 Analysis of Ozone Episodes

Apart from the analysis of general seasonal and spatial $O_3$ pattern, study of pollution episodes can also provide insights into the effect of meteorological indices on the elevated $O_3$ days (Xu et al., 1999). In addition, understanding of the dependence of ground-level $O_3$ accumulation on the emissions of its precursors is fundamental to developing scientifically sound $O_3$ pollution control strategies. In general, major episodes of elevated concentrations of $O_3$ associated with high concentrations of other chemical pollutants usually occurred under the influence of slow-moving, high-pressure weather systems, causing the subsidence of air (Seinfeld and Pandis, 1998). For example, $O_3$ pollution studies in Shanghai (Xu et al., 1999) showed that incidents were characterized by high pressure systems and northwestern wind currents while there was a relatively smaller influence by wind speed and temperature. In the eastern US (Kasibhatla et al., 1998), episodes were also characterized by relatively stagnant meteorological conditions. Apart from that, others showed that these episodes occurred during warm, sunny, and relatively stagnant conditions associated with slow-moving high pressure systems in summer (Vukovich et al., 1977; Logan et al., 1981).

## 1.4 Overseas Ozone Studies and their Comparison

Extensive overseas $O_3$ studies have been conducted during the last two decades and they have supplied a large amount of $O_3$ data from around the world. Such information is essential to the evaluation of our local pollution and the formation of an appropriate migration strategy. This section will review the overseas $O_3$ studies and provide information about the urban and rural $O_3$ levels from around the world.

### *1.4.1 Overseas Ozone Studies*

#### **(a) Western Countries**

Atmospheric $O_3$ research has been widely studied in many regions of the world (e.g. McKendry, 1993; Bower et al. 1994; Sunwoo et al., 1994; Lin et al., 2000 and Pochanart et al, 2001a). In North America and Europe, over 30 major field studies have been carried out examining tropospheric $O_3$ chemistry, meteorology, precursor emissions, modelling etc during the past few decades (Solomon et al., 2000). Key findings include:

(i) reaffirmation that tropospheric $O_3$ is a multi-scale phenomenon extending to continental boundaries;

(ii) aerometric conditions aloft are important to ground-level $O_3$;

(iii) biogenic sources make important contributions to VOC and $NO_x$ emissions in parts of eastern North America and southern Europe;

(iv) emissions estimates are among the most uncertain components of predictive models for $O_3$;

(v) recirculating flow over complex terrain and large water bodies are universally important factors affecting accumulation of $O_3$ at the ground;

(vi) nonlinearities in $O_3$ response to precursor changes create important degrees of freedom in management strategies - VOC and $NO_x$

sensitivities vary extensively in the urban and rural areas, making decisions about emissions management complicated;

(vii) measurement methods for many precursors, intermediates, and products of photochemical reactions have improved greatly; and

(viii) additional analysis and interpretation of existing data from many of these field studies should pay handsome dividends at relatively modest cost.

Rodriguez and Guerra (2001) summarized that high surface $O_3$ concentrations photochemically produced from anthropogenic $O_3$ precursors have been extensively described in continental regions surrounding the North Atlantic, i.e., Eastern US (e.g. Logan, 1989; Trainer et al., 1993; Ryan et al., 1998), Western Europe (e.g. De Muer et al., 1997) and Western Mediterranean (e.g. Millan et al., 1991). During the late 1980s and early 1990s the high $O_3$ concentrations measured at remote sites in the North Atlantic were attributed to the transport of $O_3$ or its precursors from Europe and / or North America (e.g. Schmitt et al., 1988; Schmitt and Carretero, 1995).

In addition, the frequencies and characteristics of regional $O_3$ pollution episodes in the industrially-developed western regions (e.g. the Canadian / US subcontinent and Europe) has been studied extensively (e.g. Vukovich, 1979; King and Vukovich, 1982; Vukovich, 1995; Lin et al., 2001). For the seasonal variation of $O_3$, maximum levels in summer and minimum levels in winter were reported in different North American and European countries (e.g. Angle and Sandhu, 1989; McKendry, 1993; Bower et al., 1994; Rodriguez et al., 2001; Pochanart et al., 2001b and Varotsos et al., 2001). Further, Pochanart et al. (2001b) observed two main types of $O_3$ seasonal variation in Europe. The first type includes a single spring maximum or spring maximum-summer minimum found in the relatively clean sites at higher latitude and the second type with a spring-summer broad maximum and winter minimum type being observed more in central or southern Europe (Monks, 2000).

### (b) Eastern Countries

Extensive ground-level $O_3$ studies have also been conducted over the East Asian areas (e.g. Liu et al, 1990 and 1994; Sunwoo et al., 1994; Xu et al., 1999 and Cheng, 2001). For example, there was a seasonal variability in the measured $O_3$ concentrations with its peak in spring and a significant summer minimum in Japan (Sunwoo et al., 1994). Pochanart et al. (2001a) revealed the basic picture of surface $O_3$ characteristics in Thailand and showed dry season maximum – wet season minimum were controlled primarily by the long-range transport of $O_3$ under the Asian monsoon. In India, maximum $O_3$ concentrations were observed during autumn and winter months due to higher amounts of precursor gases, in spite of lower solar radiation (Lal et al., 2000). At Mt Abu of India, monthly average $O_3$ mixing ratios showed a systematic seasonal variation with maximum value of about 46 ppbv during late autumn and winter (October – February). A monthly minimum $O_3$ mixing ratio (about 25 ppbv) was observed in summer with the prevailing monsoon (Naja et al., 2003). Pochanart et al. (2002) analyzed the surface $O_3$ data at four remote islands in Japan and indicated that East Asian anthropogenic emissions significantly influence the boundary layer in Japan. Under the influence of the ‘regionally polluted’ continental outflow, the background $O_3$ levels were as high as 41-46 ppbv in winter and 54-61 ppbv in spring. General characteristics and trends of ground-level $O_3$ were also investigated in Korea for the period of 1990-1995. It was found that seasonal $O_3$ variations were characterized by a spring peak with decreased levels in the summer, followed by increases in the autumn (Ghim and Chang, 2000).

Detailed studies of atmospheric chemistry over the western Pacific were conducted under NASA’s Pacific Exploratory Mission-West A in autumn 1991 and West B in spring 1994 (Smyth et al., 1999 and references therein). Such projects increased our understanding of the abundance and distribution of important trace gases and aerosols in the western Pacific, the transport of $O_3$, combustion-based and industrial pollutants and also the transport of dust storms from the Asian continent to the remote Pacific (Wang et al., 1997). For eastern China, Luo et al. (2000) reported that, under the influence of the Asian Monsoonal Circulation, enhanced $O_3$ concentrations were observed during the autumn and early winter. From the measurement of $O_3$ and other primary air pollutants (trace gases, VOC and aerosol) at Lin’an, a rural/agricultural site in the fast developing Yangtze Delta region of China, it was reported that elevated $O_3$ and CO levels were associated with large-scale stagnation, intense solar radiation, minimum rainfall and were suggested to be a partial result of incomplete biomass burning. The results also strongly suggested that CO emissions in eastern China had been underestimated and highlighted the importance of characterizing trace gases and aerosol within source regions of the Asian continent. (Cheung and Wang, 2001; Wang et al., 2001a; 2002; 2004).

### (c) African Countries

By comparison, there have been limited studies on the surface $O_3$ levels in the African continent. Lacaux et al. (1993) reported about 30-40 ppbv of surface $O_3$ in Central Africa during 1983 and 1988 while Combrink et al. (1995) presented variations in the range of 25-50 ppbv at two different stations in South Africa. The mean $O_3$ levels ranged from 33 to 48 ppbv in Eastern Highlands of Zimbabwe (Jonnalagadda et al., 2001).

### *1.4.2 Comparison of Ozone Levels around the World*

It is of interest to compare the ambient $O_3$ levels between HK and other metropolises by studying the highest 1-hour maximum $O_3$ levels during the period. Figure 1.4 compares the highest 1-hour maximum $O_3$ concentrations measured in different international cities between 1999 and 2002. HK was found on the higher side among the metropolises with the highest hourly $O_3$ concentration (379 $\mu g/m^3$), which is much higher than its air quality objective of 240 $\mu g/m^3$.

Urban $O_3$ levels are normally titrated by the fresh emissions from vehicles and industries. It is therefore worth understanding and comparing the background $O_3$ levels at remote sites. Such background $O_3$ measurements from remote sites around the world are routinely measured by the Climate Monitoring and Diagnostics Laboratory (CMDL) of the National Oceanic and Atmospheric Association (NOAA), an agency responsible for monitoring *in situ* greenhouse gas and $O_3$ depleting substances on a global scale (Vingarzan, 2004). Table 1.1 presents the range of annual mean surface $O_3$ concentrations measured by CMDL at six remote cities around the world (CMDL, 2004). Additional long-term data on background $O_3$ is also available from the Clean Air Status and Trends Network (CASTNet, 2004) from sites designated as protected areas. Table 1.2 presents a summary of annual medians and maxima compiled for 11 national parks in the US. Annual medians at US parks range from 13 to 47 ppbv, while annual maxima range from 49 to 109 ppbv (CASTNet, 2004). In Canada, the Canadian Air and Precipitation Network has been recording surface $O_3$ concentrations at the rural sites over the past two decades. Table 1.3 presents a summary of annual $O_3$ statistics from these sites. Annual median $O_3$ concentrations at Canadian background sites range from 23 to 34 ppbv, while annual maxima range from 63 to 108 ppbv (CAPMoN, 2003). Direct comparison of $O_3$ data at different sites must be done with caution as the surface $O_3$ varies distinctively with the topography, seasons and urban characteristics of the site.

*Figure 1.4 Inter-city comparison of 1-hour maximum $O_3$ concentrations.*

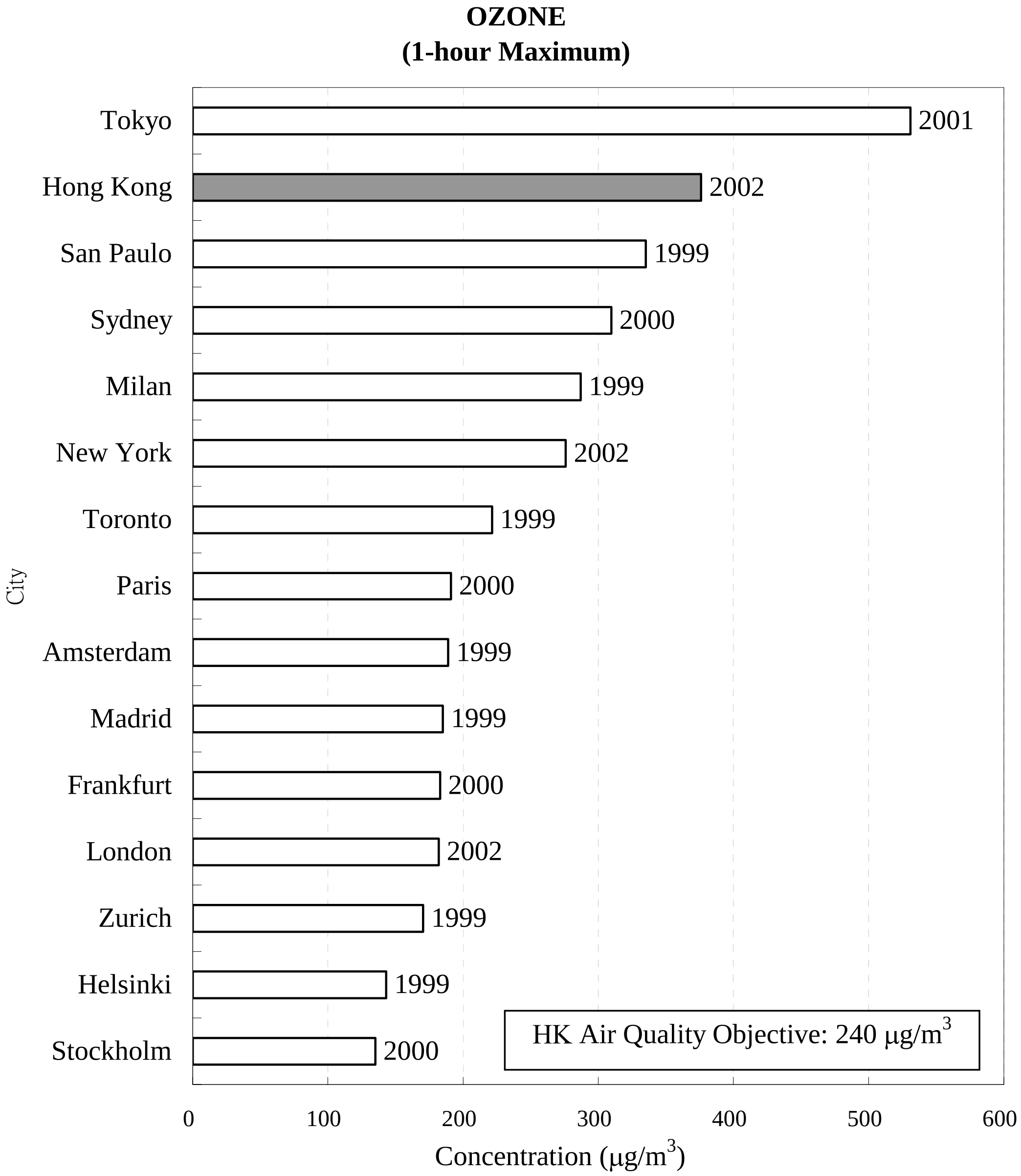

**Data Sources**
**Tokyo:** Japanese EPA website (http://www.nies.go.jp/igreen/index.html)
**Hong Kong:** Hong Kong EPD Air Quality Report 2002
**San Paulo, Toronto, Zurich and Helsinki:** "Air Quality in Ontario 1999" annual report, Ministry of the Environment, Ontario, Canada.
**Syndey:** Suzanne Quigley - Manager of Scientific service and Research unit, Atmospheric Science Branch (www.epa.nsw.gov.au)
**Milan, Amsterdam and Madrid:** European Topic Centre on Air and Climate Change (http://air-climate.eionet.eu.int/databases/ozone99.html)
**New York:** USA EPA AIRSData (http://www.epa.gov/air/data/monsum.html)
**Paris:** Paris Summary of Statistics from Central Paris Air Quality Information Sheet
**Frankfurt:** Frankfurt Air Quality Information Sheet
**London:** UK National Air Quality Information Archive (http://www.aeat.co.uk/netcen/airqual/statbase/concns/auto2.html)
**Stockholm:** Stockholm Air website (http://www.slb.mf.stockholm.se/)

*Table 1.1 Range of annual (January–December) hourly ozone concentrations (ppbv) at background sites around the world (CMDL, 2004)*

| Location | Elevation (m) | Period of record | Range of annual means |
|---|---|---|---|
| Pt. Barrow, Alaska | 11 | 1992–2001 | 23–29 |
| Ny Alesund, Svalbard, Spitsbergen[a] | 475 | 1989–1993 | 28–33[b] |
| Mauna Loa, Hawaii[c] | 3397 | 1992–2001 | 37–46[d] |
| American Samoa | 77 | 1995–2001 | 11–14 |
| South Pole, Antarctica | 2835 | 1992–2001 | 26–30[d] |
| Arrival Heights, Antarctica | n/a | 1997–1999 | 23–26 |

[a] University of Stockholm Meteorological Institute.

[b] Annual medians.

[c] 10:00–18:00 UTC.

[d] High elevation site.

*Table 1.2 Range of annual (January–December) hourly median and maximum ozone concentrations (ppbv) at background stations in protected areas of the United States (CASTNet, 2004)*

| Location | Elevation (m) | Period of record | Range of annual medians | Range of annual maxima |
|---|---|---|---|---|
| Denali National Park, Alaska | 640 | 1998–2001 | 29–34 | 49–68 |
| Glacier National Park, Montana | 976 | 1989–2001 | 19–27 | 57–77 |
| Voyageurs NP, Montana | 429 | 1997–2001 | 28–35 | 74–83 |
| Theodore Roosevelt NP, North Dakota | 850 | 1983–2001 | 29–43 | 61–82 |
| Yellowstone NP, Wyoming | 2469 | 1996–2001 | 37–45[a] | 68–79[a] |
| Rocky Mountain NP, Colorado | 2743 | 1994–2001 | 40–47[a] | 68–102[a] |
| Olympic National Park, Washington | 125 | 1998–2001 | 19–22 | 50–63 |
| North Cascades NP, Washington | 109 | 1996–2001 | 14–18 | 48–69 |
| Mount Rainier National Park, Washington | 421 | 1995–2001 | 13–20 | 54–98 |
| Lassen National Park, California | 1756 | 1995–2001 | 38–43[a] | 81–109[a] |
| Virgin Islands NP, US Virgin Islands | 80 | 1998–2001 | 19–24 | 50–64 |

[a] High elevation site.

*Table 1.3 Range of annual (January–December) hourly median and maximum ozone concentrations (ppbv) at Canadian background stations (CAPMoN, 2003)*

| Location | Elevation (m) | Period of record | Range of annual medians | Range of annual maxima |
|---|---|---|---|---|
| Kejimkujik, Nova Scotia[a] | 127 | 1989–2001 | 25–34 | 76–116 |
| Montmorency, Quebec | 640 | 1989–1996 | 28–32 | 73–99 |
| Algoma, Ontario[a] | 411 | 1988–2001 | 27–33 | 76–108 |
| Chalk River, Ontario[a] | 184 | 1988–1996 | 25–31 | 79–107 |
| Egbert, Ontario[a] | 253 | 1989–2001 | 27–32 | 90–113 |
| E.L.A., Ontario | 369 | 1989–2001 | 28–33 | 64–87 |
| Bratt’s Lake, Saskatchewan | 588 | 1999–2001 | 26–29 | 63–68 |
| Esther, Alberta | 707 | 1995–2001 | 26–31 | 63–78 |
| Saturna Island, British Columbia | 178 | 1992–2001 | 23–27 | 65–82 |

[a] Stations affected by long-range transport of anthropogenic emissions.

## 1.5 Ozone Studies in Hong Kong

In HK, the general ground-level $O_3$ are monitored by the air quality monitoring network of the Environmental Protection Department (EPD, 2000). Figure 1.5 presents the EPD's air quality monitoring network; $O_3$ levels are measured at all the eleven general stations. Due to the efficient scavenging of $O_3$ from the roadside vehicular NO emissions, the low roadside $O_3$ level is not monitored by the EPD in HK. Comparison of their spatial and temporal (annual, monthly and diurnal) $O_3$ patterns reveals the various impact of $O_3$ pollution to the areas with different site characteristics. Details can be found at the annual air quality reports prepared by the EPD (http://www.epd-asg.gov.hk/english/report/report.php).

In addition, the HK Polytechnic University Regional Air Monitoring and Research Group has set up an air monitoring station at a coastal site, Hok Tsui (HT) for the study of the regional impact on air quality of the southeast China region since 1993 (Chan et al., 1998; Wang et al., 1997; 1998; 2001b and c; Lam et al., 2001). The site is in the southeastern tip of HK Island and has a $240^o$ ocean view stretching from the northeast to the west. Under the prevailing easterly winds, the HT site is upwind of urban areas of HK and provides invaluable background $O_3$ information of the region.

*Figure 1.5 EPD's Air Quality Monitoring Network of Hong Kong.*

(Source: http://www.epd-asg.gov.hk/english/backgd/quality.php)

Apart from the regular $O_3$ monitoring, a number of studies were conducted on the $O_3$ behaviours in or before 1997. Chan et al. (1998) analyzed the $O_3$ data from 1990 to 1994 collected at several urban locations and reported a peak in autumn and a trough in summer. Wang et al. (1998) showed several $O_3$ episodes observed at a coastal site in 1994 and discussed small-scale re-circulation and transport of aged air masses. An aircraft study in autumn 1994 (Kok et al., 1997) also showed high concentrations of $O_3$ and other pollutants in western parts of HK and presented evidence to suggest transport of local and regional pollution to the western sector. Wang et al. (2001b) also presented the relationship of $O_3$ to meteorological parameters particularly to the wind flow over HK, by using 1996 data collected in five sites in HK. Wang and his co-workers (Wang et al., 2001c) further analyzed the measurements of several trace gases at HT in autumn 1997 and compared them with the aircraft measurements obtained in 1994 by Kok et al. (1997). Examination of 10-day isentropic back trajectories showed that the measured trace gases could be influenced by maritime air masses, outflow of pollution-laden continental air and mixing of the two. Chan and Chan (2000) also studied the effect of meteorology and air pollutant transport on $O_3$ episodes in HK. All the results provided us with the information of $O_3$ variation and formation in HK.

The above studies were concentrated on the general $O_3$ surface pattern and its relationship with meteorological factors in or before 1997. However, not much or significant work has been carried out to study the chemical processes on $O_3$ formation. During the past few years, moreover, there has been a rapid economic development and significant change in land use in HK and other cities of the PRD. The recent industrial developments in the region may affect the $O_3$ levels on both local and regional scales. It is therefore of interest to have an updated analysis of $O_3$ distribution as well as the spatial correlation of $O_3$ and other air pollutants among the territories. Moreover, details of the chemical processes on $O_3$ formation and its relationship with the other $O_3$ precursors (e.g. VOC) relationship are still not clear. Therefore, this thesis will attempt to fill the above data gaps and help identify the processes in contributing to the $O_3$ formation in HK.

## 1.6 Overseas Studies on Volatile Organic Compounds and their Comparison

VOC are well known $O_3$ precursors and play a critical role on photochemical $O_3$ formation, caused by their gas-phase reactions with $NO_x$ in the presence of sunlight (e.g. Finlayson and Pittis, 1976; Logan et al., 1981). Different VOC have various abundances and reactivities which differ in their effects on $O_3$ formation. Therefore, it is essential for us to obtain a clear and accurate VOC picture prior to our understanding of the $O_3$ formation in an area. Prior to our study of the local VOC pattern, it is necessary to provide some background information about their sources and overseas measurements.

In general, the production of VOC and $NO_x$ in urban environments is often dominated by vehicular emissions involving gasoline distribution, evaporation and automobile exhaust (Watson et al., 2001). Non-methane hydrocarbons (NMHC), a major class of VOC, are especially important among VOC in photochemical $O_3$ production. They mainly come from anthropogenic sources in the cities, such as vehicle exhaust emissions, gasoline evaporation and spillage, leaks of commercial natural gas, emissions from petroleum manufacturing plants and refineries, and chemical solvents (Warneck, 2000). Alkanes are generally associated with gasoline evaporation, liquefied petroleum gas (LPG) and natural gas leakage (e.g. Blake and Rowland, 1995; Chen et al., 2001). Unsaturated hydrocarbons like ethene and ethyne are characteristic products of internal combustion engines, while $C_5$-$C_8$ hydrocarbons are mainly contributed by unburned vehicular emissions

(Mayrsohn and Crabtree, 1976). Aromatic hydrocarbons, usually representing a significant fraction of total NMHC, are emitted by fuel combustion and evaporation of fuels and solvents. VOC emitted from natural sources like isoprene also play an important role on photochemical $O_3$ formation. Therefore, it is crucial to characterize the sources, composition and distribution of different types of VOC in the atmosphere.

Measurements of VOC have been extensively conducted and Table 1.4 compares the key VOC levels in different megacities including HK. The VOC levels in HK were on the middle/lower side together with metropolises like Sydney and London. By comparison, Karachi, Kathmandu, Mexico City and Santiago had much higher levels. For example, the annual average mixing ratio of benzene (0.5 ppbv) in HK was much less than the regulatory limit of 10 $\mu g/m^3$ (3.1 ppbv) implemented in several countries, but the levels in Karachi, Mexico city and Santiago were all over the limit (4.6 – 6.0 ppbv) (Barletta et al., 2002). Further discussion on the VOC data of HK will be given in Chapters 5 and 6.

*Table 1.4 Comparison of selected hydrocarbons measured in Hong Kong (average of three urban sites) and in other cities (units are in ppbv unless otherwise specified).*

| Compound | Hong Kong | Karachi[a] | Kathmandu[b] | Mexico City[c] | Santiago[d] | Athens[e] | Taipei[f] | Osaka[g] | Hamburg[h] | Sydney[i] | Chicago[j] | London[k] |
|---|---|---|---|---|---|---|---|---|---|---|---|---|
| Sampling Period | (Sep 02 to Aug 03) | (Dec 98 to Jan 99) | (Nov 98) | (Feb 93) | (Jun 96) | (Jun 93, May & Jul 94) | (Jan 97) | (Not provided) | (Apr 86 to Apr 87) | (Sep 79 to Jun 80) | (Nov 86 to Feb 87) | (1996) |
| Methane (ppmv) | 2.0 | 6.3 |  | 2.6 | 2.2 |  |  |  |  |  |  |  |
| Ethane | 1.9 | 93 | 7.7 | 14 | 9.4 |  | 8.3 |  |  | 7.5 | 6.4 | 4.2 |
| Propane | 1.8 | 41 | 6.0 | 158 | 137.5 | 1.2 | 6.4 | 8.9 | 2.1 | 5.9 | 3.2 | 2.0 |
| *n*-Butane | 1.7 | 19.8 | 42.2 | 70.4 | 27.0 | 2.1 | 5.2 | 11 | 7.8 | 7.5 | 6.0 | 3.2 |
| *n*-Pentane | 0.3 | 13.4 | 24.8 | 14.4 | 6.6 | 4.2 | 4.3 | 7.7 | 5.1 | 5.0 | 3.8 | 0.6 |
| *n*-Hexane | 0.3 | 7.4 | 13.8 | 12.2 | 4.1 | 1.6 | 2.3 | 5.5 | 3.8 | 2.1 | 2.0 | 0.2 |
| Ethene | 1.8 | 19 | 48.4 | 21.6 | 29.4 |  | 14.1 | 23.3 | 5.3 | 12.5 | 3.5 | 3.4 |
| Propene | 0.4 | 5.5 | 12.8 | 5 | 8.0 | 3.9 | 4.6 | 6.1 | 2.9 | 7.4 | 1.4 | 1.4 |
| *i*-Butene | 0.2 | 1.2 |  | 1.8 | 2.8 |  | 2.7 |  |  | 1.4 |  |  |
| 1-Butene | 0.1 | 1.1 | 2.5 | 2.1 | 2.4 | 0.9 | 0.9 |  |  | 1.0 |  | 0.2 |
| Isoprene | 0.2 | 0.8 | 0.3 | 0.1 | 0.5 |  |  |  |  |  |  | 0.1 |

*(to be continued)*

*Table 1.4 continued*

| Compound | Hong Kong | Karachi[a] | Kathmandu[b] | Mexico City[c] | Santiago[d] | Athens[e] | Taipei[f] | Osaka[g] | Hamburg[h] | Sydney[i] | Chicago[j] | London[k] |
|---|---|---|---|---|---|---|---|---|---|---|---|---|
| Sampling Period | (Sep 02 to Aug 03) | (Dec 98 to Jan 99) | (Nov 98) | (Feb 93) | (Jun 96) | (Jun 93, May & Jul 94) | (Jan 97) | (Not provided) | (Apr 86 to Apr 87) | (Sep 79 to Jun 80) | (Nov 86 to Feb 87) | (1996) |
| 1,3-butadiene | 0.1 | 0.8 |  |  | 1.5 |  |  |  |  |  |  |  |
| Ethyne | 2.2 | 18 | 36 | 31.6 | 25.9 |  | 15.1 |  | 8.8 | 10.1 | 4.1 | 4.6 |
| Benzene | 0.5 | 5.2 |  | 4.6 | 6.0 | 5 |  | 5.1 | 3.2 | 2.6 | 2.4 | 1.1 |
| Toluene | 3.1 | 7.1 |  | 21 | 21.8 | 14.3 |  | 31.1 | 8.2 | 8.9 | 3.8 | 2.2 |
| 1,3,5-Trimethylbenzene | 0.1 | 0.4 |  |  | 1.4 |  |  | 1.2 |  | 0.5 |  |  |
| 1,2,4-Trimethylbenzene | 0.2 | 1.0 |  |  | 3.1 |  |  | 2.9 |  | 1.3 |  |  |
| *o*-Xylene | 0.2 | 1.1 |  |  | 3.8 | 3.7 |  | 2.8 | 1.8 | 1.5 | 0.4 | 0.4 |
| *m*-Xylene | 0.4 | 2.1 |  |  | 7.0 |  |  | 5.4 |  |  |  |  |
| *p*-Xylene | 0.3 | 1.0 |  |  | 3.3 |  |  | 2.3 |  |  | 1.5 |  |

[a]Barletta et al. (2002); [b]Sharma et al. (2000); [c]Blake and Rowland (1995); [d]Chen et al. (2001); [e]Moschonas and Glavas (1996); [f]Ding and Wang (1998); [g]Tsujino and Kuwata (1993); [h]Bruckmann et al. (1988); [i]Nelson et al. (1983); [j]Aronian et al. (1989); [k]Derwent et al. (2000).

## 1.7 Volatile Organic Compounds Studies in Hong Kong

In HK, there were limited VOC studies and they only focused on the spatial and temporal VOC pattern. Sin et al. (2000) reported the annual variation and correlations of major VOC at the two toxic air pollutants monitoring stations of the EPD from July 1997 to June 1998. Lee et al. (2002) studied the VOC levels at different areas from September 1997 to September 1999 and analyzed the respective winter to summer ratio, spatial patterns as well as benzene, toluene, ethylbenzene and xylene (BTEX) pictures in HK. Chan et al. (2002) and Ho et al. (2002) also investigated the VOC levels at the roadside sites in 1998 and 1999 respectively. However, the above studies only focused on the general VOC patterns and BTEX data in the industrial and roadside areas. There have been very limited studies on the sensitivity of $O_3$ precursors [$NO_x$ versus hydrocarbons controls] to $O_3$ formation, analysis of hydrocarbon emission pattern and identification of reactive hydrocarbons that are specifically important to $O_3$ formation in HK. Such information is critical to an effective control strategy assessment of our $O_3$ problem. In-depth relevant studies should be further conducted to better characterize the photochemical environment of this region.

## 1.8 Background of Reactive Nitrogen Compounds

Reactive nitrogen compounds also play a controlling role in the chemistry of the lower atmosphere and they are involved in the production and loss of atmospheric $O_3$ on urban and regional scales. It is therefore essential to understand the budget and partitioning of the reactive nitrogen species in the atmosphere in order to evaluate the dependence of $O_3$ on the reactive nitrogen compounds in a photochemically aged air mass. Here, a brief introduction about the reactive nitrogen compounds is provided.

Total reactive nitrogen ($NO_y$) is defined as the sum of $NO_x$ ($NO + NO_2$) and all compounds that are atmospheric products of $NO_x$ are named as $NO_z$ ($NO_y - NO_x$). This includes the compounds of nitric acid ($HNO_3$), nitrous acid ($HNO_2$), nitrate radical ($NO_3^-$), dinitrogen pentoxide ($N_2O_5$), peroxynitric acid ($HNO_4$), peroxyacetyl nitrate (PAN, $RC(O)OONO_2$) and its homologues, alkyl nitrates ($RONO_2$), peroxyalkyl nitrates ($ROONO_2$), and nitro-aromatic compounds ($RNO_2$). In general, nitrous oxide ($N_2O$) and ammonia ($NH_3$) are not considered as reactive nitrogen compounds (Seinfeld and Pandis, 1998; Roberts, 1995).

The most important molecule in atmospheric chemistry is $NO_x$ and its emissions are mainly from combustion of fossil fuels in transportation, power plants and industrial sources. $HNO_3$ is the major oxidation product of $NO_x$ in the atmosphere and is rapidly deposited on water surfaces because of its extreme water solubility. In urban locations, where the local NO sources are typically large, NO and $NO_2$ are probably the dominant constituents of the $NO_y$. The proportion of $HNO_3$, PAN and other oxides of nitrogen to $NO_y$ is believed to be relatively small in urban areas. In contrast, the proportion of $NO_z$ to $NO_y$ can be substantial in rural and remote locations.

The measurement of reactive nitrogen compounds provides an important means of following the chemistry of the atmosphere. The concentrations of individual nitrogen species relative to $NO_y$ provide a useful way to assess the importance of each species and the interconversion of one species to another. For completeness, a schematic representation of the $NO_y$ chemistry pertaining to the troposphere is given in Figure 1.6 (Seinfeld and Pandis, 1998).

*Figure 1.6 Schematic of* $NO_y$ *chemistry*

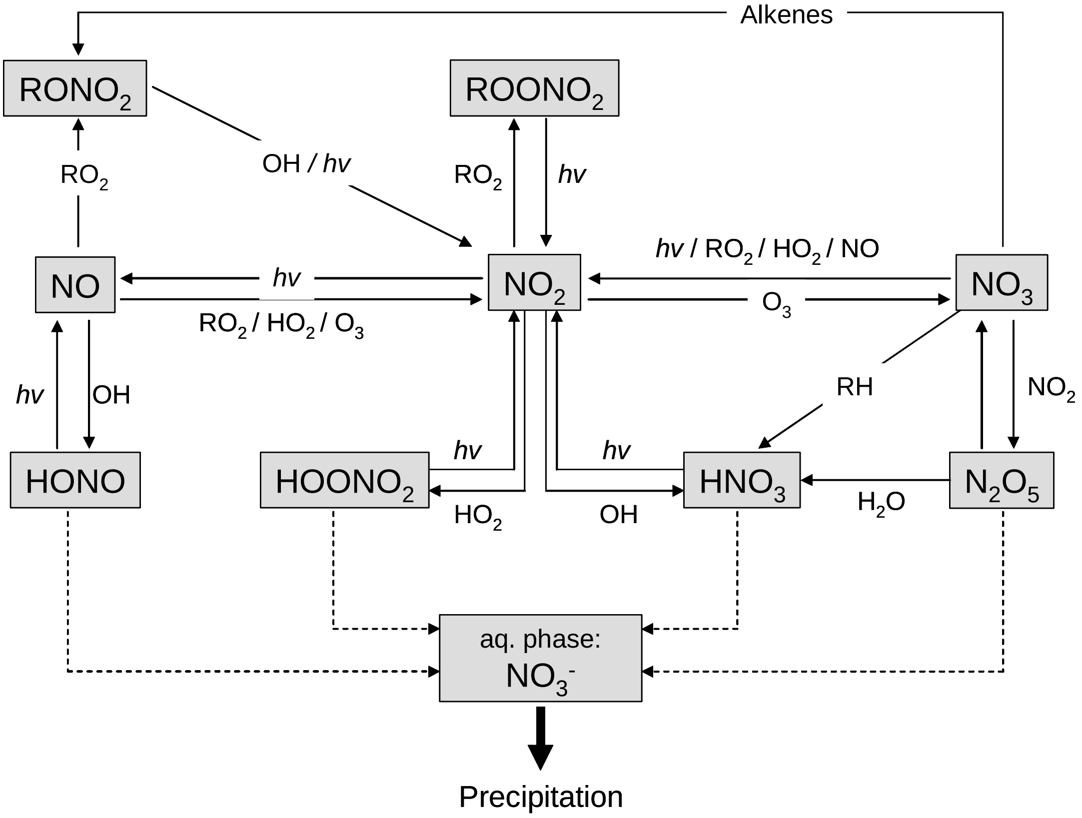

(Sources: Seinfeld and Pandis, 1998)

## 1.9 Objectives of this Thesis

This thesis is aimed at filling our knowledge gap on the sources and formation of ground-level $O_3$ in HK. Understanding of the $O_3$-$NO_x$-VOC chemistry and the sensitivity for different $O_3$ precursors in controlling $O_3$ formation in HK are also the key objectives of this thesis. As a corollary, measurement data of different sites in HK and the PRD are analyzed with the assistance of various statistical techniques like principal component analysis and the photochemical box model. The scientific findings of this thesis are anticipated to assist in the policy formulation in reducing photochemical pollution in the regions of HK and the PRD.

This thesis consists of nine chapters which are outlined below:

**Chapter 1** (this chapter) sets out the $O_3$ problems in HK, summarizes the background information and presents the objectives of this thesis..

**Chapter 2** outlines the statistical, mathematical and modelling methods to be applied to the data analysis in this thesis.

**Chapter 3** lists the data sets to be analyzed in this thesis. It also provides the background information of all the measurement sites and presents the respective measurement techniques and instrumental details.

**Chapter 4** discusses our work on the study of local and regional influence of $O_3$ to HK (So and Wang, 2003).

**Chapters 5 and 6** present our characterization of VOC in HK from different areas of spatial-temporal variations, source-receptor relationship and photochemical reactivity. Such findings provide important information about the VOC pattern and help understand the formation of $O_3$ in HK (So and Wang, 2004; Guo et al., 2007).

**Chapter 7** quantifies the roles of different $O_3$ precursors in the formation of $O_3$ at sites in HK and the PRD, using measurement indicators and modelling tools. Measurement data and model results will be used to highlight the $O_3$-$NO_x$-VOC chemistry and elevate the sensitivity for different VOC in controlling $O_3$ formation. The overall findings identify the similarities and differences of VOC mix between two rural PRD sites, suggesting that different VOC reduction plans should be implemented in different PRD areas in order to attain the largest overall reduction in regional $O_3$ pollution.

**Chapter 8** makes further use of the photochemical box model to evaluate the sources of $O_3$ production (local production versus long-range transport) between the sites in HK and the PRD. Two cases of $O_3$ episodes will also be studied to infer the photochemistry and $O_3$ formation from the measurement data and modelling results. This highlights the variation of intermediates, partitioning of reactive nitrogen compounds, $O_3$ budget and production efficiency during the elevated $O_3$ days.

**Chapter 9** summarizes the results, presents the conclusions, addresses the significance of this thesis and provides recommendations on the future work.

# CHAPTER 2 METHODOLOGY

This thesis will make use of various statistical, mathematical and modelling methods for the analysis of the data sets. The temporal and spatial variation patterns of $O_3$, VOC and other trace gases will be studied in order to obtain the background information about the trace gases in HK. The chemical properties of the air masses concerned will be further examined by using their chemical ratios in accordance with their different properties in reactivity. Principal component analyses will be used to explain the sources of the pollutants and their relationship. Moreover, the reactivity of VOC will be compared to identify the VOC which play significant roles on $O_3$ formation at a site. In order to quantitatively evaluate the roles of VOC, NO and CO on $O_3$ formation, an observation-based model will be applied to our data set of VOC and trace gases to compare their relative roles on $O_3$ formation under various sites and conditions. Details of the above methods to be used for data analyses will be described in this chapter.

## 2.1 Analyses of Spatial and Temporal Variation

Spatial and temporal (seasonal and diurnal) variations of trace gases, VOC and their ratios will be analyzed in this thesis. The air pollutants levels at a site can be compared with measurements made at other locations to help study the chemical environment of the region. The spatial analysis of upwind, urban and downwind sites measurement can also help assess the transport of pollutants and sources characterization of different sites. Seasonal and long term trends analyses will provide a general picture of pollutants variation due to the change of land use and meteorological conditions. In addition, diurnal variation of atmospheric species gives an insight into the interplay of emission and chemical and physical processes operating on a diurnal cycle. The above analyses are aimed at enhancing our understanding of the chemistry and formation of $O_3$ at areas with different characteristics in HK.

## 2.2 Chemical Ratios Analysis

Elevated $O_3$ events tend to occur on calm days when there is a lack of a homogeneous regional wind, although it is often difficult to attribute an $O_3$ episode to a particular source region by using limited wind data alone. The analysis of chemical ratios rather than absolute levels is therefore an appropriate approach in the examination of chemical composition in different areas or scenarios like high $O_3$ cases. Various chemical ratios to be applied in this thesis are described below.

**(a) Ratios of $SO_2/NO_x$ and $CO/NO_x$ for Different Emission Patterns:** Analysis of chemical ratios of gaseous pollutants in such elevated $O_3$ cases can provide valuable and complementary information. This methodology is particularly useful for studying air pollution transport between HK and the nearby PRD areas because the emission pattern in HK is quite different from that in the surrounding mainland of Guangdong. For example, due to the use of low sulphur-content fuel and more efficient combustion technology in HK, the emission ratio of $SO_2$ and CO to $NO_x$ is much smaller in HK than in mainland cities. The measurement studies have indeed shown that the air mass from the mainland is laden with relatively abundant CO and $SO_2$ (Kok et al., 1997; Lind and Kok, 1999 and Wang et al., 2001b). Therefore, the measured $SO_2/NO_x$ and $CO/NO_x$ can help find out the possible source region/sector of a high-$O_3$ plume.

**(b) $O_3$+$NO_2$ for Total Ozone Potential:** According to *[Equation 1.3]*, the summation of $O_3$ and $NO_2$ gives the information of the total $O_3$ potential (TOP=$O_3$+$NO_2$) (Clapp and Jenkin, 2001). Assessment of this quantity with the level of $NO_x$ (i.e. ratio of TO to $NO_x$) provides insights into the atmospheric sources of TOP, particularly at urban locations with major vehicular emissions. With reference to the analysis in the UK (Clapp and Jenkin, 2001), for example, the level of TOP could be made up of $NO_x$-dependent and $NO_x$-independent contributions.

**(c) Ratio of VOC/$NO_x$ and $O_3/NO_y$ for $O_3$-$NO_x$-VOC chemistry:** Ratio of VOC/$NO_x$ is also a useful indicator for our analysis of $O_3$-$NO_x$-VOC chemistry. As discussed above, an area with a low ratio of VOC/$NO_x$ (i.e. 4) is generally VOC-limited whereas the ratio greater than 15 is considered as $NO_x$-limited. In a VOC-limited area, $O_3$ levels would respond more delicately to VOC emission controls while in a $NO_x$-limited area, $NO_x$ control measures are usually much more effective (NRC, 1991). The study of VOC to $NO_x$ ratios across the territory will enhance our understanding of the $O_3$-$NO_x$-VOC system in HK.

The formation of nitric acid ($HNO_3$) in *[Equation 1.12]* represents the major sink for odd hydrogen sources under the condition of high abundance of $NO_x$ in urban areas (with small VOC/$NO_x$ ratio). This regime is VOC-sensitive as the $O_3$ production rate decreases with the increase in $NO_x$. High afternoon value of $NO_y$ (>20 ppbv) is expected which can be explained in terms of VOC/$NO_x$ ratio if reactivity-weighted VOC remains relatively constant (Sillman, 1995). Small ratio of $O_3/NO_y$ (<6-8) is associated with the VOC-sensitive chemistry as $O_3$ and $NO_y$ are assumed to be proportional to $S_H$ and $S_N$, respectively, as explained in Section 1.1 (Sillman and He, 2002).

In contrast, under conditions of high abundances of $HO_x$ and low level of $NO_x$ (usually in rural / remote areas), the $O_3$ production rate increases approximately linearly with $NO_x$ and such $NO_x$-sensitive photochemical regime is dominated by *[Equations 1.13 and 1.14]*. A large (>10) VOC/$NO_x$ ratio, low afternoon value of $NO_y$ and high afternoon ratio of $O_3/NO_y$ are therefore expected.

**(d) Ratios of Hydrocarbons for Ages of Air Mass:** Ratios of different VOC are used as indicators of $O_3$ formation potential and tracers of urban emissions. Under the assumption that the ratio of the interested species in the emission is relatively constant throughout the day, the relative abundance of the more reactive (shorter lifetime) species should decrease with time during the daylight hours. Examples are alkenes and more reactive aromatic hydrocarbons such as toluene. In contrast, the relative abundance of less reactive (longer lifetime) species (e.g. alkanes and the less reactive aromatic hydrocarbons like benzene) will appear to increase. Therefore, ratios of more reactive to less reactive VOC can be used as indicators of the relative changes in species composition and age. Comparison of the ratios among sites can be made to estimate the relative age of air parcels and help provide evidence of transport. Moreover, this ratio analysis can indicate whether the site is dominantly affected by fresh local emission or aged regional source. Ratios including xylenes to benzene (Sin et al., 2000), toluene to benzene (Liu et al. 2000) and propane to propene (Boudries et al., 1994) are often used for the above analysis of air mass ages. In addition, ratio of isomers like *m*, *p*-xylenes to ethylbenzene (Nelson and Quigley, 1983) and *i*-butane to *n*-butane (Jobson et al., 1994) are also used to identify their photochemical reactivity among different sites. In this thesis, different ratios of VOC will be selected to evaluate the impact of air mass and chemistry of different species among the territory.

## 2.3 Principal Component Analysis

Principal component analysis (PCA) can be applied to an air data set to further understand the relationship of air pollutants and factors affecting their variations at each site. The principle of PCA is to transform the original set of variables into a smaller set of linear combinations that account for most of the variance of the original set. PCA compresses the system variance into the first few components. The first component accounts for the maximum possible variance in the data set and each succeeding component accounts for the maximum portion of the remaining variance (Liu et al., 1996). In general, varimax rotation is applied to the components to make the results clearer. Therefore, the major goals of PCA in $O_3$ and other air pollutants are: (1) to determine the dominant pollutant sources in different sampling sites; and (2) to examine the variation of $O_3$ with respect to the other pollutants (Buhr et al. 1995). Comparing the results of chemical ratios analysis, a clear picture of photochemical reactions of $O_3$ across the territory will be obtained. For the data set of VOC with several tens or more different parameters, PCA will be very useful in the data examination and significant in the evaluation of the major emission source(s) at the studied areas (Borbon et al., 2002). As a result, the number of principal component(s) extracted as well as the relationship between parameters within the components provides valuable information about the sources and chemistry of air pollutants concerned.

## 2.4 Photochemical Reactivity of VOC on Ozone Formation

VOC can be removed and transformed in the troposphere by photolysis and chemical reaction with OH radicals, $NO_3$ radicals and $O_3$. In addition, different VOC react at differing rates in the troposphere because of their differing rate constants for photolysis and reaction with OH radicals, and even $NO_3$ radicals and $O_3$. Therefore, it is not appropriate in our evaluation of VOC on $O_3$ formation if only their abundances are considered. In order to better estimate the contribution of different VOC species, we have to consider the atmospheric VOC concentration, its rate of reaction with OH (and $NO_3$

radicals and $O_3$), and the number of $O_3$ molecules produced each time the species is oxidized. Apart from the study of VOC concentration, therefore, this research will also evaluate the roles of various $O_3$ precursors by calculating the product of VOC concentrations and their OH rate constants (propene-equivalent concentration) and the $O_3$-forming capability of the VOC using the Maximum Incremental Reactivity (MIR) coefficient.

**(a) OH Reactivity (Propene-Equivalent Concentration):** To account for the combined effect of OH reactivity and concentration, Chameides et al. (1992) defined a propene-equivalent concentration, PE(j), for each hydrocarbon j. This equivalent concentration is given by *[Equation 2.1]*:

$$\mathrm{PE(j)} = \mathrm{Concentration(j)} \times \frac{k_{OH}(j)}{k_{OH}(C_3H_6)} \qquad \textit{[Equation 2.1]}$$

where Concentration(j) is the concentration of hydrocarbon j expressed in ppbC;

$k_{OH}$(j) is the rate constant for the reaction between hydrocarbon j and OH; and

$k_{OH}(C_3C_6)$ is the rate constant for the reaction between propene and OH.

Therefore, PE(j) is a measure of the concentration of hydrocarbon j on an OH-reactivity-based scale normalized to the reactivity of propene. Since hydrocarbon oxidation is usually initiated by a reaction with OH, the PE provides an estimate of the relative contribution made by each hydrocarbon species to the flux of organic carbon being oxidized in the area. Literally, it is the concentration of propene required to yield a carbon oxidation rate equal to that of hydrocarbon j (NRC, 1991; Seinfeld and Pandis, 1998).

**(b) Ozone-forming Potential (Maximum Incremental Reactivity):** For the estimation of $O_3$ formation, the product of the VOC concentration and the Maximum Incremental Reactivity (MIR) coefficient (dimensionless, gram of $O_3$ produced per gram of hydrocarbon j) *[Equation 2.2]* can also be used to indicate how much the VOC may contribute to $O_3$ formation in the air mass (Carter, 1994):

$$O_3 \text{ formation (j)} = \text{Concentration(j)} * \text{MIR coefficient} \qquad \textit{[Equation 2.2]}$$

Whenever possible, the OH reaction rate constants ($k_{OH}$) and MIR coefficients used in this study are taken from Atkinson (1994) and Carter (1994) respectively. In cases of coelution, reaction rates as well as MIR coefficients will be calculated as an average value from the corresponding individual reaction rates of hydrocarbons.

In short, comparison of different parameters like PE, $O_3$ formation as well as concentration of VOC at different sites is helpful to better understand the photochemical $O_3$ reactivity in the territory from different perspectives.

## 2.5 Observation-based Model

**(a) Emission- versus Observation-based Models:** In order to estimate the effectiveness of $O_3$ reduction under the control of $NO_x$ and VOC, modelling tools have been playing a significant role in this area. Traditionally, the design of smog-control strategies has depended upon the use of emission-based models (EBMs). However, EBMs require the use of accurate emission data which is very challenging in developing countries because they either lack the emission data or have difficulty to update the database in pace with their rapid development. For example, underestimation of China's emission inventory had been reported and the accuracy of the EBM's results were therefore adversely affected (Wang et al., 2004; Lam et al., 2005). By comparison, application of measurement parameters and observation-based models can provide an initial insight into the $O_3$ precursors on photochemical $O_3$ formation without using challenging emission data (Cardelino and Chameides, 1995; Sillman, 1995). Such a relatively easy approach can effectively assist the policy makers to address the $O_3$ problem. In this connection, more empirical or observation-based approaches have been developed to provide an alternate and complimentary method for assessing $O_3$ precursor relationships in areas (Hidy, 2000). One such alternate approach is the observation-based model (OBM) developed by Cardelino and Chameides (1995).

The OBM uses measurements of ambient concentrations of $O_3$ and its precursors along with appropriate analytical techniques and photochemical algorithms to evaluate the accuracy of existing emissions inventories and for assessing the relative benefits of various proposed emission control strategies. For example, OBM can be used to estimate the relative efficacy of $NO_x$ and VOC emissions for mitigating photochemical smog. For any given VOC-control strategy, OBM can help assess the relative benefits of strategies that target specific individual components and/or source sectors (e.g. mobile, stationary, natural sources). Since OBM neither uses emission inventories nor requires the simulation of boundary layer dynamics, it avoids some of the uncertainties inherent in EBM and thus provides a useful independent verification on the results obtained using EBM. On the other hand, because OBM is diagnostic rather than prognostic, it cannot be used in a predictive mode to estimate exactly how much emission reduction is needed to reduce $O_3$ concentrations. For this reason, OBM should be viewed as a complement to, rather than a substitute for, EBM.

**(b) Background of the OBM:** Details of the OBM can be found in the previous work of Cardelino and Chameides (1995). Briefly, the OBM uses measurements of ambient concentrations of $O_3$ and its precursors like NO, CO and VOC along with an algorithm for simulating the photochemical production and destruction of $O_3$. The major goal of the model is to assess the sensitivity of net $O_3$ production in an area to changes in the emissions of NO, CO as well as individual and various groupings of VOC without the use of emission inventories and simulation of boundary layer dynamics as in emission-based model (Cardelino and Chameides, 1995 and 2000).

The OBM is a zero dimension time-dependent numerical model originally developed by Cardelino and Chameides (1995), using the Carbon Bond Chemical Mechanism (Version IV) (CBM-IV). The CBM-IV is a lumped structure chemical mechanism in which organics are grouped according to bond type (Gery et al., 1989). This mechanism is actually a hybrid of explicit chemistry, surrogate approximations, and lumped/generalized chemistry designed to simulate the broad features of urban smog and the regional $O_3$ formation.

The CBM-IV mechanism (Gery et. al., 1989) consists of 33 chemical species and 81 chemical reactions. These 33 compounds include the odd-oxygen species (O, $O(^1D)$, and $O_3$); the odd-hydrogen species (OH, $HO_2$, and $H_2O_2$); the odd-nitrogen species (NO, $NO_2$, $NO_3$, $N_2O_5$, $HNO_2$, $HNO_3$, and $HO_2NO_2$); CO and water vapour ($H_2O$); and 18 functional groups. These functional groups are designed to represent two kinds of hydrocarbon in the atmosphere.

Measured hydrocarbon species from both anthropogenic and natural sources are grouped into nine functional groups as ETH, FORM, PAR, OLE, ALD2, TOL, XYL, ISOP and NR. Table 2.1 shows the carbon number of carbon-bond groups for each primary functional group. ETH represents ETHene ($CH_2=CH_2$). FORM represents FORMaldehyde ($CH_2=O$). PAR is used to represent the carbon-carbon single bond (i.e., PARffinic bond) of the alkane. OLE represents the fast reacting double bond (i.e., OLEfinic bond) of the alkenes. ALD2 represents the high molecular weight aldehydes (RCHO, R>H). Aromatic HCs are represented by TOL and XYL. TOL represents the monoalkylbenzenes including TOLuene, and XYL represents the di- and trialkylbenzenes including the XYLenes. ISOP represents ISOPrene, NR represents the non-reactive part of different molecular species such as benzene, ethane, and ethyne.

After the concentrations of $O_3$, NO, CO and nine measured hydrocarbon functional groups are specified as a function of time, non-measured species are calculated by the model for determining the net $O_3$ production. The net $O_3$-forming potential at site S ($P^S_{O_3-NO}$) can be easily determined by integrating net amount of $O_3$ formed and NO consumed over a 12-hour period from Local Standard Time (LST) 0700 to 1900.

*Table 2.1 Carbon Number of Carbon-Bond Groups for Primary Species under CBM-IV*

| Carbon-Bond Group | Carbon Number (carbon atoms per molecule) |
|---|---|
| PAR | 1 |
| ETH | 2 |
| OLE | 2 |
| TOL | 7 |
| XYL | 8 |
| FORM | 1 |
| ALD2 | 2 |
| ISOP | 5 |
| NR | 1 |

**(c) Relative Incremental Reactivity (RIR):** Following Carter and Atkinson (1989), the incremental reactivity (IR) of precursor X at site S is defined as:

$$\mathrm{IR}^{\mathrm{S}}(\mathrm{X}) = \frac{\mathrm{P}^{\mathrm{S}}_{\mathrm{O_3-NO}}(\mathrm{X}) - \mathrm{P}^{\mathrm{S}}_{\mathrm{O_3-NO}}(\mathrm{X}-\Delta\mathrm{X})}{\Delta\mathrm{S}(\mathrm{X})}$$ *[Equation 2.3]*

where X represent a group of or specific hydrocarbon, NO or CO;

S(X) is the integrated amount of species X emitted or transported to the measurement site that results in the concentration of X at the site; and

ΔX is the change in the concentration of X caused by a hypothetical change in S(X), ΔS(X).

For example, the functions $IR^S(HC)$, $IR^S(NO)$, $IR^S(CO)$ represent an estimate of the integrated amount of $O_3$ photochemically produced at site S over the time period per hydrocarbon molecule, NO molecule and CO molecule, respectively. While the IR function gives an estimate of the absolute amount of $O_3$ produced per hydrocarbon, NO or CO molecule. The relative incremental reactivity, $\mathrm{RIR}^{\mathrm{S}}(\mathrm{X})$ is the percentage decrease in $O_3$ production at site S per percentage decrease in the concentration of a given precursor compound or class of compounds X at site S:

$$\mathrm{RIR}^{S}(X) = \frac{\dfrac{P^{S}_{O_3-NO}(X) - P^{S}_{O_3-NO}(X-\Delta X)}{P^{S}_{O_3-NO}(X)}}{\dfrac{\Delta S(X)}{S(X)}} \qquad \textit{[Equation 2.4]}$$

In other words, the sensitivity of each given parameter ($O_3$ precursor) at site S can be assessed by evaluating the respective RIR value, giving a relative measure of the effectiveness of reducing the emissions of one compound or group of compounds on the reduction of $O_3$ production. For example, if RIR(VOC) is calculated to be 1, it suggests that for each percent reduction in VOC emissions, a 1% reduction of $O_3$ production would result. If the RIR(NO) is calculated to be -1, this result estimates a 1% increase of $O_3$ production under each percent reduction in NO emissions. Therefore, the higher the RIR value, the more effective in controlling $O_3$ under the reduction of such precursor. In contrast, a negative RIR value of a precursor indicates the control of such precursor will however enhance the $O_3$ production.

**(d) Sensitivity to ΔS:** Because of the non-linear nature of the $O_3$ chemistry, RIR functions calculated by the OBM may be sensitive to the change of ΔS. Therefore, Cardelino and Chameides (1995) conducted a series of sensitivity test to ΔS reductions from 5 to 40%; results of which are given in Figure 2.1. The findings indicated that the variability of RIR under different ΔS was small and the relative importance of each precursor group was not affected. Therefore, a value of 10% (of ΔS) as the percent change in precursor source was adopted to compute the RIR.

*Figure 2.1 Area-averaged RIR calculated from the multiple day analysis dataset in Atlanta for nitric oxide (NO), anthropogenic hydrocarbons (AHC), natural hydrocarbons (NHC), and carbon monoxide (CO) as functions of the percent change in precursor source.*

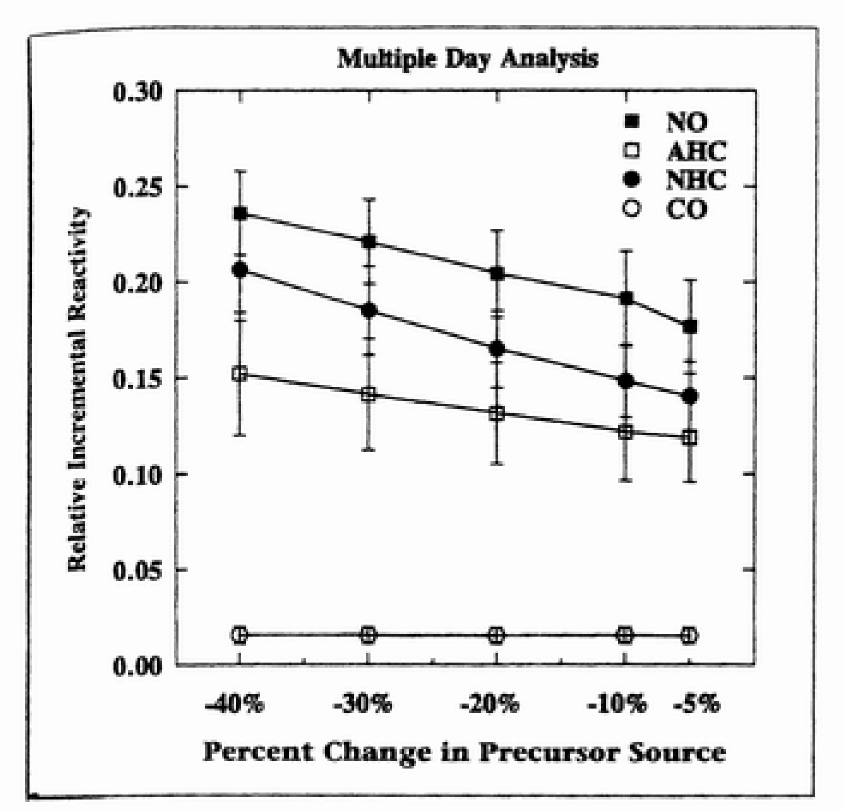

(Source: Cardelino and Chameides,1995)

**(e) Treatment of Entrainment, Mixing Height and Deposition in the OBM:** Several assumptions are made in the operation of the OBM and one of the most critical assumptions is that the horizontal transport is neglected in solving for the concentrations of the non-measured species.

The entrainment of air pollutants aloft is calculated from the diurnal variation of mixing height following the method described for the OZIPM4 model (Hugo and Grey, 1988). The mixing height was estimated based on the principle that heat transferred from the surface to the atmosphere results in convection, vigorous vertical mixing, and establishment of a dry-adiabatic lapse rate (Holzworth, 1967). Here, upper air soundings and hourly temperature were used to compute morning and afternoon mixing heights. The upper air soundings are reported by National Climate Data Center (NCDC) and available at the NOAA website (http://raob.fsl.noaa.gov/). The approach of Holzworth (1967) was followed with the exception that 2°C instead of 5°C was used to account for the temperature difference between rural and urban environments and for some initial surface heating just after sunrise while calculating the morning mixing height, since HK has a latitude of 22.32°N and the daily temperature difference between different areas is probably not as much as that at mid-latitudes. The hourly mixing height profiles were obtained by interpolating between the morning and afternoon mixing heights, considering that the mixing height increases rapidly after sunrise and slowly in early afternoon until it reaches the afternoon mixing height.

The deposition rate is a function of deposition velocity and the height of mixing layer. Therefore, the rates of change of the pollutants in the model due to deposition process, $(dc_i/dt)_{Deposition}$, can be expressed as:

$$(dc_i/dt)_{Deposition} = V_d * C_i / H(t) * 0.6 \qquad \textit{[Equation 2.5]}$$

where $V_d$ is the deposition velocity in units of cm/s, which is determined by surface type and the individual species' resistance to surface uptake. In general, $NO_x$, $HNO_3$, PAN, $H_2O_2$, and $O_3$ have high deposition rates (Liu et al., 1983; Sillman et al., 1993), whereas organic compounds have very low deposition rates. H(t) is the height of the mixing layer (m) at time t, and 0.6 is the conversion from cm/s to m/min (Hogo and Gery., 1988).

**(f) Applications of the OBM:** In this thesis, the RIR of $O_3$ precursor or groups of compounds at a site will be estimated to determine the sensitivity of the $O_3$ photochemical production at sites in HK and the PRD subject to changes in precursor concentrations. The RIR values will be calculated by using a 10% reduction in $\Delta S$, which is following the practice of Cardelino and Chameides (1995). Such information can help evaluate the roles of different $O_3$ precursors on photochemical $O_3$ production. In addition to the calculation of RIR, the OBM will also be used to estimate the sources of $O_3$ pollution (local production versus regional transport) and get insights into the variation of non-measured intermediates, partitioning of reactive nitrogen compounds, $O_3$ budget and production efficiency during the elevated $O_3$ days.

The instantaneous net (production – loss) $O_3$ production rates will be calculated by the OBM and compared with the observed rate.  The observed rate of change of $O_3$ ($dO_3/dt$) is defined by a finite difference formula *[Equation 2.6]* as defined by Kleinman et al. (1994).  For hour = n,

$$\frac{dO_3}{dt} = \frac{O_3(n+1) - O_3(n-1)}{2} \qquad \textit{[Equation 2.6]}$$

The differences between calculated and predicated rates of change of $O_3$ will allow us to understand the combined effects of vertical motions, deposition and transport of pollution to the site (Kleinman et al., 1995).

# CHAPTER 3 DATA USED IN THIS THESIS AND EXPERIMENTAL DETAILS FOR DATA

This chapter summarizes the data set used in this thesis and describes the experimental details including sites environment and instrumental methods for these data.

## 3.1 Summary of Data Sets used in this Thesis

Table 3.1 summarizes the different data sets which are studied in this thesis. Trace gases of $O_3$; CO; NO/$NO_x$/$NO_y$; $SO_2$; RSP and VOC, coupled with respective meteorological data of both HK and PRD sites are analyzed. They are used to provide information about the local and regional influences on $O_3$ formation; on spatial, temporal and emission patterns of $O_3$ precursors, and how they contributed to the photochemical $O_3$ formation in HK and PRD sites.

## 3.2 Environment of Hong Kong and Pearl River Delta Region

HK is a small territory with a land area of about 1095 $km^2$ located on the eastern side of the Pearl Estuary on the South China coast. The whole territory consists of HK Island, Kowloon Peninsula, the New Territories, Lantau Island, and a number of outlying islands (see Figure 3.1). The territory has a complex terrain, with hilly areas making up about 70% of the total land. The highest peak is Tai Mo Shan (957 m above the sea level). The climate of HK is governed by the Asian monsoons. Prevailing synoptic winds arriving in HK are from the north and northeast in winter, east in spring and autumn, and south and southwest during the summer months (Chiu and So, 1986).

*Figure 3.1 Location of six EPD's air quality monitoring stations, two HKPU's air quality monitoring stations and HKO's meteorological station.*

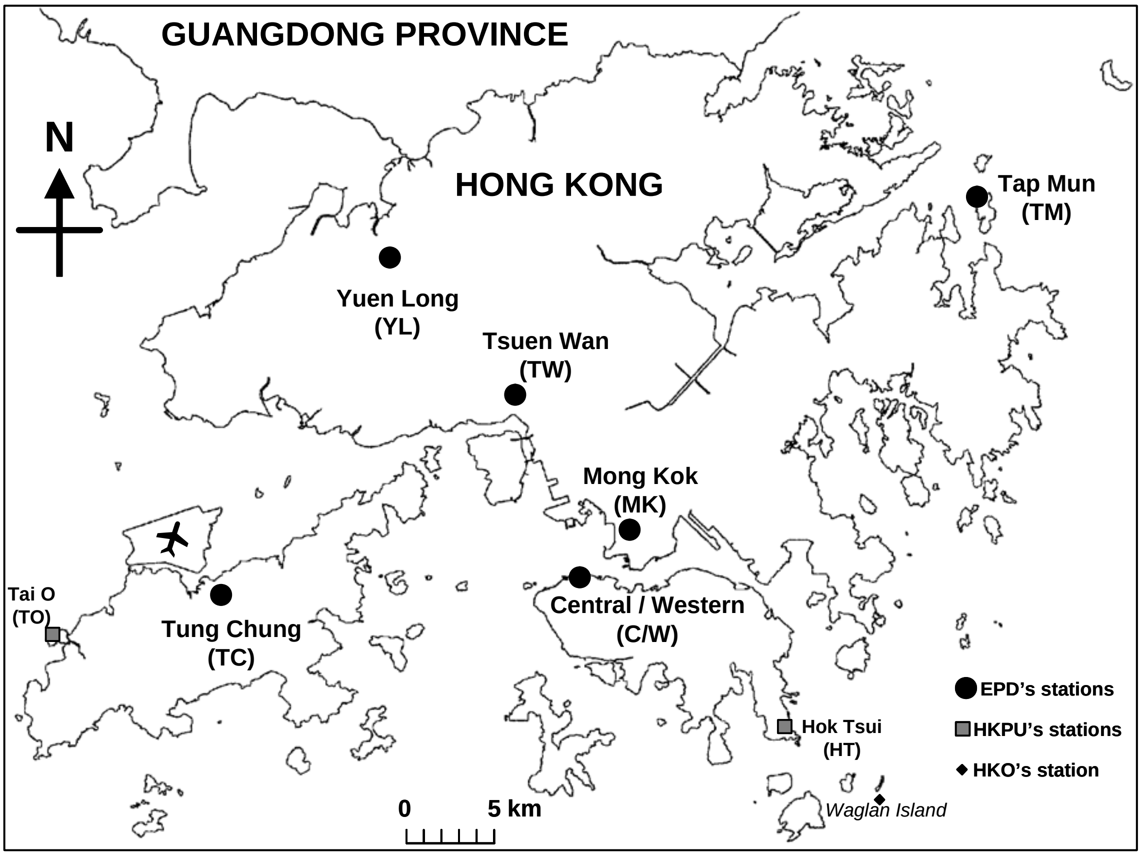

*Table 3.1 Summary of data sets used in this thesis*

| **Chapter** | **Parameters** | **Types of Sites** | **Period** | **Study Objectives** |
|---|---|---|---|---|
| 4 | $O_3$; CO; $NO_x$; $SO_2$; RSP | 3 HK sites: Industrial (TW); New Town (TC); Rural (TM) | June 1999 to May 2000 | Local and regional influence on $O_3$ formation |
| 5 | $C_3$ to $C_{12}$ hydrocarbons | 4 HK sites: Industrial (TW); Residential (C/W); Rural (HT); Roadside (MK) | November 2000 to October 2001 | VOC seasonal and temporal patterns, photochemical ages of air mass and VOC reactivity on $O_3$ formation |
| 6 | $C_1$ to $C_8$ hydrocarbons | 4 HK sites: Residential (C/W); Rural (TM); New Town (TC and YL) | September 2002 to August 2003 | |
| 7 and 8 | $O_3$; CO; NO; $NO_y$;<br>$C_1$ to $C_{10}$ hydrocarbons | HK site: Coastal Rural (TO)<br>PRD site: Inland Rural (WQS) | September to November 2002<br>April to June 2004 | Roles of different $O_3$ precursors and photochemistry on $O_3$ production |

As of 2004, the population of HK was about 6.8 million and was concentrated on the two sides of Victoria Harbour and in new towns of the New Territories. Power stations and the airport are located on the western side of HK. In contrast, northeast of HK are mostly rural areas.

The PRD is situated on the South China Coast and is home to several large Chinese cities, including HK. This region has experienced astonishing economic and industrial developments in the past two decades. Shenzhen (population: 4 million) and Guangzhou (population: 10 million) are the other two large population centres in the region (Wang and Kwok, 2003). There are also a number of mid-sized cites in the region with populations ranging from 280,000 to 430,000. The region's power plants, airports, and seaports are mainly located along the two sides of the Pearl Estuary (Wang et al., 2003b).

## 3.3 Site Characteristics

### *3.3.1 EPD's Stations*

In this thesis, the measurement data from six EPD's air quality monitoring stations will be analyzed; five of them are ambient air quality monitoring stations and one is a roadside air quality monitoring station. The five ambient stations, in Central/Western (C/W), Tsuen Wan (TW), Yuen Long (YL), Tung Chung (TC) and Tap Mun (TM), are located on the roof-tops of buildings with an elevation ranging from 11 to 21 m above the ground level (EPD, 2000). C/W is an urban residential area on HK Island. TW is a mixed residential / commercial / industrial area. YL is in the northwestern new town which is about 15 km southwest of Shenzhen, a large and developing industrial city in Guangdong Province. There is also an industrial estate within 1 km to the northeast of the YL site. TC is in the southwestern new town in proximity to the Chek Lap Kok Airport and TM is a rural area in the northeastern part of HK.

The roadside site is in Mong Kok (MK) which is a mixed commercial / residential area with heavy traffic and is surrounded by some moderately tall buildings. Figure 3.1 presents the spatial distribution and Table 3.2 shows the area characteristics, sampling height above ground and sea level of the six EPD's stations.

*Table 3.2 Site information of six EPD's air quality monitoring stations*

| **Air Quality Monitoring Station** | **Area Type** | **Sampling Height (above sea level)** | **Above Ground** |
|---|---|---|---|
| Central/Western (C/W) | Urban: Residential | 78 m | 18 m |
| Tsuen Wan (TW) | Urban: Mixed residential / commercial / industrial | 21 m | 17 m |
| Tung Chung (TC) | New Town: Residential | 28 m | 21 m |
| Tap Mun (TM) | Background: Rural | 26 m | 11 m |
| Mong Kok (MK) | Urban Roadside: Mixed residential / commercial area surrounded by some moderately tall buildings | 8.5 m | 3 m |
| Yuen Long (YL) | New Town: Residential | 31 m | 25 m |

### *3.3.2 HKPU's Stations*

The measurements reported in this study were also made at the two atmospheric research stations established by the Hong Kong Polytechnic University (HKPU) at Hok Tsui (HT) and Tai O (TO) in HK and another monitoring site at Wan Qing Sha (WQS) in Guangdong Province. Figure 3.2 shows the locations of the three sites and details of the sites characteristics are described below.

*Figure 3.2 Map of the PRD showing Tai O, Hok Tsui and Wan Qing Sha.*

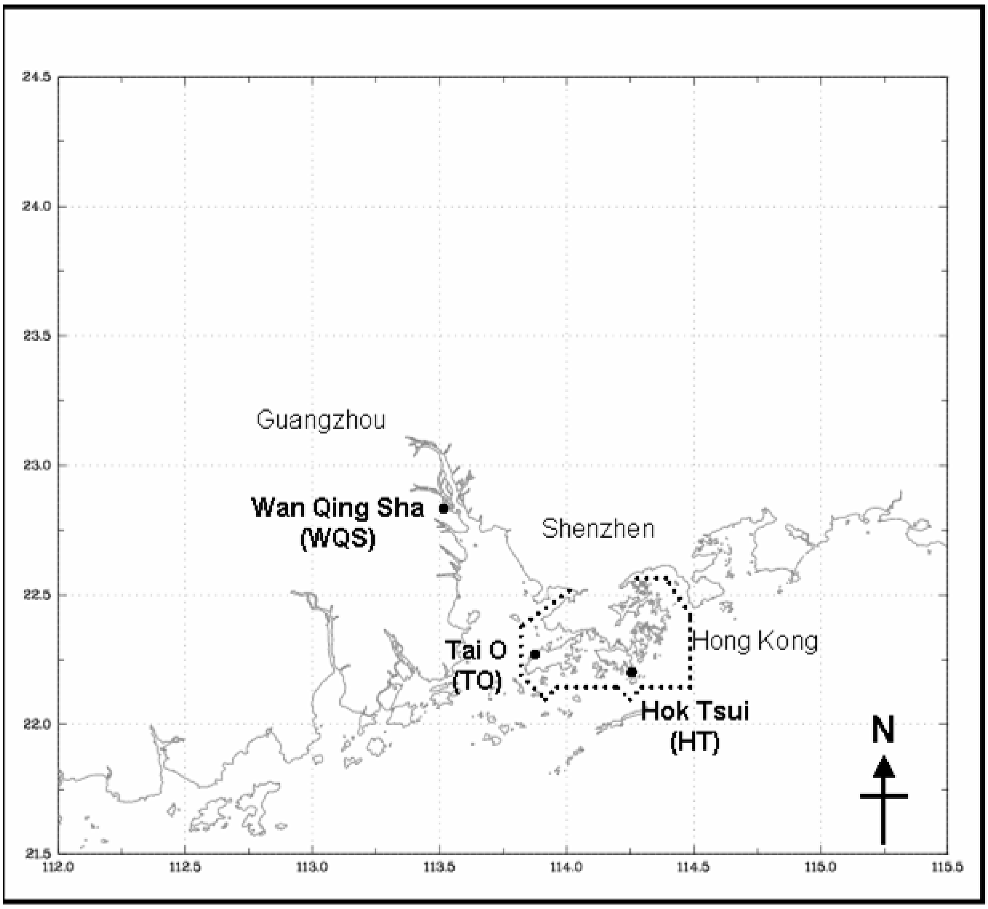

The HT site is on the southeastern tip of HK Island and the air monitoring station is 60 m above the sea level with 240° of ocean view from northeast to southwest. In the vicinity of the station, there are relatively few anthropogenic activities. Emissions from ships in the nearby ocean may occasionally affect the measured pollutant levels (Wang et al., 1997, 1998 and 2001b).

The TO site is a sparsely populated coastal area on Lantau Island, situated roughly in the north-south centreline of the Pearl River estuary with HK’s urban centre 32 km to the east and Macau/Zhuhai, China, to the west at about the same distance. The study site is located on a hill 80 m above sea level, overlooking the Pearl River estuary to the west and north and the South China Sea to the south. Local emissions from TO are small because of the sparse population and the light traffic in the area. Major sources of emissions from traffic and power plants in the region are located in the east, north, and southwest directions (Wang and Kwok, 2003; Wang et al., 2003b).

WQS is a rural / inland site situated at the mouth of Pearl River Estuary (see Figure 3.2), with Panyu urban centre 30 km to the northwest, Dongguan city 40 km to the northeast, and Zhuhai about 50 km to the south. The measurement was conducted on a roof-top of a secondary school, which is about 22 m above the ground level. The pollution from local emissions is not significant because of the sparse population and light traffic there. This site is at the geographical centre in the PRD region and the measurement data can therefore represent the regional pollution in the inland of the PRD region.

## 3.4 Measurement Techniques

### *3.4.1 Trace Gases*

For the EPD's stations, $O_3$ was monitored with a commercial UV photometric analyzer (Thermo Environmental Instruments, Inc. (TEI), model 49 / Advanced Pollution Instrumentation (API), model 400); $NO_x$ was measured by a commercial chemiluminescence instrument (Monitor Laboratories Inc. (ML), model 8840 / API, model 200A). $SO_2$ was monitored using UV fluorescence technique (ML, model 8850 / TEL, model 43A), and CO was detected with a non-dispersive infra-red absorption with gas filter correlation (TEL, model 48C). RSP was measured using the principle of oscillating microbalance (Rupprecht & Patashnick (R&P), model TEOM Series 1400a-AB-PM10). All the instruments were regularly calibrated, tested, and audited by standards with known traceability (EPD, 2000).

High resolution measurement data were collected from the HKPU's sites in HT, TO and WQS and brief descriptions of the respective measurement techniques are given below.

$O_3$ was measured using a commercial UV photometric instrument (TEI, model 49), which had a detection limit of 2 ppbv and a 2-sigma (2-$\sigma$) precision of 2 ppbv for a 2-minute average.

$SO_2$ was measured by pulsed UV fluorescence (TEI, model 43S), with a detection limit of 0.06 ppbv and 2-$\sigma$ precision of 3% for ambient levels of 10 ppbv (2-minute average). The uncertainty was estimated to be about 9%.

CO was measured with a gas filter correlation, non-dispersive infrared analyzer (Advanced Pollution Instrumentation, Inc., model 300) with a heated catalytic scrubber (as purchased) to convert CO to carbon dioxide ($CO_2$) for baseline determination.  Tests showed that nearly 100% of the water vapour was able to pass through the converter, although it could take a few minutes for the signal to reach equilibrium.  In our study zeroing was conducted every two hours, each lasting 12 minutes. The 2-minute data at the end of each zeroing were taken as the baseline. The detection limit was 30 ppbv for a 2-minute average. The 2-$\sigma$ precision was about 1% for a level of 500 ppbv (2-minute average) and the overall uncertainty was estimated to be 10%.

NO and $NO_y$ were detected with a modified commercial molybdenum oxide (MoO) / chemiluminescence analyzer (TEI, model 42S).  The modification was made to relocate the internal catalytic converter to a separate enclosure which was placed outside the laboratory near the sample inlet.  This was done in order to reduce the loss of $NO_y$ in the sample line prior to the catalytic converter.  The enclosure also housed a temperature controller (for the MoO catalyst) and solenoid valves for zero and span tests. $NO_y$ was converted to NO on the surface of MoO, which was maintained at 350°C, with NO subsequently measured by the chemiluminescent detector.  The instrument automatically switched among zero, NO and $NO_y$ modes.  A bypass pump was installed in the $NO_y$ line to maintain a flow of 1.5 litres per minute through the converter when the instrument was in NO mode.  The analyzer had a detection limit of 0.05 ppbv. The 2-$\sigma$ precision of this instrument was 4% (for NO = 10 ppbv) and the uncertainty was about 10%.

The analyzers were calibrated by injecting scrubbed ambient air (TEI, model 111) and a span gas mixture. A NIST-traceable standard (Scott-Marrin, Inc., California) containing 156.5 ppmv CO (± 2%), 15.64 ppmv $SO_2$ (± 2%), and 15.55 ppmv NO (± 2%) was diluted using a dynamic calibrator (Environics, Inc., model 6100). The $NO_y$ conversion efficiency on MoO was checked using a 5 ppm n-propyl nitrate (NPN) standard (Scott-Marrin, Inc., California), which was chosen as the surrogate for $NO_y$ (Jaffe et al., 1996). The zero and span were carried out every day in the early morning. Over the study period, the instrument sensitivity varied by less than 10%, and the conversion efficiency for NPN on the catalyst was 98% and remained so over the period. The conversion of $NO_2$ (generated by the gas phase titration method using the calibrator) was also tested manually and the efficiencies were 100%. A data logger (Environmental Systems Corporation, model 8816) was used to control the zero/span calibration and to collect 1-second data, which were averaged to 1-minute values.

In addition to the above chemical measurements, several meteorological parameters were measured at the sites. They include wind speed and direction, temperature, relative humidity, total ultraviolet radiation (TUV; 320-400 nm), and global solar radiation.

### *3.4.2 Volatile Organic Compounds*

For the VOC measurement at the EPD's stations (to be discussed in Chapter 5), air samples were collected by certified clean 6-L evacuated SUMMA® canisters with sampling system (Xontech Inc., model 910A) and the canister samples were sent to the HK Government Laboratory (GL) for analyses. A total of 143 $C_3$-$C_{12}$ VOC including 39 alkanes, 32 alkenes, 2 alkynes, 27 aromatics and 43 halocarbons in the air samples were determined by a technique of cryogenic preconcentration and gas chromatographic-mass spectrometric detection (Sin et al., 2001). The method detection limits and practical quantification limits were sensitive at 0.02 and 0.10 ppbv, respectively. For the VOC samples collected at four EPD's stations from September 2002 to August 2003 (to be discussed in Chapter 6), they were sent to the University of California at Irvine (UCI) for $C_1$ to $C_8$ analysis which will be described below.

VOC measurement was also conducted at TO and WQS, but the samples collection and analyzing method were different to those of the EPD's samples. Cleaned and evacuated 2-L electro-polished stainless steel canisters at the UCI were used to collect whole air samples. After collecting the air sample into the canister for about one minute, they were shipped to UCI for chemical analysis. The concentration of methane ($CH_4$) and $C_2$ to $C_8$ non-methane hydrocarbons (NMHC) in the canister samples were determined using a combination of gas chromatography with flame ionization detection and gas chromatography with electron capture detection and mass spectrometric detection techniques (Blake et al., 1994; Colman et al., 2001). The detection limits of $CH_4$ and $C_2$ to $C_{10}$ NMHC are 5 ppbv and 3 pptv, respectively. CO was also quantified from the canister samples by first reducing CO to $CH_4$ followed by gas chromatographic analyses with a flame ionization detection with a detection limit of 5 ppbv.

### *3.4.3 Meteorological Data*

In addition to the above chemical measurements, several meteorological parameters were measured at the HKPU's stations. They include wind speed and direction, temperature, relative humidity, total ultraviolet radiation (TUV; 320-400 nm), and global solar radiation. In addition, wind speed and direction measured by the Hong Kong Observatory (HKO) at Waglan Island is also used to present the corresponding seasonal patterns in HK. Waglan Island (see Figure 3.2) is about 6 km southeast of HT. The wind there is considered to be a better indication of the large-scale synoptic flow as the site is less affected by the hilly topography of HK.

# CHAPTER 4 GROUND-LEVEL OZONE STUDY IN HONG KONG DURING 1999/2000

Chapter 1 pointed out that the previous $O_3$ studies in HK were focused on the $O_3$ data in or before 1997. During the past few years, however, there has been a rapid economic development and significant change in land use in HK and in other cities of the PRD. The recent industrial developments in the region may have affected the $O_3$ levels on both local and regional scales. It is therefore of interest to have an updated analysis of the $O_3$ distribution. In addition, $O_3$ data from additional areas in HK have become available recently. In 1998 and 1999, two new air quality monitoring stations were established by the HKEPD, including one at an upwind northeastern rural site (TM) and another in the downwind southwestern new town (TC), respectively. This expanded network provides a more complete data set to allow a detailed examination of the spatial distribution of $O_3$. In this chapter, the $O_3$ data together with other major pollutants data recorded at three EPD's stations are presented. The three sites cover upwind rural (TM), urban (TW), and downwind suburban (TC) areas. The influence of local and regional emissions on $O_3$ variation is studied through analysis of chemical species ratios. PCA technique is also used to further elucidate the relationship of air pollutants and the factors affecting the variation of $O_3$ at each site. Finally, analysis of four high $O_3$ episodes in August and September 1999 can help understand $O_3$ formation and transport processes during the episodes. The results are significant and published in the Journal of Environmental Pollution titled “Local and Regional Influence on Ground-level Ozone Concentrations in Hong Kong” (So and Wang, 2003).

## 4.1 Spatial Distribution of Ozone and Other Pollutants

Table 4.1 shows the annual average values of the air pollutants ($O_3$, CO, $NO_x$, $SO_2$ and RSP) measured at the three sites during the study period (June 1999 to May 2000). As expected, the primary pollutants show the highest levels at the urban (TW) site and lowest in the upwind rural (TM) site. The opposite is true for the secondary pollutant $O_3$. Both primary and secondary pollutants in the suburban new town (TC) lie in the middle of the concentration ranges. The spatial patterns reflect the land use types and thus the emission characteristics around each site. TM is a rural area without major sources of anthropogenic emissions. As a result, the lowest levels of CO and $NO_x$ are observed with together the highest $O_3$ level in regionally polluted air mass. By comparison, TW is a populated urban area surrounded by mountains preventing the dispersion of local pollutants. The strong local emissions result in high levels of $NO_x$ which efficiently scavenge $O_3$ in regional air mass advected to the site. The new town TC in the southwest produces pollutant levels between the urban and rural areas with $O_3$ levels between those of the other two sites.

*Table 4.1 Annual averages of major air pollutants and respective chemical ratios at TM, TC and TW from June 1999 to May 2000*

| **Pollutant / Ratio** | **TM** | **TC** | **TW** |
|---|---|---|---|
| $O_3$ (ppbv) | 34 | 20 | 12 |
| $SO_2$ (ppbv) | 3 | 6 | 7 |
| $NO_x$ (ppbv) | 7 | 37 | 74 |
| CO (ppbv) | 491 | 598 | 861 |
| RSP (μg $m^{-3}$) | 41 | 50 | 53 |
| TOP (= $O_3$ + $NO_2$) (ppbv) | 40 | 45 | 44 |
| $[O_3]/[TO]$ (ppbv/ppbv) | 0.82 | 0.48 | 0.26 |
| $SO_2/NO_x$ (ppbv/ppbv) | 0.55 | 0.18 | 0.11 |
| $CO/NO_x$ (ppbv/ppbv) | 7.85 | 5.25 | 2.38 |

## 4.2 Temporal Variation of Ozone

The monthly variations of $O_3$ for the three sites are shown in Figure 4.1(a). For the rural TM, it is clear that a low value of about 17 ppbv is found in summer and high values of 30 to 45 ppbv are observed in the other three seasons. The range of maximum (March 2000) and minimum (July 1999) is 28 ppbv. The seasonal difference is not as large at the urban (TW) and suburban (TC) sites. The range of maximum and minimum monthly value for the TC and TW sites is 13 and 12 ppbv, respectively. The low summer $O_3$ level found in 1999-2000 is similar to the result reported by Wang et al. (2001b) for the 1996 data showing a trough in summer and a peak in autumn. Such a pattern is primarily due to the variations of prevailing wind direction in different seasons of a year. It is also attributable to southwesterly winds which bring in clean oceanic air and unstable rainy weather. It is interesting to see a new $O_3$ peak in spring from the recent data, with a value comparable to the autumn peak. It is possible that the spring peak is due to the transport of regional pollutants under the prevailing northeasterly winds.

It is well known that $O_3$ reacts quickly with NO following the reaction $O_3 + NO \rightarrow NO_2 + O_2$ *[Equation 1.3]*. The summation of $O_3$ and $NO_2$ gives the information on the total $O_3$ potential ($TOP=O_3+NO_2$). Assessment of this quantity provides insights into the chemistry of NO and $O_3$ in the three air sheds (Clapp and Jenkin, 2001). As shown in Table 4.1, the annual mean levels of TO for TM, TC and TW are 40, 45 and 44 ppbv respectively. The difference between the maximum (suburban TC) and minimum (rural TM) values of TOP is about 11%. The seasonal variations of TOP at the three sites are shown in Figure 4.1(b) indicating a similar seasonal pattern at each site. This result suggests that, on average, there is little production of $O_3$ as an air mass moves from northeast to southwest across HK. The slightly higher TOP levels at the urban and suburban sites may be attributed to the additional sources of $NO_2$ from vehicles and/or aircrafts.

The annually averaged diurnal $O_3$ variations at the three sites are shown in Figure 4.1(c). A diurnal pattern of $O_3$ is quite obvious, especially for the rural site TM. A daily low and a peak are found at LST 0700 and 1500, respectively. At the urban TW, there exists two peaks at LST 0300 and 1400 and the diurnal variation at this site is relatively smaller than those at the other two sites.

In general, $O_3$ reaches a daily peak in the afternoon because of the high solar radiation facilitating photochemical production of $O_3$ and downward mixing from the overlying air mass. An obvious peak is seen at the non-urban TM and TC. For the urban TW, the afternoon peak is relatively small and an additional peak in the morning is found. Such bimodal diurnal patterns have been observed in HK (Chan et al., 1998) and Taiwan (Liu et al., 1990). The pattern of two peaks or troughs is mainly related to the local traffic and industrial activities. At night, $O_3$ level approaches that of the background air when the local traffic and industrial activities are minimal. When the urban activities start in the morning (LST 0700-0900), $O_3$ gradually decreases and there is a trough because of the titration effect of the fresh vehicular emission (e.g. NO). With the sunlight and vertical mixing during daytime, the level of $O_3$ increases and reaches its maximum in the afternoon (LST 1300-1500).

*Figure 4.1* *Monthly averaged concentration of (a)* $O_3$*, (b) TOP (*$O_3 + NO_2$*) and (c) annual averaged diurnal* $O_3$ *variation measured at TM, TC and TW for June 1999 to May 2000.*

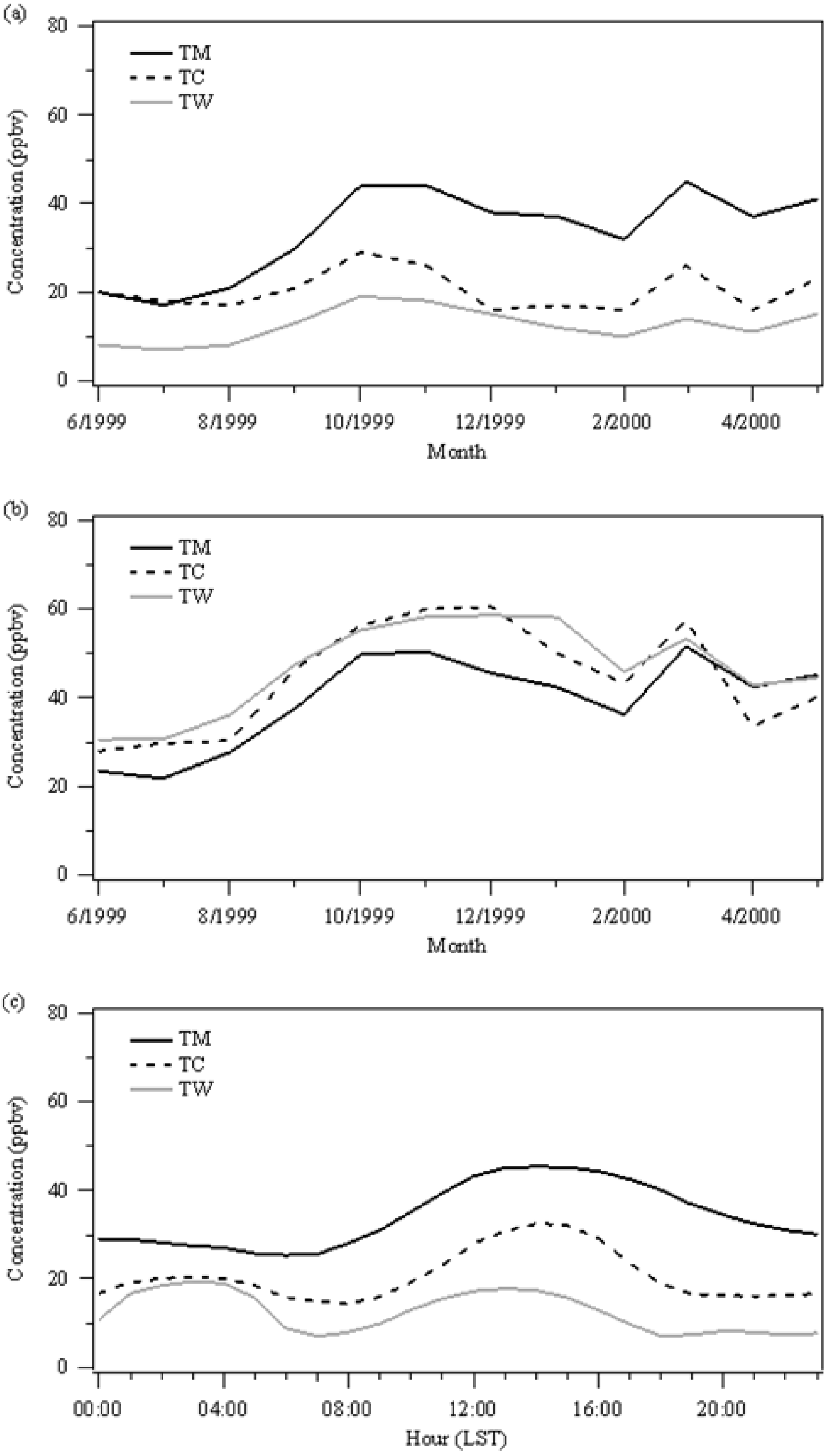

## 4.3 Chemical Ratio Analysis

Air chemistry data can provide useful information on the source(s) of pollutants measured at a site. In the present study, relevant chemical species ratios at each site can help us to understand air pollution transport between HK and the PRD region. Previous measurement studies have shown that air mass from the mainland is laden with relatively abundant CO and $SO_2$ (Kok et al., 1997; Lind and Kok, 1999; Wang et al., 2001b). For example, the emission ratios of $SO_2$ and CO to $NO_x$ is much smaller in HK than in mainland cities due to the use of low sulphur-content fuel and more efficient combustion technology in HK. According to the emission inventory, the ratio of $SO_2/NO_x$ is 0.4 (ppbv/ppbv) for HK (http://www.info.gov.hk/epd) and 1.4 for Guangdong Province (Streets and Waldhoff, 2000). In ambient air of urban areas, the ratio has been found to be 0.4 in Guangzhou (Zhang et al., 1998) and 0.1 in HK (EPD, 2000). The lower observed ratios in the urban areas can be attributable to the fact that the inventory-derived values have considered emissions from both area sources and power stations (normally at higher elevation) whereas the measurement at ground level is mainly affected by low-level sources. During our study period (June 1999 to May 2000), the $SO_2/NO_x$ ratios for TM, TC and TW are found to be 0.55, 0.18 and 0.11 respectively (see Table 4.1). The relatively high ratio at TM is consistent with the fact that TM is normally upwind of HK's urban centre, implying that the rural site is predominantly affected by air pollutants emitted from regional sources. The higher CO to $NO_x$ ratio (7.85, see Table 4.1) at TM provides further evidence for the influence of regional emissions. For suburban TC, the $SO_2$ to $NO_x$ ratio (0.18) is higher than the ambient HK ratio, which may be partly due to occasional influence of air mass from the PRD region. The ratio for TW (0.11) matches the HK's ambient ratio (0.11) highlighting that the site is heavily impacted by local emissions.

### 4.4 Principal Component Analysis

In this section, PCA is applied to the data set to further understand the relationship of air pollutants and factors affecting their variations at each site. Hourly data from June 1999 to May 2000 are subject to PCA using commercial software (SPSS for windows Release 9.0, 1999). Table 4.2 shows the factor loadings (after varimax rotation) for the three sites. For simplicity, only factors with eigenvalue larger than 1 and factor loading larger than 0.2 are shown in the table. In addition, the eigenvalue and its corresponding percentage of variance for each factor are provided. For the three sites, two factors are resolved among the pollutants but the composition of each factor is different among the sites. For the urban site TW, Factor 1 (with a higher eigenvalue and percentage of variance) is dominated by strong loadings of RSP and $NO_2$. The Factor 2 (with a lower eigenvalue and percentage of variance) is characterized by strong loadings of NO and $O_3$ but with negative correlation. The results highlight that TW is mainly affected by the local emissions of RSP and $NO_2$. The negative correlation between NO and $O_3$ suggests the $O_3$ level at TW is strongly influenced by local titration. Similar results are observed at the new town TC, but Factor 1 is also characterized with a strong loading of $SO_2$ and moderate loading of CO. The high loading of $SO_2$ may be due to the influences of $SO_2$ emissions from the airport activities, coal-fired power stations in the western sector and the possible influence of PRD emissions. For the rural site of TM, a different picture is obtained. Factor 1 is dominated by a strong positive correlation between $NO_x$ and $SO_2$, and Factor 2 is characterized by a significant positive correlation between RSP and $O_3$. Since there is no major anthropogenic source of emission at TM, the strong loading of $SO_2$ for Factor 1 suggests the influence of PRD region, which is consistent with the result from the chemical ratios analysis as discussed in Section 4.3. The positive relationship between $O_3$ and RSP at the rural site indicates that the regional chemical processes are responsible for the secondary pollutants like $O_3$ and RSP.

*Table 4.2 Factor loadings of concentrations of the different air pollutants at TM, TC and TW (Varimax rotated factor pattern and strong factor loadings are in bold)*

| **Pollutant** | **TM** | | **TC** | | **TW** | |
|---|---|---|---|---|---|---|
| | **Factor 1** | **Factor 2** | **Factor 1** | **Factor 2** | **Factor 1** | **Factor 2** |
| $O_3$ | -0.307 | **0.813** | | **-0.922** | 0.275 | **-0.882** |
| $SO_2$ | **0.753** | 0.415 | **0.828** | | 0.523 | 0.568 |
| $NO_2$ | **0.899** | | **0.843** | 0.273 | **0.822** | 0.277 |
| NO | **0.766** | -0.217 | 0.430 | **0.754** | 0.425 | **0.762** |
| CO | 0.238 | 0.582 | 0.759 | 0.201 | 0.674 | |
| RSP | | **0.889** | **0.923** | | **0.919** | |
| Eigen-value | 2.153 | 2.025 | 3.027 | 1.560 | 2.464 | 1.790 |
| % of Variance | 35.884 | 33.743 | 50.446 | 26.000 | 41.059 | 29.838 |

The above annual hourly data set was also divided into four seasons and separately analyzed by PCA. Similar factor loadings are obtained for all the three sites. When the data were further divided into morning and afternoon periods (LST 0700-1200 and 1300-1700), no obvious difference was found. Thus, the result of PCA analysis based on annual data set is generally applicable. Consistent with emission characteristics and land use types around each site, PCA results suggest that the variations of air pollutants at the urban TW site and, to a lesser degree, the suburban TC is dominated by local emission sources, while the rural TM site is primarily influenced by emissions and chemical processes occurring on a regional scale.

## 4.5 Analysis of Ozone Episodes

Here, high $O_3$ episodes are analyzed to show the meteorological and chemical conditions associated with elevated $O_3$ days. Figure 4.2 shows daily maximum 1-hour $O_3$ levels at the three sites over a one-year period from June 1999 to May 2000. It can be seen that a number of moderately high $O_3$ (hourly concentration > 80 ppbv) cases occurred at the rural and suburban sites. By comparison, $O_3$ levels at the urban TW remained low throughout the year. The HK Air Quality Objective for $O_3$ is 240 $\mu g/m^3$ (122 ppbv) over a 1-hour period. Table 4.3 shows the summary of the $O_3$ exceedences at the three sites during June 1999 to May 2000. The rural TM and suburban TC had four and five days of exceedences, respectively. Figure 4.2 shows that while low $O_3$ levels are generally found in summer months, some of the highest $O_3$ cases are observed in the same season. This is attributed to meteorological conditions in the subtropical part of East Asia. The normally low $O_3$ in summer is due to southeast summer monsoon which brings in clean oceanic air and rainy conditions. However, when a tropical cyclone is formed in the East China Sea at about 600-700 km east of HK, the descending of large-scale air mass is often found over HK, resulting in calm and stable conditions that are favourable to $O_3$ formation and build up.

*Figure 4.2 Daily maximum 1-hour $O_3$ at (a) TM, (b) TC and (c) TW from June 1999 to May 2000.*

(a)

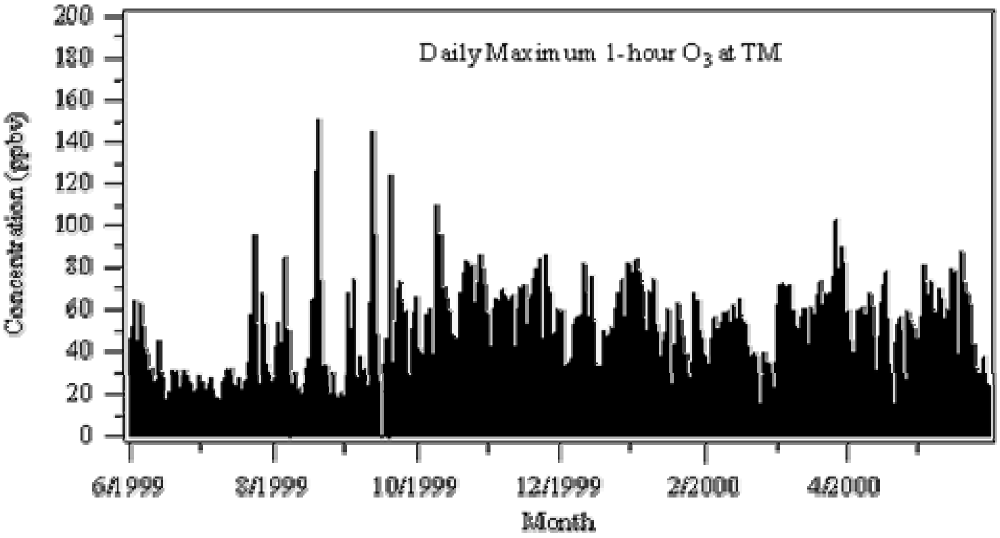

(b)

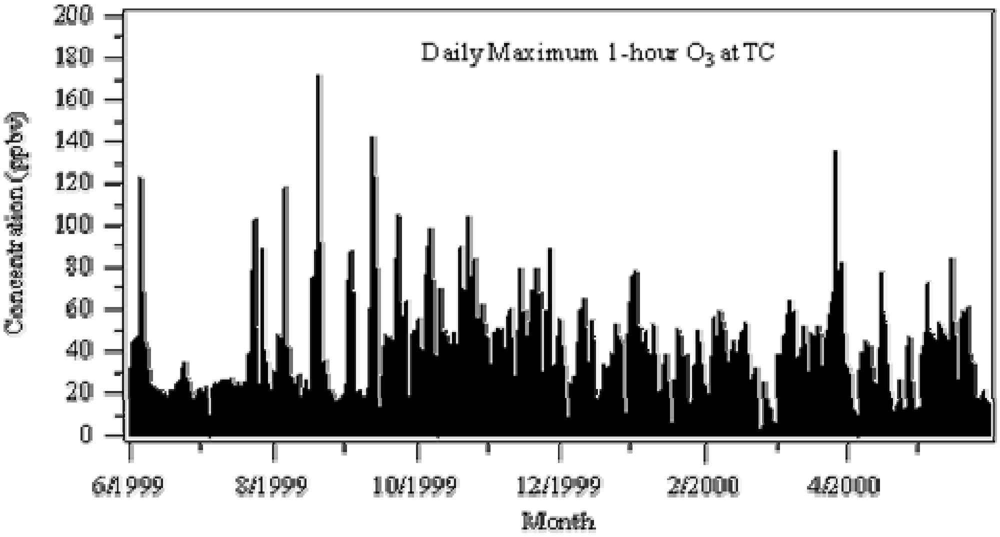

*(to be continued)*

*Figure 4.2 continued*

(c)

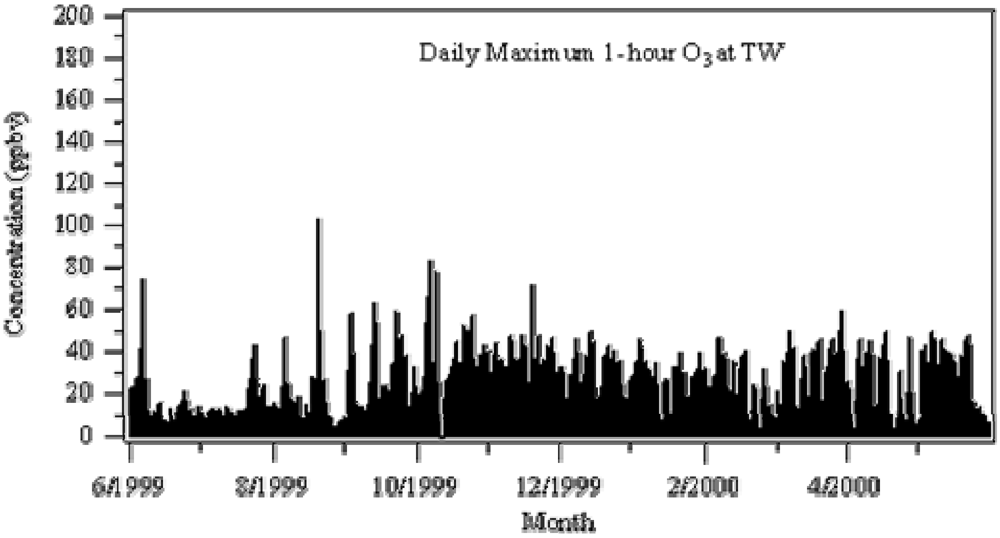

*Table 4.3 Summary of $O_3$ episodes (hourly $O_3$ concentration > 122 ppbv) at TM, TC and TW from June 1999 to May 2000*

| **Sites** | **TM** | **TC** | **TW** |
|---|---|---|---|
| No. of days with $O_3$ episodes | 4 | 3 | 0 |
| No. of hours with $O_3$ episodes | 8 | 5 | 0 |

Huang et al. (2005) analyzed the $O_3$ episodes in HK from 1999 to 2003 and classified them into three categories: typhoon cyclone (62%), anticyclone (21%) and low pressure trough (17%). Here, a case study of $O_3$ episode due to typhoon cyclone was selected for discussion because it was a territory wide event and elevated $O_3$ levels were measured at both upwind (TM) and downwind (TC) areas. The event occurred on 19 and 20 August 1999 when Typhoon Sam was approaching HK. Figure 4.3 shows the synoptic weather maps on these two days. During the period, $O_3$ levels exceeding the HK Air Quality Objective of 122 ppbv were recorded in TM, TC but not TW. Influenced by the low-pressure system, hot and stagnant atmospheric conditions were observed in HK. The maximum temperature was $32.7^oC$ and $33.2^oC$ on 19 and 20 August 1999, respectively. The total number of bright sunshine hours was more than eight hours on both days. Among the three sites, the suburban TC recorded the highest hourly $O_3$ level (171 ppbv) at LST 1400 on 20 August 1999. Figure 4.4 shows the diurnal variations of $O_3$, $SO_2$, $NO_x$ and TO observed at the three sites. An interesting feature is an obvious enhancement of $SO_2/NO_x$ during the periods of $O_3$ peaks (see Figure 4.4).

As discussed above, the high $SO_2/NO_x$ is a characteristic of emission in Mainland China. Therefore, the values of $SO_2/NO_x$ can be used as the “fingerprints” for distinguishing local (HK) air masses from those originating from the rest of the PRD. Table 4.4 lists averaged concentrations of $O_3$ and $SO_2/NO_x$ between LST 1300 and 1700 at each site. It can be seen that elevated levels of $O_3$ observed in the afternoon were associated with high ratios (0.58-1.50) of $SO_2/NO_x$ at the rural and the suburban sites. Much lower ratios (0.24-0.33) were found for the urban TW site. Another two $O_3$ episodes of September 1999 were also studied and similar results were obtained with

$O_3$ laden air masses enriched with $SO_2$ (relative to $NO_x$) at the rural and suburban sites (see Table 4.4). The high $SO_2$ to $NO_x$ ratios is considered as the evidence of the transport of emissions from other cities in the PRD, whose air is known to contain much higher $SO_2$ to $NO_x$ ratios. Therefore, it is possible that during the episode days, HK was affected by regional $O_3$ pollution.

*Table 4.4 Averaged $O_3$ levels and $SO_2/NO_x$ during the 4 days of $O_3$ episode (LST 1300 to 1700)*

| Date of 1999 | TM | | TC | | TW | |
|---|---|---|---|---|---|---|
| | $O_3$ (ppbv) | $SO_2/NO_x$ (ppbv/ppbv) | $O_3$ (ppbv) | $SO_2/NO_x$ (ppbv/ppbv) | $O_3$ (ppbv) | $SO_2/NO_x$ (ppbv/ppbv) |
| 19 Aug | 112 | 1.50 | 77 | 0.58 | 25 | 0.24 |
| 20 Aug | 134 | 0.90 | 139 | 1.17 | 78 | 0.33 |
| 12 Sep | 98 | 0.74 | 87 | 0.68 | 29 | 0.30 |
| 20 Sep | 84 | 0.62 | 34 | 0.24 | 9 | 0.15 |

*Figure 4.3 Synoptic weather maps for 19 and 20 August 1999.*

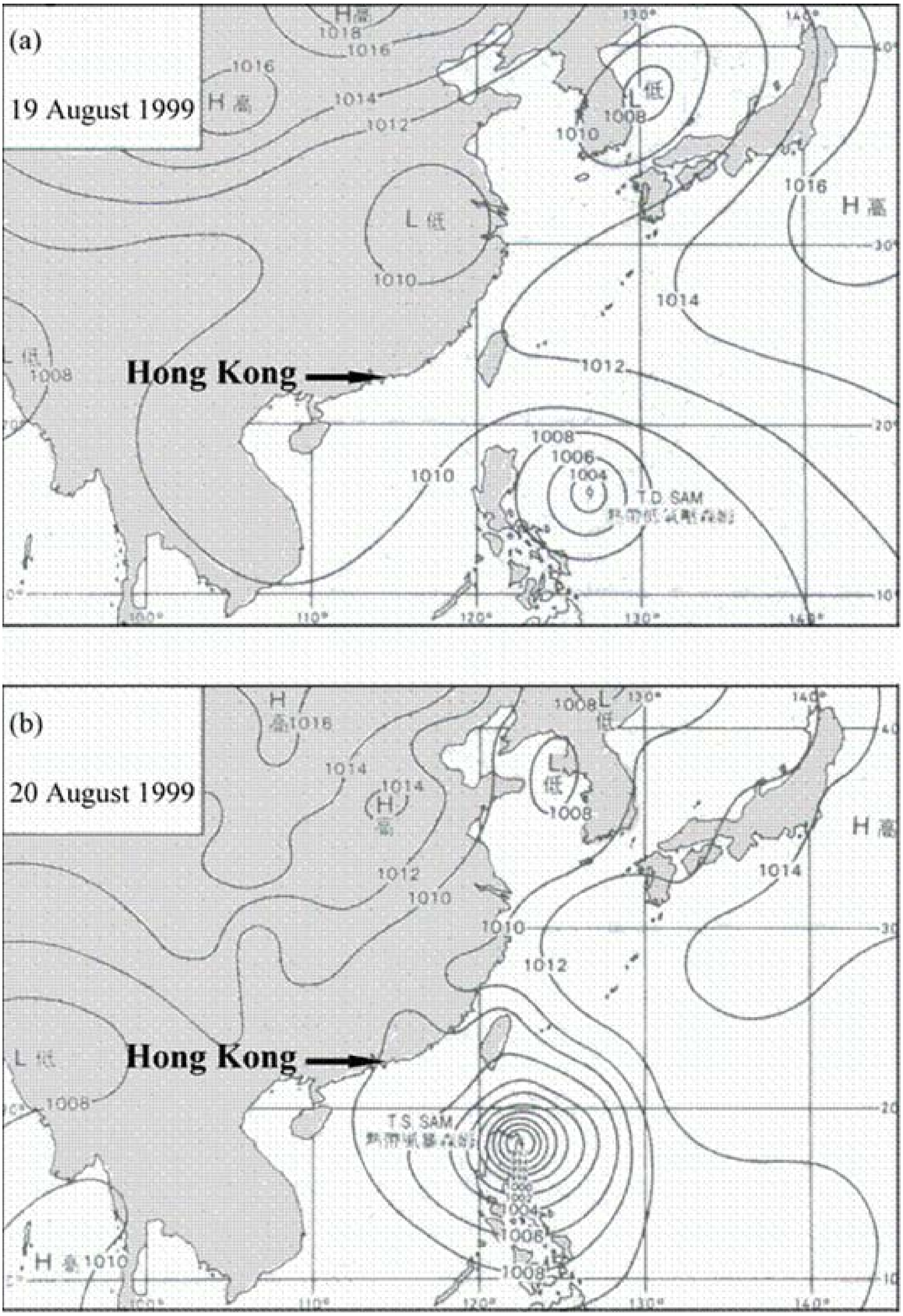

*Figure 4.4 Multiple pollutants variation at (a) TM, (b) TC and (c) TW on 19 and 20 August 1999.*

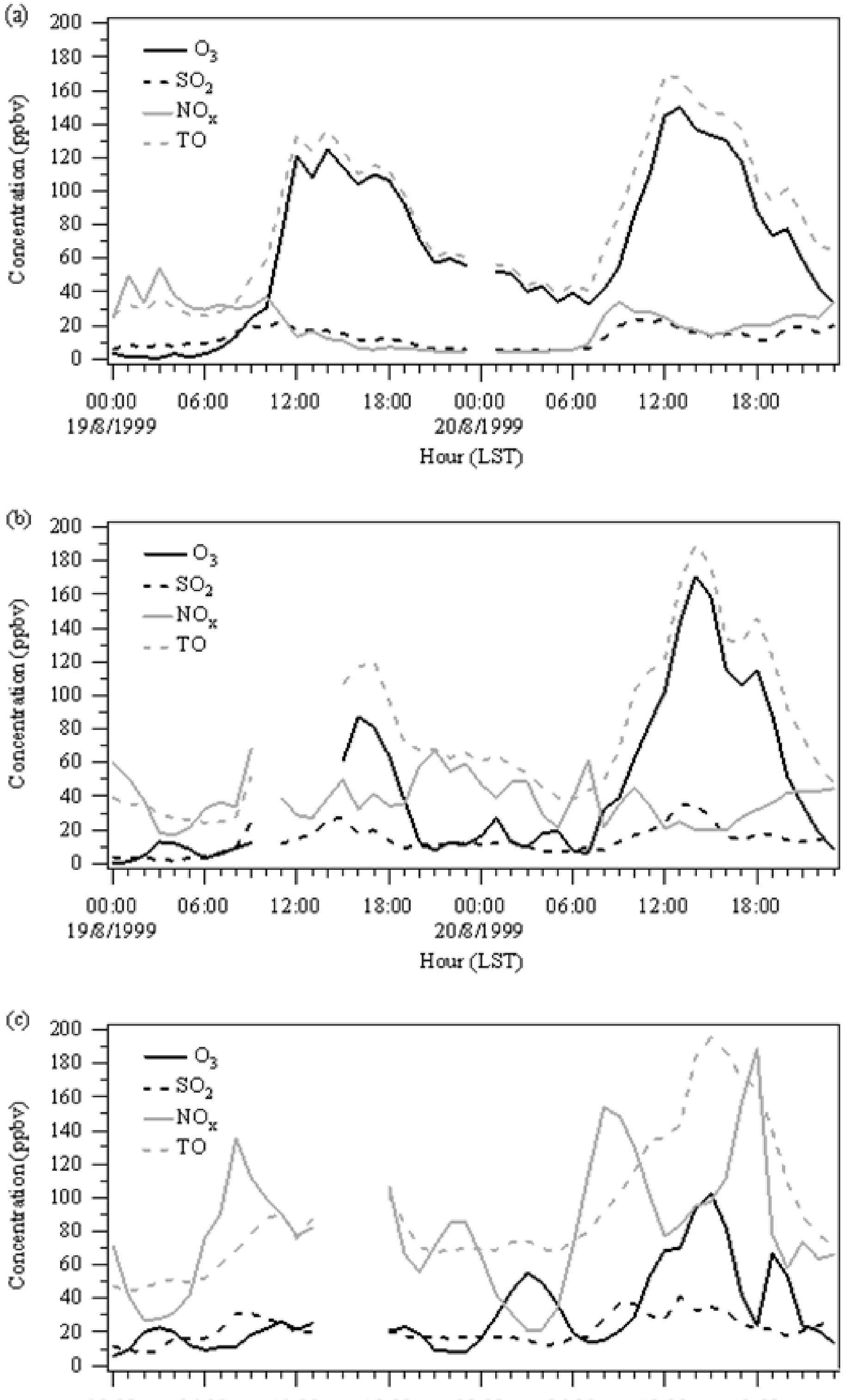

## 4.6 Chapter Summary

In this chapter, more recent (1999/2000) measurement data on $O_3$ and other air pollutants obtained at the rural (upwind), urban, and suburban (downwind) sites were analyzed to show the temporal and spatial distribution of $O_3$ in HK in connection with the rapid development of the PRD cities over the years. The rural northeastern site TM showed the highest monthly $O_3$ levels and an obvious diurnal cycle. The urban TW site had the lowest $O_3$ among the three sites. Low $O_3$ level was observed in summer but $O_3$ maxima were found in both autumn and spring, which was somewhat different from the previous study of the 1996 data indicating a single peak in autumn.

Examination of the chemical species ratios such as $SO_2/NO_x$ and $CO/NO_x$ revealed the different characteristics of emission sources impacting each of the study sites. The rural site was characterized by high levels of CO and $SO_2$ (relative to $NO_x$), indicating frequent influences of regional air masses from the inland region. The urban site, as expected, was predominantly affected by local emissions (containing higher levels of $NO_x$). The suburban site was impacted by both local and regional pollution. Application of PCA also shows that the variation of pollutant at the rural site was strongly influenced by regional emissions and chemical and transport processes, whereas the urban and suburban sites were impacted more by fresh emission.

The analysis of $O_3$ episodes showed that stagnant conditions were associated with a tropical cyclone situated over the East China Sea. Elevated ratio of $SO_2$ to $NO_x$ was found during the high $O_3$ days, suggesting evidence for transport to HK of regional air masses containing high ratios of $SO_2$ to $NO_x$.

This chapter shows that in a relatively small territory of HK, different parts may be influenced by local and regional emissions to a varying extent. It is possible that the regional impact could become more significant in the coming years in light of the continuing economic expansion in the PRD. To better understand the cause(s) of $O_3$ pollution in HK, it is imperative to look into the patterns and roles of major $O_3$ precursors (VOC) which will be discussed in the following chapters.

# CHAPTER 5 STUDY OF $C_3$ TO $C_{12}$ HYDROCARBONS IN HONG KONG DURING 2000/2001

In this chapter, an analysis of comprehensive data set on NMHC ($C_3$ to $C_{12}$ hydrocarbons) is conducted to establish their seasonal and spatial trends, to identify their possible sources and to assess their impact on $O_3$ formation. The NMHC data were obtained from November 2000 to October 2001 at four sites in HK, including one rural (HT), one urban residential (C/W), one urban industrial (TW) and one roadside site (MK). For the urban sites (C/W and TW), the NMHC sample was collected once every 6 days, and there were a total of 60 samples from each of the two sites. The sampling frequency at the other two sites, rural (HT) and roadside (MK), was twice per month and there were 23 samples (only 1 sample was collected in January 2001) from November 2000 to October 2001. For each sample, concentrations of 100 NMHC (39 $C_3$-$C_{12}$ alkanes, 32 $C_3$-$C_{10}$ alkenes, 2 $C_3$-$C_4$ alkynes and 27 $C_6$-$C_{12}$ aromatic hydrocarbons) were determined. Since the concentrations of alkynes (propyne and 1-butyne) were less than 0.6% of the 100 NMHC (in ppbC) for all the samples, the analysis is focused on alkanes, alkenes and aromatic hydrocarbons as well as total NMHC (summation of 39 alkanes, 32 alkenes and 27 aromatic hydrocarbons in ppbC).

The spatial and seasonal patterns of total and selected NMHC are examined and compared with other overseas cities. PCA is utilized to evaluate the relationships of different NMHC and to shed lights on the source characteristics at each site. The ratios of selected NMHC are used to assess the ages of air masses sampled in each site, especially the emission ratio at the roadside. Finally, the NMHC to $NO_x$ ratios are calculated to assess the photochemical reactivity of NMHC. The results are significant and published in the Journal of Science of Total Environment titled “$C_3$-$C_{12}$ Non-methane Hydrocarbons in Subtropical Hong Kong: Spatial-temporal Variations, Source-receptor Relationships and Photochemical Reactivity” (So and Wang, 2004).

## 5.1 Spatial Distribution, Seasonal Variation and Inter-city Comparison of Non-methane Hydrocarbons

The spatial distribution and seasonal variation of total NMHC levels among the four sites are shown in Figure 5.1. As expected, the total NMHC and the three major functional groups of NMHC were the highest at the roadside site and lowest at the rural site. In general, the descending order of the average concentrations of hydrocarbons was roadside > industrial > residential > rural. The highest total NMHC level at the roadside site is attributed to the heavy vehicular emissions and the surrounding buildings preventing effective dispersion of the vehicle emissions. The industrial site (TW) was impacted by the emissions from surrounding industrial and local traffic sources (Guo et al., 2004). The total NMHC level at this site was slightly lower than those of roadside because the samples were collected on the roof-top, with less influence from direct emissions. Compared to the roadside and industrial sites, the total NMHC level at the residential site (C/W) was further lower due to fewer industrial activities and a lower traffic volume around the site. As expected, the lowest level of total NMHC was observed at the rural HT site.

*Figure 5.1 Seasonal variations of alkanes, alkenes, aromatic hydrocarbons and their summations (total NMHC) at the four sites in HK: HT (rural); C/W (residential); TW (industrial) and MK (roadside). Winter: November 2000-February 2001; spring: March 2001-April 2001; summer: May 2001-August 2001; autumn: September 2001-October 2001.*

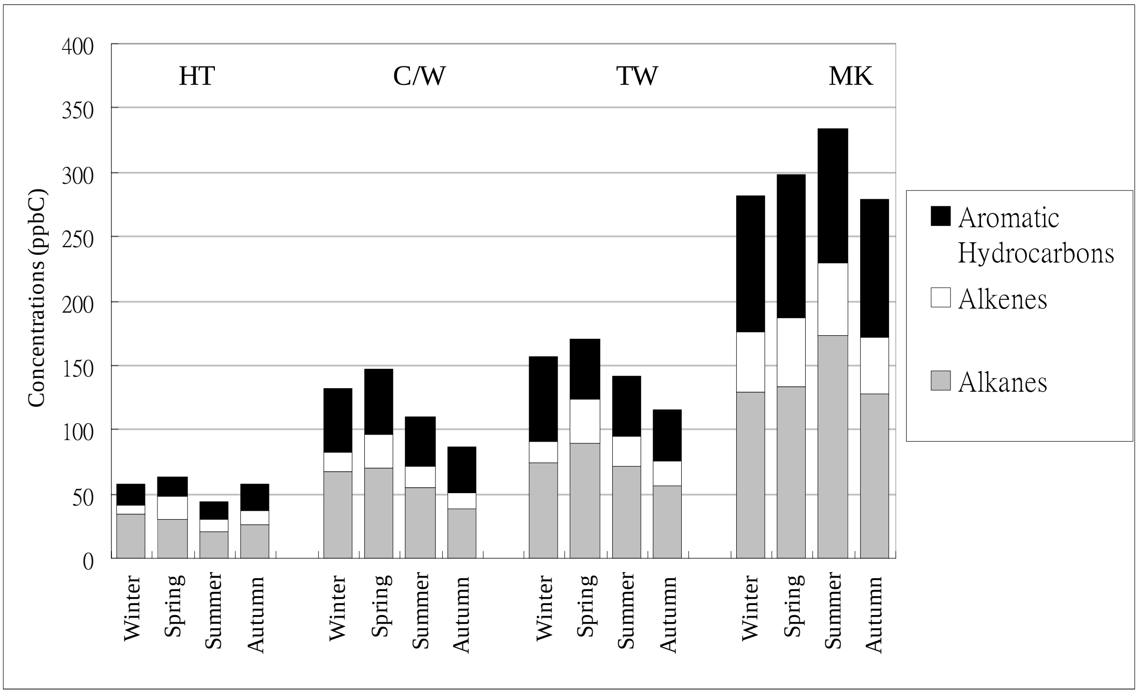

To examine the seasonal pattern of NMHC in HK, the data were classified into four seasons including winter (November to February), spring (March to April), summer (May to August), and autumn (September to

October) (Lee et al., 2002). The total NMHC levels at the residential and industrial sites followed a general seasonal variation with high levels in winter and spring and low level in summer and autumn. A similar seasonal pattern has also been observed for other air pollutants such as $NO_2$ and RSP (EPD, 2001) indicating that the two sites were under the similar seasonal and regional influence. The total NMHC level at the rural site was lowest in summer, with comparable levels in the other three seasons. Such a seasonal variation is similar to that of $O_3$ in the rural areas of HK (e.g. Wang et al., 2001b; So and Wang, 2003). The seasonal variations of the abundances of air pollutants in subtropical HK are mainly influenced by the Asian Monsoons which bring in clean maritime air and unstable weather in summer and pollutant-laden continental air in winter. In contrast to the rural site, the roadside site had the highest levels of total NMHC and alkanes in summer. In particular, the compounds, such as *n*-butane, *i*-butane and *i*-pentane, which mainly come from vehicle exhausts, evaporation of gasoline, and the leakage from LPG, all showed the highest levels at the roadside in summer and the lowest concentrations in winter. As the roadside site is situated by a road with heavy traffic and surrounded by buildings, the NMHC concentrations at this site are thus dominated by the emission strength from vehicles and are less affected by the changes in regional-scale air flow patterns, as compared to other three sites. The high temperature in summer could enhance the fuel evaporation, contributing to a higher level of *n*-butane, *i*-butane, *i*-pentane and other NMHC in the summer season. Similar observations of elevated summertime concentrations of typical fuel components like butanes and pentanes have also been reported in other countries (Field et al., 1994; Hansen and Palmgren, 1996; Na and Kim, 2001).

Table 5.1 compares 11 key hydrocarbons at the HK roadside site with those observed in other overseas cities. The NMHC levels in HK are on the lower side together with London and Edmonton. By comparison, Karachi, Mexico City and Santiago have much higher levels. For example, the annual average concentration of roadside benzene (1.58 ppbv) in HK was about half of the regulatory limit of 10 $\mu g/m^3$ (3.1 ppbv) implemented in several countries, but the levels in Karachi, Mexico city and Santiago were all over the limit (4.6 – 5.2 ppbv) (Barletta et al., 2002). Isoprene was an exceptional hydrocarbon which had a quite high concentration in HK (annual average = 0.65 ppbv), comparable to the levels observed in Karachi (0.8 ppbv) and Santiago (0.5 ppbv). The following section examines the sources of isoprene observed at different sites in HK.

## 5.2 Sources of Isoprene at Different Sites in Hong Kong

Isoprene (2-methyl-1,3-butadiene, $C_5H_8$) is highly reactive with OH radicals and plays a crucial role on photochemical $O_3$ formation. It is well known that isoprene is released by biogenic sources in rural areas and its emission increases with the increase of ambient temperature (e.g. Jobson et al. 1994). Recent studies also reported elevated levels of isoprene in vehicle exhausts in urban areas (e.g. Borbon et al., 2001; Barletta et al., 2002). In HK, the annual average concentration of isoprene was 0.46, 0.30, 0.43 and 0.65 ppbv at the rural, residential, industrial and roadside sites, respectively. Figure 5.2 shows the variation of isoprene among the four sites during a year, using the 24-hour data. At the rural site (HT), the isoprene concentration showed the maximum in August presumably because higher temperatures caused increasing emissions of isoprene from biogenic sources. The results of high level in summer and low level in winter indicated that the biogenic emission was the major source of isoprene at the rural site. By comparison, there was no obvious seasonal variation of isoprene at the roadside site (MK) and most of the data were within the range between 0.5 to 1.0 ppbv. Such pattern could be explained by the contribution of local vehicular emissions which did not have a significant seasonal variation in a year. It is not clear about the three high isoprene data (over 1.0 ppbv) in spring and further research is needed to look into the source. The summertime peak of isoprene was also observed in the other urban sites (C/W and TW), suggesting biogenic emission was also a dominant source of isoprene in these areas. Depending on the site environment, there is a mixed contribution of isoprene from both vehicular and biogenic sources in an urban area. With reference to the results in other urban areas (Karachi of Pakistan and Toronto of Canada), about 20 to 30% of isoprene was estimated coming from vehicular emissions (Roberts et al., 1998; Barletta et al. 2002).

*Table 5.1* *Comparison of selected NMHC measured in Hong Kong (roadside area) and other cities*

| NMHC (Unit: ppbv) | HK | Taipei [a] | Osaka [b] | Karachi [c] | Mexico City [d] | Santiago [e] | Edmonton [f] | Athens [g] | Munich [h] | London [i] |
|---|---|---|---|---|---|---|---|---|---|---|
| Sampling period | Nov 00 to Oct 01 | Jan 97 | Not provided | Dec 98 to Jan 99 | Feb 93 | Jun 96 | Dec 91 to Nov 93 | Jun 93, May & Jul 94 | Aug 93 | 1996 |
| Propane | 4.01 | 6.4 | 8.9 | 41 | 158 | 137.5 | 8.32 | 1.2 | | 2 |
| Propene | 2.80 | 4.6 | 6.1 | 5.5 | 5 | 8.0 | 1.56 | 3.9 | | 1.4 |
| *n*-butane | 6.53 | 5.2 | 11 | 19.8 | 70.4 | 27.0 | 5.43 | 2.1 | | 3.2 |
| *i*-butane | 2.87 | 2.4 | 5.1 | 11.0 | 33.1 | 16.1 | 1.31 | 1.1 | | 1.4 |
| 1-butene / *i*-butene | 2.24 | 3.6 | | 2.3 | 3.9 | 5.2 | | | | |

*(to be continued)*

*Table 5.1 continued*

| NMHC (Unit: ppbv) | HK | Taipei [a] | Osaka [b] | Karachi [c] | Mexico City [d] | Santiago [e] | Edmonton [f] | Athens [g] | Munich [h] | London [i] |
|---|---|---|---|---|---|---|---|---|---|---|
| Pentane | 1.71 | 4.3 | 7.7 | 13.4 | 14.4 | 6.6 | 1.50 | 4.2 |  | 0.6 |
| *i*-pentane | 4.48 | 12.8 | 10.6 | 12.1 | 19.4 | 14.2 | 3.65 | 11.7 |  | 2.6 |
| Isoprene | 0.65 |  |  | 0.8 | 0.1 | 0.5 |  |  |  | 0.1 |
| 2-methyl-pentane | 1.78 |  | 3.9 | 4.7 | 8.1 | 4.8 | 1.08 | 3.3 | 2.2 |  |
| Benzene | 1.58 |  | 5.1 | 5.2 | 4.6 | 6.0 | 1.06 | 5 | 3.6 | 1.1 |
| Toluene | 8.24 |  | 31.1 | 7.1 | 21 | 21.8 | 1.89 | 14.3 | 7.0 | 2.2 |

[a] Taipei, Ding and Wang (1998); [b] Osaka, Tsujino and Kuwata (1993); [c] Karachi, Barletta et al. (2002); [d] Mexico City, Blake and Rowland (1995); [e] Santiago, Chen et al. (2001); [f] Edmonton, Cheng et al. (1997); [g] Athens, Moschonas and Glavas (1996); [h] Munich, Rappenglück and Fabian, (1999); [i] London, Derwent et al. (2000)

*Figure 5.2 Daily variations of isoprene at the four sites: TW (industrial); C/W (residential); HT (rural); and MK (roadside).*

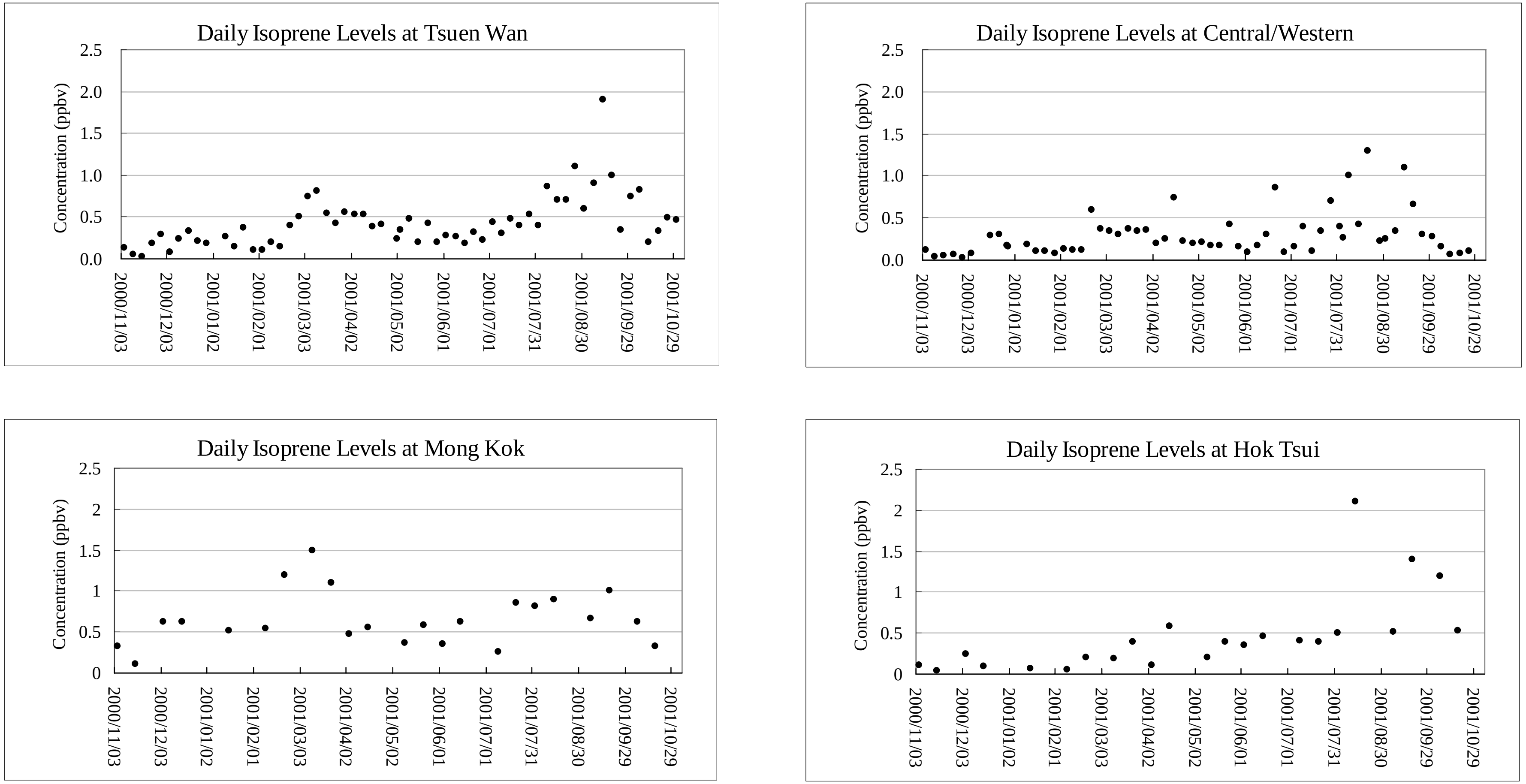

In order to better understand the source of isoprene at different sites, PCA was applied to a subset of NMHC including isoprene and the other 19 key NMHC (see Table 5.2). These compounds were selected for PCA because of their relative abundance and their ability to serve as tracers for major sources such as vehicle exhausts, fuel evaporation and LPG leakage. PCA reduces a data set containing a number of variables to a new data set with several PCs which explains the most variability contained in the original data set. The first component accounts for the maximum possible variance in the data set and each succeeding component accounts for the maximum portion of the remaining variance. A varimax rotation was applied to maximize the variance of the squared loadings for each component (Liu et al., 1996; Borbon et al., 2001). Table 5.2 shows the loading (with values of 0.4 or above shown), the eigenvalue, and the corresponding percentage of variance for each PC. Three to five PCs were extracted from the data set for the four sites and the composition of each component was different.

The rural site has five PCs extracted from the data set. PC1 to PC4 were characterized by tracers of anthropogenic sources while PC5 was only dominated by isoprene The lack of association of isoprene with the anthropogenic emissions indicated that isoprene at the rural site was not from vehicular sources but from biogenic emissions.

For the roadside site, four PCs were extracted and they were all related to the sources of vehicles combustion and fuel evaporation. The loadings of isoprene in PC1 (0.42), PC2 (0.59) and PC4 (0.52) were similar and suggested that isoprene was emitted from the busy vehicular activities at the roadside area.

Three and four PCs were extracted from the industrial and residential sites, respectively. PC1 for both sites were dominated by tracers of vehicles combustion like propene, butene and 1,3-butadiene. The high loadings of isoprene in PC1 of the two urban sites indicated that isoprene was to a certain extent related to vehicular activities in the urban sites. It is of interest to estimate the relative contribution of different sources to isoprene by applying multiple linear regression to the data set. Guo et al. (2004) conducted a source apportionment of hydrocarbons data (including isoprene) at two urban sites in HK and reported that biogenic emissions were not significant there. The results were based on annual average data and no seasonal factor was studied. To better estimate the relative contribution of vehicular and biogenic emissions to isoprene at different sites in various seasons, it is recommended to perform source apportionment on a more comprehensive data set (including diurnal isoprene and other VOC data) in the further work.

*Table 5.2 Results of principal component analysis of 20 NMHC at the four sites (Only PCs with eigenvalue larger than 1 and loading larger than 0.4 are shown)*

| | HT (Rural) | | | | |
|---|---|---|---|---|---|
| NMHC | PC1 | PC2 | PC3 | PC4 | PC5 |
| Propane | | | 0.93 | | |
| Propene | | 0.67 | 0.55 | | |
| *n*-butane | 0.44 | 0.50 | 0.70 | | |
| *i*-butane | 0.56 | | 0.66 | | |
| 1-butene / *i*-butene | | 0.82 | | | |
| *cis*-2-Butene | | 0.83 | | | |
| *trans*-2-butene | 0.49 | 0.45 | | 0.48 | |
| 1,3-butadiene | 0.49 | 0.56 | | 0.48 | |
| Pentane | | 0.52 | 0.75 | | |
| 1-pentene | | 0.94 | | | |
| Isoprene | | | | | 0.87 |
| Hexane | 0.86 | | | | |
| Benzene | | | 0.94 | | |
| Heptane | 0.87 | | | | |
| Toluene | 0.94 | | | | |
| *m,p*-xylene | 0.89 | | | | |
| *o*-xylene | 0.85 | | | | |
| Ethylbenzene | 0.73 | | 0.57 | | |
| Styrene | | 0.80 | | | |
| Naphthalene | | | | 0.82 | |
| Eigenvalue | 5.77 | 4.61 | 4.29 | 1.53 | 1.52 |
| % of Variance | 28.86 | 23.05 | 21.47 | 7.63 | 7.58 |

*(to be continued)*

*Table 5.2 continued*

| | C/W (Residential) | | | |
|---|---|---|---|---|
| NMHC | PC1 | PC2 | PC3 | PC4 |
| Propane | | | 0.93 | |
| Propene | 0.56 | | 0.70 | |
| *n*-butane | 0.65 | | 0.62 | |
| *i*-butane | | 0.45 | 0.69 | |
| 1-butene / *i*-butene | 0.88 | | | |
| *cis*-2-Butene | 0.93 | | | |
| *trans*-2-butene | 0.84 | | | |
| 1,3-butadiene | 0.78 | | | |
| Pentane | | | 0.86 | |
| 1-pentene | 0.74 | | 0.42 | |
| Isoprene | 0.63 | | | |
| Hexane | 0.49 | 0.64 | | |
| Benzene | | | 0.83 | |
| Heptane | 0.41 | 0.78 | | |
| Toluene | | 0.80 | | |
| *m,p*-xylene | | 0.86 | | |
| *o*-xylene | | 0.87 | 0.41 | |
| Ethylbenzene | | 0.80 | | |
| Styrene | | | | 0.79 |
| Naphthalene | 0.56 | | | -0.60 |
| Eigenvalue | 5.68 | 4.69 | 4.47 | 1.69 |
| % of Variance | 28.39 | 23.45 | 22.37 | 8.46 |

*(to be continued)*

*Table 5.2 continued*

| | TW (Industrial) | | |
|---|---|---|---|
| NMHC | PC1 | PC2 | PC3 |
| Propane | | 0.67 | 0.65 |
| Propene | 0.73 | | 0.48 |
| *n*-butane | 0.64 | 0.40 | 0.61 |
| *i*-butane | 0.55 | | 0.58 |
| 1-butene / *i*-butene | 0.87 | | |
| *cis*-2-Butene | 0.87 | | 0.42 |
| *trans*-2-butene | 0.94 | | |
| 1,3-butadiene | 0.86 | | |
| Pentane | 0.48 | 0.45 | 0.71 |
| 1-pentene | 0.50 | | 0.78 |
| Isoprene | 0.67 | | |
| Hexane | 0.62 | 0.64 | |
| Benzene | | 0.64 | 0.60 |
| Heptane | | 0.89 | |
| Toluene | 0.46 | 0.78 | |
| *m,p*-xylene | | 0.94 | |
| *o*-xylene | | 0.94 | |
| Ethylbenzene | | 0.91 | |
| Styrene | | | 0.84 |
| Naphthalene | 0.82 | | |
| Eigenvalue | 6.70 | 6.11 | 4.02 |
| % of Variance | 33.49 | 30.56 | 20.12 |

*(to be continued)*

*Table 5.2 continued*

| | MK (Roadside) | | | |
|---|---|---|---|---|
| NMHC | PC1 | PC2 | PC3 | PC4 |
| Propane | | 0.90 | | |
| Propene | 0.65 | 0.63 | | |
| *n*-butane | 0.87 | | | |
| *i*-butane | 0.87 | | | |
| 1-butene / *i*-butene | 0.87 | | | |
| *cis*-2-Butene | 0.90 | | | |
| *trans*-2-butene | 0.87 | | | |
| 1,3-butadiene | 0.84 | 0.44 | | |
| Pentane | 0.62 | 0.69 | | |
| 1-pentene | 0.56 | 0.58 | | |
| Isoprene | 0.42 | 0.59 | | 0.52 |
| Hexane | 0.85 | | | |
| Benzene | | 0.90 | | |
| Heptane | 0.85 | | | |
| Toluene | 0.53 | | | 0.53 |
| *m,p*-xylene | | | 0.94 | |
| *o*-xylene | | | 0.94 | |
| Ethylbenzene | | | 0.91 | |
| Styrene | | | | 0.87 |
| Naphthalene | 0.91 | | | |
| Eigenvalue | 8.57 | 3.96 | 3.05 | 1.79 |
| % of Variance | 42.83 | 19.79 | 15.25 | 8.96 |

## 5.3 Photochemical Age and Evaluation of Emission Ratios

Previous studies have shown that elevated $O_3$ levels in HK's rural areas such as HT and TO are attributable to the re-circulation/transport of aged air masses to these sites (e.g. Wang et al, 1998; Wang et al., 2003b). The "photochemical age" of an air mass can be assessed by examining ratios of two species with similar emissions source(s) but different chemical lifetimes in the atmosphere. Ratios of *m,p*-xylene to ethylbenzene, butane to propane and toluene to benzene have been widely used for the assessment of photochemical age (Nelson and Quigley, 1983; Laurila and Hakola, 1996; Grosjean et al., 1999).

Figure 5.3a shows scatter plots of monthly averages of *m,p*-xylene to ethylbenzene for the four sites. The rural site had the smallest slope and the roadside site had the largest. Since the principal pathway of decay for aromatic hydrocarbons in the atmosphere is by reaction with the OH, (Darnall et al., 1976) and the OH rate constant ($k_{OH}$) of ethylbenzene ($7.1\times10^{-12}$ $cm^3$ $molecule^{-1}$ $s^{-1}$) is smaller than those of *m,p*-xylene ($23.6\times10^{-12}$ and $14.3\times10^{-12}$ $cm^3$ $molecule^{-1}$ $s^{-1}$ for *m*-xylene and *p*-xylene respectively) (Atkinson, 1994), a reduced ratio is expected in rural areas due to a faster removal of xylenes compared to ethylbenzene. The ratio measured at the roadside and two urban stations represented the emission ratio from traffic and overall urban sources (including traffic) in HK, respectively. The emission ratio (1.77) at the roadside site was lower than that observed in Sydney (3.6) and New York (4.3) (Nelson and Quigley, 1983).

Figure 5.3b shows butane versus propane in HK. The slope ranged from 0.39 at the rural site to 1.31 at the roadside. A reduced ratio was observed at the rural site because of the faster removal rate of butane ($k_{OH}$=2.54×$10^{-12}$ $cm^3$ $molecule^{-1}$ $s^{-1}$) compared to propane ($k_{OH}$=1.15×$10^{-12}$ $cm^3$ $molecule^{-1}$ $s^{-1}$) (Atkinson, 1994). The butane to propane emission ratio of 1.31 in HK was somewhat smaller than the value of 2.0 found in the Helsinki city area (Laurila and Hakola, 1996). The lower ambient ratios for the above pairs in HK compared to other cities (Sydney, New York and Helsinki) could be due to the variations in fuel compositions, vehicle types, sites characteristics, and sampling period among different cities.

*Figure 5.3 Scatter plots of monthly data from November 2000 to October 2001 for (a) m,p-xylene versus ethylbenzene and (b) butane versus propane at the four sites: HT (rural); C/W (residential); TW (industrial) and MK (roadside).*

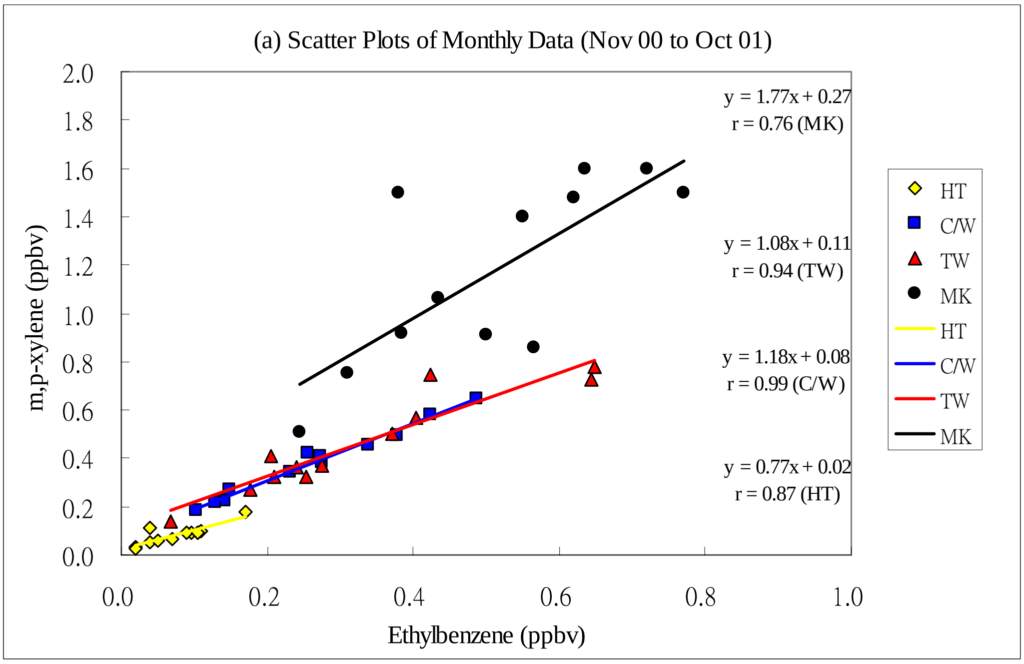

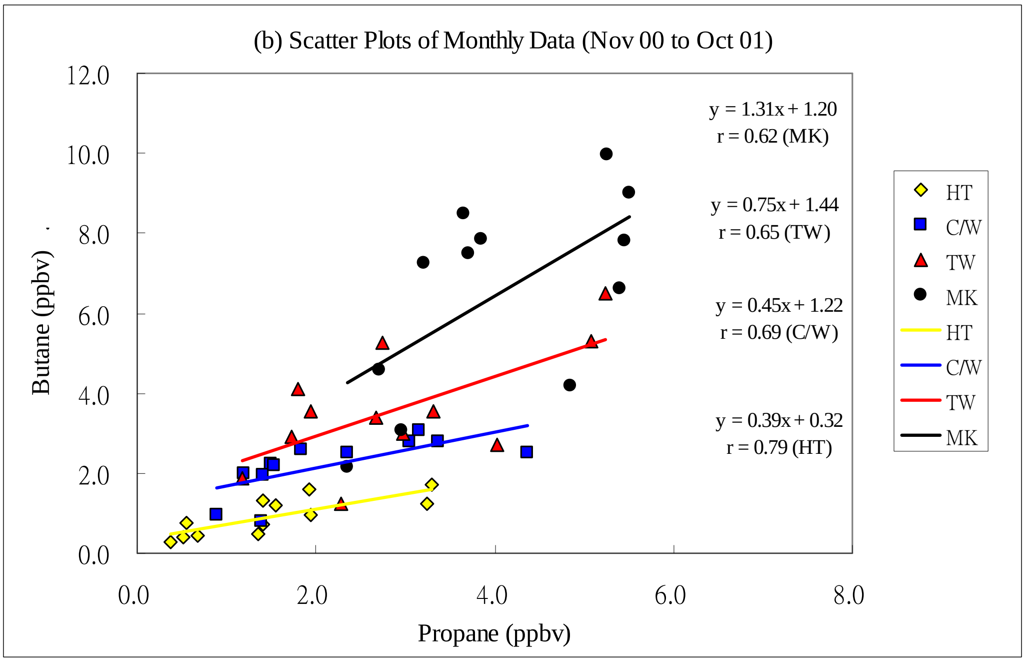

There was a larger degree of scatter in the butane versus propane plot than in the *m,p*-xylene versus ethylbenzene scatter plot, which may be due to the more pronounced variations of background concentrations for the less reactive compounds such as butane and propane compared to *m,p*-xylene and ethylbenzene. The regression slopes for each of the two pairs differed at different sites, indicating the spatial variation of the sources of these species and the difference in photochemical ages of the air masses at these sites. Vehicle exhausts and solvent usages are the main sources of *m,p*-xylene and ethylbenzene. The roadside data are expected to mainly reflect vehicular emissions whereas the urban sites can be affected by both vehicular emissions and solvent use. The similar *m,p*-xylene to ethylbenzene ratio at TW and C/W sites suggests similarity of sources and photochemical ages of air masses sampled at these two urban sites. By comparison, butane and propane could be generated from more diverse sources such as vehicle exhausts, fuel evaporation, LPG and industrial processes. The well distinguished butane-propane slopes among the four sites could therefore be due to the variation of sources in addition to the different degree of atmospheric processing including mixing and photochemical reactions.

The emission ratio of toluene to benzene inferred from the roadside data in HK was 6.20, which was much higher than those (0.7 to 3.5) in cities in the US (Grosjean et al., 1999). The higher emission ratio in HK was attributed to the widespread use of aromatic-rich unleaded fuels in the territory (Sin et al., 2000). Unleaded petrol was introduced to HK in April

1992, and the sale and supply of leaded petrol was banned in HK from April 1999 (Census and Statistic Department, 1999). The aromatic (mainly toluene) content of unleaded fuels was increased in order to maintain the volatility as well as the octane number of leaded fuels. The composition of benzene was reduced to 1% in the unleaded fuels. In general, unleaded fuels with aromatic levels of more than 40% are widely used in Asian cities including HK, and toluene-to-benzene ratios of 10 have also been reported in Bangkok and Manila (Gee and Sollars, 1998; Lee et al., 2002). By comparison, the regulatory limit in the US for aromatic hydrocarbons of unleaded fuels is 25% (the Clean Air Act Amendments of 1990), which may explain the relatively lower toluene-to-benzene ratio observed in the US cities. In addition, the relatively high ratio is also contributed to the extensive use of toluene-rich solvent in HK (Wang et al., 2005)

## 5.4 Ratios of Total NMHC to $NO_x$ in Hong Kong

The ratio of VOC/$NO_x$ can be used to evaluate whether $O_3$ production is controlled by $NO_x$ or VOC (Sillman, 1999). Table 5.3 compares the ratios of total NMHC to time-matched $NO_x$ at the three urban sites and to total reactive nitrogen ($NO_y$) measured at the rural HT site (Wang et al, 2003a). A low NMHC-to-$NO_x$ ratio of 2-3 (ppbC/ppbv) was seen at the three urban sites. While $NO_x$ was not measured at the rural HT during the period of VOC sampling, it was estimated to comprise about half of $NO_y$ (Wang et al., 2001b). Thus, the NMHC-to-$NO_x$ ratio was approximately 10 at HT, which is at the borderline of 8-10 between the VOC and $NO_x$ limiting regime (NRC, 1991). These results suggest that $O_3$ formation in the urban HK plume was strongly controlled by NMHC, as in many other urban areas (NRC, 1991).

## 5.5 Photochemical Reactivity and Ozone Formation

As discussed above, the low total NMHC-to-$NO_x$ ratios suggest a controlling role of NMHC on $O_3$ formation. To estimate and compare the photochemical reactivity of the NMHC at different sites, propene-equivalent concentrations (PE) (Chameides et al., 1992) and Maximum Incremental Reactivity (MIR) (Carter, 1994) for each individual NMHC are examined in this section.

Table 5.4 lists the top 10 hydrocarbons ranked by mass concentration (ppbC), PE (ppbC) and $O_3$ Formation ($\mu g/m^3$) at the four sites. The results were calculated from the annual averages of the NMHC. Toluene, *n*-butane and propane were the most abundant NMHC in terms of ppbC for all the four sites and benzene, 2-methylpentane, *i*-pentane as well as *i*-butane were also the major contributors. Although the mass concentration of isoprene at the roadside site was higher than that of the rural site, isoprene was not in the top 10 list because of the relatively high concentration of other NMHC at the roadside site. Naphthalene was only found on the lists of three urban sites as it mainly came from combustion sources.

*Table 5.3 Summary of the average ratios of total NMHC to $NO_x$ ($NO_y$ for HT) with standard deviations at the four sites*

| Ratio (Unit: ppbC/ppbv) | 19 February to 31 April 2001 | | | 5 November 2000 to 31 October 2001 | | |
|---|---|---|---|---|---|---|
| | Average | Standard deviation | No. of samples | Average | Standard deviation | No. of samples |
| Total NMHC/$NO_y$ at HT (Rural) | 5.23 | 0.99 | 5 | - | - | - |
| Total NMHC/$NO_x$ at C/W (Residential) | 3.12 | 1.19 | 12 | 2.60 | 1.08 | 60 |
| Total NMHC/$NO_x$ at TW (Industrial) | 2.28 | 0.73 | 10 | 2.09 | 0.82 | 59 |
| Total NMHC/$NO_x$ at MK (Roadside) | 1.51 | 0.30 | 5 | 1.60 | 0.37 | 19 |

*Table 5.4 Top 10 NMHC ranked according to mass concentration, PE and $O_3$ formation in MIR calculated from the annual averages of NMHC at the four sites*

| Rank | HT (Rural) | | C/W (Residential) | | TW (Industrial) | | MK (Roadside) | |
|---|---|---|---|---|---|---|---|---|
| Mass Concentration (in ppbC) | | | | | | | | |
| 1 | Toluene | 6.23 | Toluene | 23.56 | Toluene | 24.45 | Toluene | 57.67 |
| 2 | Propane | 4.33 | *n*-butane | 8.73 | *n*-butane | 14.26 | *n*-butane | 26.14 |
| 3 | *n*-butane | 3.53 | Propane | 6.40 | Propane | 8.53 | *i*-pentane | 22.39 |
| 4 | Benzene | 3.23 | 2-methylpentane | 5.77 | *i*-pentane | 7.87 | Propane | 12.04 |
| 5 | 2-methylpentane | 3.21 | *i*-pentane | 5.10 | *i*-butane | 5.79 | *i*-butane | 11.46 |
| 6 | *i*-pentane | 2.98 | Naphthalene | 4.41 | 2-methylpentane | 5.53 | 2-methylpentane | 10.68 |
| 7 | Isoprene | 2.30 | *i*-butane | 4.39 | Naphthalene | 5.03 | Naphthalene | 9.86 |
| 8 | 1-butene / *i*-butene | 1.92 | Hexane | 4.34 | Benzene | 4.72 | Benzene | 9.51 |
| 9 | *i*-butane | 1.78 | Benzene | 3.64 | 1-butene / *i*-butene | 4.28 | *m,p*-xylene | 9.31 |
| 10 | Pentane | 1.52 | *m,p*-xylene | 3.06 | Pentane | 3.68 | 1-butene / *i*-butene | 8.96 |

*(to be continued)*

*Table 5.4 continued*

| Rank | HT (Rural) | | C/W (Residential) | | TW (Industrial) | | MK (Roadside) | |
|---|---|---|---|---|---|---|---|---|
| PE (in ppbC) | | | | | | | | |
| 1 | Isoprene | 8.82 | Isoprene | 5.70 | Isoprene | 8.27 | 1-butene / *i*-butene | 14.09 |
| 2 | 1-butene / *i*-butene | 3.02 | Toluene | 5.34 | 1-butene / *i*-butene | 6.73 | 2-methyl-2-butene | 13.69 |
| 3 | Toluene | 1.41 | 1-butene / *i*-butene | 4.57 | Toluene | 5.54 | Toluene | 13.07 |
| 4 | 2-methyl-2-butene | 1.05 | 2-methyl-2-butene | 2.62 | 2-methyl-2-butene | 3.77 | Isoprene | 12.49 |
| 5 | Propene | 1.04 | Propene | 2.43 | Propene | 3.43 | Propene | 8.41 |
| 6 | 2-methyl-1-butene | 1.02 | *m,p*-xylene | 2.20 | *m,p*-xylene | 2.61 | *m,p*-xylene | 6.71 |
| 7 | 2-methylpentane | 0.68 | 2-methyl-1-butene | 1.67 | 2-methyl-1-butene | 2.24 | 2-methyl-1-butene | 5.61 |
| 8 | 1-pentene | 0.61 | 2-methylpentane | 1.23 | 1,3-butadiene | 1.86 | 1,3-butadiene | 5.51 |
| 9 | *m,p*-xylene | 0.48 | 1,3-butadiene | 1.14 | 1,2,4-trimethylbenzene | 1.54 | *trans*-2-butene | 4.16 |
| 10 | *i*-pentane | 0.44 | 1-pentene | 0.98 | *trans*-2-butene | 1.42 | *i*-pentane | 3.32 |

*(to be continued)*

*Table 5.4 continued*

| Rank | HT (Rural) | | C/W (Residential) | | TW (Industrial) | | MK (Roadside) | |
|---|---|---|---|---|---|---|---|---|
| $O_3$ Formation in MIR (in μg/m3) | | | | | | | | |
| 1 | Isoprene | 11.62 | Toluene | 34.20 | Toluene | 35.49 | Toluene | 83.70 |
| 2 | Toluene | 9.04 | Propene | 13.05 | Propene | 18.47 | Propene | 45.28 |
| 3 | 1-butene / *i*-butene | 7.81 | *m,p*-xylene | 12.26 | 1-butene / *i*-butene | 17.39 | *m,p*-xylene | 37.33 |
| 4 | Propene | 5.57 | 1-butene/ *i*-butene | 11.80 | *m,p*-xylene | 14.53 | 1-Butene / *i*-butene | 36.41 |
| 5 | 2-methylpentane | 2.83 | Isoprene | 7.51 | Isoprene | 10.90 | *i*-pentane | 18.20 |
| 6 | *m,p*-xylene | 2.65 | *n*-butane | 5.28 | *n*-butane | 8.63 | Isoprene | 16.46 |
| 7 | *i*-pentane | 2.42 | 2-methylpentane | 5.07 | *i*-pentane | 6.40 | *n*-butane | 15.81 |
| 8 | *n*-butane | 2.13 | *i*-pentane | 4.14 | 1,2,4-trimethylbenzene | 5.97 | 2-methyl-2-butene | 15.18 |
| 9 | 1-pentene | 1.81 | 1,2,4-trimethylbenzene | 3.79 | 2-methylpentane | 4.86 | 1,3-butadiene | 13.08 |
| 10 | *i*-butane | 1.28 | *o*-xylene | 3.60 | 1,3-butadiene | 4.42 | 1,2,4-trimethylbenzene | 12.22 |

Taking into consideration its reaction rate with OH, isoprene was the most dominant NMHC at HT, C/W and TW sites. It also occupied a very high position at the roadside site even though its mass concentration was low at this site. Other NMHC like 1-butene/*i*-butene, toluene, 2-methyl-2-butene, propene, 2-methyl-1-butene and *m,p*-xylene were also important in terms of their OH-reactivity. As expected, 1,3-butadiene was not in the top 10 list at the rural site reflecting a less significant contribution from vehicular exhaust. In general, alkenes especially isoprene accounted for a major proportion of NMHC's reactivity in HK. Isoprene was also found to be the highest ranking hydrocarbon in Atlanta in terms of the OH-reactivity (NRC, 1991). By comparison, toluene and *m,p*-xylene were the most important species in cities like the Greater Munich Area (Rappenglück and Fabian, 1999) and Seoul (Na et al., 2003).

Ranking with respect to $O_3$ formation (MIR) yielded results which were quite different from those based on reactions with OH (see Table 5.4). The largest contributor to $O_3$ formation was isoprene at the rural site and toluene at the other three urban sites. Overall, toluene, propene, *m,p*-xylene, isoprene and 1-butene/*i*-butene played a significant role on $O_3$ formation in HK. Similar results were also found in Karachi (Barletta et al., 2002) and Porto Alegre (Grosjean et al., 1998) with toluene, propene and *m,p*-xylene as the major contributors to the production of photochemical $O_3$ in these areas.

Overall, the largest value for mass concentration, OH-reactivity (PE), and $O_3$ formation (MIR) was all found at the roadside site, suggesting the dominant impact of vehicular emissions on photochemical reactivity in HK. The highest $O_3$ formation potential of toluene at the three urban sites was attributed to the widespread use of toluene-rich solvent and unleaded fuels in HK. Although the concentration of isoprene was lower than that of other NMHC in HK, it was an important species in terms of OH-reactivity and $O_3$ formation, especially in the rural area.

## 5.6 Chapter Summary

In this chapter, a comprehensive data set on $C_3$-$C_{12}$ hydrocarbons obtained in four sites (rural, residential, industrial and roadside) was examined for their spatial distribution, seasonal variation, source-receptor relationships and photochemical reactivity of NMHC. As expected, the roadside site showed the highest level of NMHC owing to the fresh emissions from vehicle exhausts, and the rural site was characterized by the aged air mass with the lowest NMHC concentrations. The seasonal variations of NMHC were different at different sites. For the rural site, NMHC had the lowest level in summer but higher concentrations in other seasons. The roadside site had the highest NMHC level in summer due to the strong fuel evaporation. In general, the average NMHC levels in HK were comparatively lower to those of other cities. However, a relatively high level of isoprene was observed in HK, especially in the roadside area. Isoprene was found to mainly come from vehicular sources at the roadside site, whereas biogenic emission was the major source of isoprene at the rural site.

Ratios of total NMHC to $NO_x$ were about 2-3 in the urban areas and 10 at the rural site, suggesting that the formation of $O_3$ in HK is generally sensitive to NMHC. Among NMHC, toluene was the most abundant species on a carbon basis and also a leading contributor to $O_3$ production, especially in the urban areas. Toluene could be produced from various kinds of sources and a detailed source apportionment of toluene is needed. Guo et al. (2004) applied a receptor-oriented source apportionment models to identify sources of ambient air pollutants and to estimate source contributions to air pollutant concentrations at two urban sites (TW and C/W) in HK. The results indicated that use of solvent, vehicle exhaust, natural gas usage and industrial sources are the major sources of toluene and related aromatic hydrocarbons in HK. To better understand the variation of emission sources over the territory with different emission characteristics, further work on the source apportionment of various VOC, not only in urban but also in rural and roadside areas, is recommended.

Isoprene, despite having a low mass concentration compared to other NMHC, had a high PE value and was a key precursor contributing to $O_3$ formation especially in the rural area. As isoprene can be generated from both anthropogenic and biogenic sources, the relative contribution of different sources to isoprene at different sites should be estimated. Having reviewed the general local VOC data, the next chapter will further study $C_1$ to $C_8$ NMHC in order to provide us with insights into the atmospheric processing in the HK atmosphere.

# CHAPTER 6 STUDY OF $C_1$ TO $C_8$ HYDROCARBONS IN HONG KONG DURING 2002/2003

Chapter 5 examined the spatial distribution, seasonal variation, source-receptor relationships and photochemical reactivity of $C_3$ to $C_{12}$ hydrocarbons at four different HK sites (rural, residential, industrial and roadside), using the data set provided by the GL. The GL's data set has its limitations of a higher detection limit (of 20 pptv) and a lower sensitivity (e.g. butane for *i/n*-butane; pentane for *i/n*-pentane; *m,p*-xylene for *m*-xylene and *p*-xylene) as compared to other international testing laboratories (Apel et al., 2003). Moreover, the GL could not provide the mixing ratios of hydrocarbons with one or two carbon atoms of air samples which are important indicators of atmospheric processing. To reconfirm the VOC patterns given by the GL's data set, it is worth using another VOC data set including $C_1$ and $C_2$ hydrocarbons which are analyzed with a higher sensitivity and a lower detection limit. Such an additional data set is also useful in filling our data gap of reactive hydrocarbons (with low carbon numbers) and their ratios to other trace gases (e.g. propane/ethane, ethene/ethane, ethyne/CO), which have been widely used to assess the atmospheric processing in an area (Smyth et al., 1999; Wang et al., 2003a). As a corollary, our knowledge on the participation of different VOC on the atmospheric processing could be enhanced.

This chapter will therefore focus on the atmospheric processes over HK by examining the measurement data from another comprehensive 12-month sampling of CO, methane ($CH_4$) and $C_2$ to $C_8$ NMHC at the four different HK sites, namely Tap Mun (TM), Central/Western (C/W), Tung Chung (TC) and Yuen Long (YL), from September 2002 to August 2003. The data set could supplement the VOC information of Chapter 5 by providing additional VOC information from sites with different characteristics. The findings of this chapter are summarized on a paper titled "$C_1$ to $C_8$ Volatile Organic Compounds in the Atmosphere of Hong Kong: Overview of Atmospheric Processing and Source Apportionment" (Guo et al., 2007).

Site information and distribution of the four sites has been given in Table 3.2 and Figure 3.1. In brief, TM is a remote island just off the northeast coast of HK, which could receive the regional air mass under the prevailing northeasterly wind. YL is a new town and highly affected by the PRD emissions subject to its close proximity to Shenzhen. Under the prevailing northwesterly wind, TC is under a significant influence due to the emissions from the Chek Lap Kok airport and Guangdong Province.

During the period, 24-hour samples of VOC were collected at the four sites once every six days and a total of 248 canisters were sent to the UCI for analysis with a detection limit of 3 pptv. Corresponding measurement of $O_3$, $SO_2$ and $NO_2$ at the four stations will also assist in our analysis of the VOC results.

## 6.1 Overall Description: Spatial and Seasonal Patterns

Table 6.1 summarizes the statistics of $O_3$, $SO_2$, $NO_2$, CO, $CH_4$, and major NMHCs during the measurement campaign. YL was found to have the highest levels of all VOC except isoprene, while TM had the lowest levels of all VOC except isoprene, which was highest. The VOC levels at the other two sites (TC and C/W) were similar, though with levels at TC somewhat lower than those of C/W, and in between the two extremes of TM and YL. The maximum VOC levels at YL are likely attributed to strong local urban activities and regional pollutants from the PRD industrial region - which has recently experienced astonishing economic and industrial developments - especially under the prevailing northwesterly wind during the seasonally high pollution period. C/W and TC are typical urban and suburban areas, respectively, and their ambient VOC levels represent the general VOC patterns in HK. The somewhat lower VOC levels at TC compared to C/W suggest an insignificant VOC contribution to TC from the nearby aircraft activities. TM is a rural area without major anthropogenic sources and generally has the lowest VOC levels compared to the other three sites. It is noteworthy that high levels of some very short-lived gases (e.g. isoprene) found at TM were due to the biogenic emissions. The highest $O_3$ level was also found at TM, which is attributed to regional chemical and transport processes (So and Wang, 2003).

*Table 6.1 Statistics (average and standard deviation (S.D.)) of trace gases and selected NMHC measured from September 2002 to August 2003 at the four sites (There were 62 canisters samples at each site and units are in pptv unless otherwise specified)*

| | TM | | | C/W | | | TC | | | YL | | |
|---|---|---|---|---|---|---|---|---|---|---|---|---|
| | Average | ± | S.D. | Average | ± | S.D. | Average | ± | S.D. | Average | ± | S.D. |
| Continuously measured trace gases (unit) | | | | | | | | | | | | |
| $O_3$ (ppbv) | 31.6 | ± | 14.5 | 20.0 | ± | 12.1 | 20.1 | ± | 11.6 | 15.3 | ± | 8.5 |
| $SO_2$ (ppbv) | 4.3 | ± | 2.6 | 6.4 | ± | 4.5 | 5.5 | ± | 5.0 | 6.2 | ± | 4.7 |
| $NO_2$ (ppbv) | 6.7 | ± | 4.2 | 24.8 | ± | 11.8 | 21.1 | ± | 13.0 | 29.1 | ± | 11.7 |
| Canisters samples of CO and VOC (unit) | | | | | | | | | | | | |
| CO (ppbv) | 310 | ± | 162 | 376 | ± | 173 | 351 | ± | 207 | 511 | ± | 236 |
| $CH_4$ (ppmv) | 1.888 | ± | 0.077 | 1.925 | ± | 0.101 | 1.901 | ± | 0.119 | 2.024 | ± | 0.176 |

*(to be continued)*

*Table 6.1 continued*

| | TM | | | C/W | | | TC | | | YL | | |
|---|---|---|---|---|---|---|---|---|---|---|---|---|
| | Average | ± | S.D. | Average | ± | S.D. | Average | ± | S.D. | Average | ± | S.D. |
| Ethane | 1787 | ± | 1088 | 1829 | ± | 1055 | 1724 | ± | 1102 | 2116 | ± | 1207 |
| Propane | 861 | ± | 569 | 1595 | ± | 874 | 1196 | ± | 1069 | 2545 | ± | 1598 |
| *i*-butane | 341 | ± | 229 | 899 | ± | 392 | 502 | ± | 410 | 1461 | ± | 731 |
| *n*-butane | 592 | ± | 386 | 1464 | ± | 644 | 951 | ± | 851 | 2625 | ± | 1432 |
| *i*-pentane | 369 | ± | 206 | 519 | ± | 251 | 450 | ± | 364 | 1143 | ± | 565 |
| *n*-pentane | 172 | ± | 105 | 250 | ± | 128 | 230 | ± | 197 | 541 | ± | 307 |
| Ethene | 859 | ± | 576 | 1465 | ± | 784 | 1297 | ± | 1041 | 2674 | ± | 1416 |
| Propene | 141 | ± | 85 | 315 | ± | 144 | 246 | ± | 166 | 606 | ± | 301 |
| *i*-butene | 114 | ± | 88 | 173 | ± | 106 | 140 | ± | 112 | 344 | ± | 141 |

*(to be continued)*

*Table 6.1 continued*

| | TM | | | C/W | | | TC | | | YL | | |
|---|---|---|---|---|---|---|---|---|---|---|---|---|
| | Average | ± | S.D. | Average | ± | S.D. | Average | ± | S.D. | Average | ± | S.D. |
| 1-butene | 52 | ± | 28 | 92 | ± | 46 | 75 | ± | 55 | 193 | ± | 96 |
| Isoprene | 334 | ± | 324 | 178 | ± | 186 | 148 | ± | 119 | 192 | ± | 96 |
| 1,3-butadiene | 19 | ± | 12 | 48 | ± | 25 | 38 | ± | 30 | 106 | ± | 54 |
| Ethyne | 1365 | ± | 940 | 1950 | ± | 1122 | 1768 | ± | 1422 | 2872 | ± | 1849 |
| Benzene | 402 | ± | 289 | 417 | ± | 280 | 464 | ± | 406 | 731 | ± | 477 |
| Toluene | 1033 | ± | 959 | 2765 | ± | 1690 | 2265 | ± | 2769 | 4340 | ± | 3499 |
| *o*-xylene | 57 | ± | 59 | 222 | ± | 157 | 163 | ± | 201 | 306 | ± | 245 |
| *m*-xylene | 95 | ± | 106 | 445 | ± | 350 | 311 | ± | 432 | 590 | ± | 524 |
| *p*-xylene | 62 | ± | 72 | 258 | ± | 184 | 178 | ± | 218 | 340 | ± | 280 |
| Ethylbenzene | 123 | ± | 134 | 395 | ± | 350 | 346 | ± | 486 | 545 | ± | 512 |

The seasonal variation of air pollutants in HK is greatly affected by the Asian monsoons, which bring in clean maritime air and unstable weather in summer and pollutant-laden continental air in winter. In general, higher NMHC concentrations were observed in winter, with lower NMHC levels in summer, consistent with the observations given in Chapter 5. Toluene is highlighted for comparison because of its relatively high abundance and variety of sources. Figure 6.1a shows the monthly average concentrations of toluene at the four sites. The winter-to-summer difference of toluene levels was largest at YL, indicating stronger local/regional sources of toluene during winter months at YL than at C/W and TC. By comparison, there was no obvious seasonal variation of toluene at TM, suggesting an insignificant seasonal effect at this rural site. However, the pattern of isoprene is different to those of toluene and other NMHC (see Figure 6.1b). The highest isoprene level was found at TM during the summertime which could be explained by the significant biogenic sources of isoprene in the rural TM area, and by the higher temperature during the summertime that accelerates the biogenic emission giving higher isoprene levels. The overall seasonal patterns of isoprene at the four sites were similar, i.e. higher level in summer and lower level in winter. It revealed that isoprene at the four sites were major contributed to the biogenic emission. Additional study on the relative contribution from biogenic and vehicular emissions is recommended.

To reconfirm the GL's VOC data as given in Chapter 5, it is of interest to compare the VOC samples measured at the same site (C/W) but analyzed by different laboratories (GL and UCI). Table 6.2 compares the annual averages (from September 2002 to August 2003) of selected hydrocarbons in C/W analyzed by the two laboratories. The two data sets are of comparable magnitude and no significant difference exists among the collocated samples. Subject to the presence of $C_2$ hydrocarbons (ethane, ethane and ethyne), the UCI's data set will be mainly used to study the atmospheric processing over HK in the following section.

*Table 6.2 Comparison of the annual averages (from September 2002 to August 2003) of selected hydrocarbons in Central/Western analyzed by the GL and UCI*

| Laboratory | GL | | | UCI | | |
|---|---|---|---|---|---|---|
| Hydrocarbons (in pptv) | Average | ± | S.D. | Average | ± | S.D. |
| Propane | 1796 | ± | 1316 | 1595 | ± | 874 |
| Propene | 448 | ± | 256 | 315 | ± | 144 |
| Isoprene | 260 | ± | 271 | 178 | ± | 186 |
| 1,3-butadiene | 81 | ± | 44 | 48 | ± | 25 |
| Benzene | 473 | ± | 315 | 417 | ± | 280 |
| Toluene | 2595 | ± | 1875 | 2765 | ± | 1690 |
| Ethylbenzene | 274 | ± | 259 | 395 | ± | 350 |

*Figure 6.1 Monthly averages of (a) toluene and (b) isoprene from September 2002 to August 2003 at the four sites in HK.*

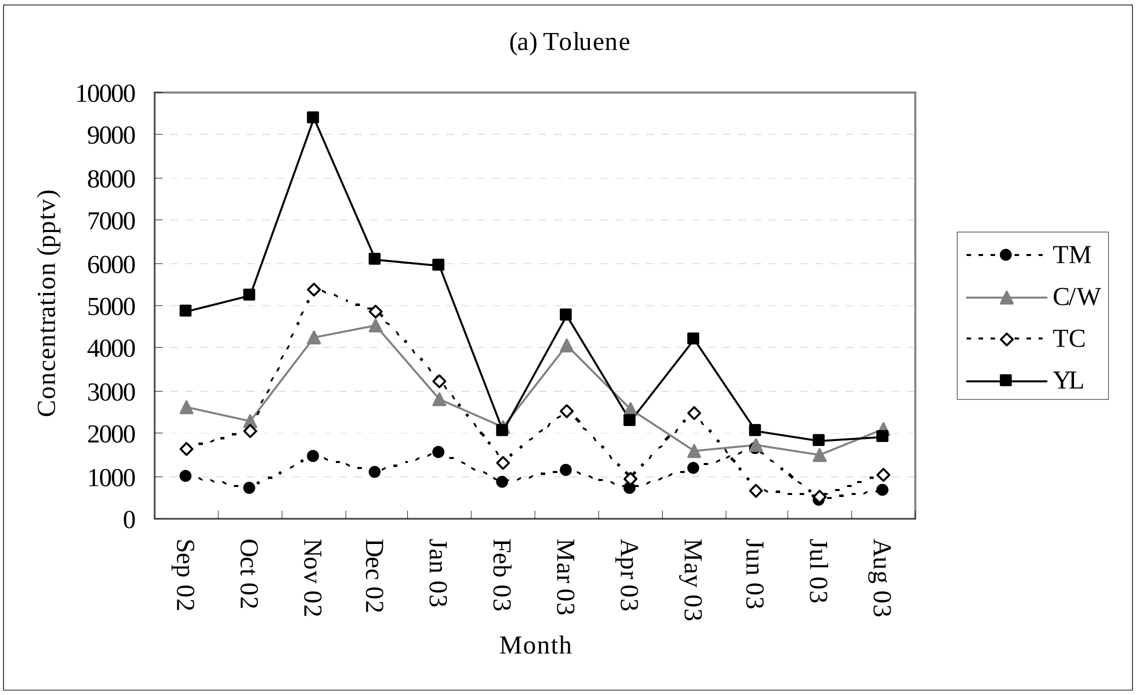

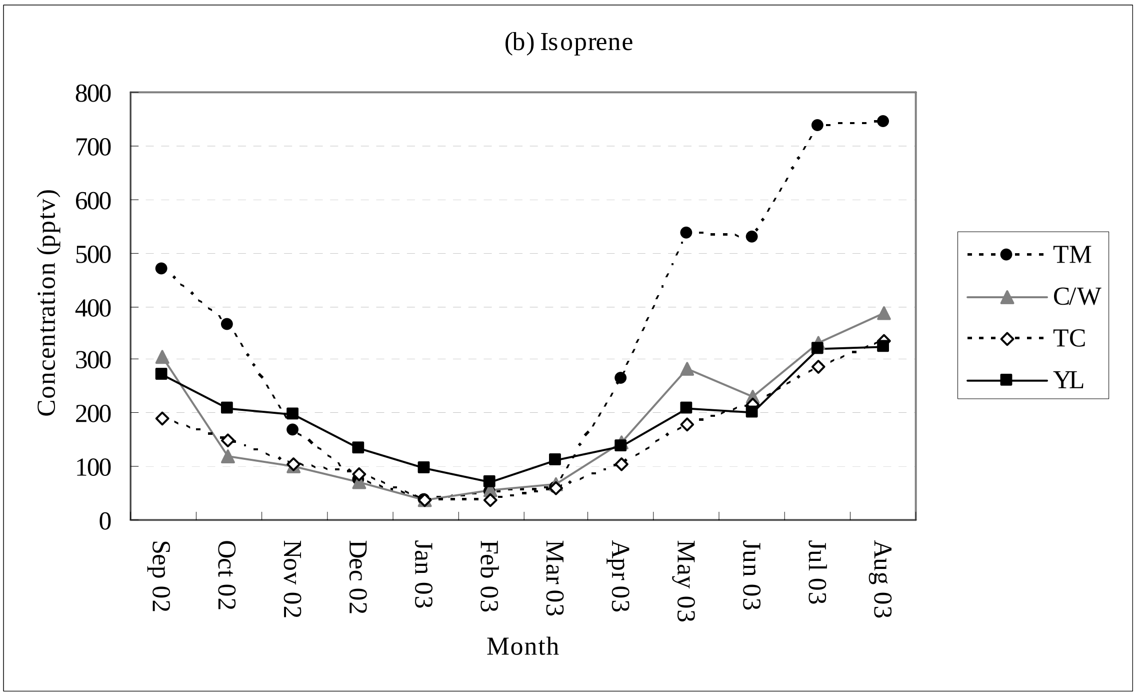

## 6.2 Atmospheric Processing of Air Masses Impacting Hong Kong

### *6.2.1 VOC Ratios*

As discussed in Chapter 5, ratios of VOC with different photochemical lifetimes can help estimate the relative ages of air masses and provide evidence of air mass transport. Moreover, this ratio analysis can indicate whether the site is dominantly affected by pollutants from local or regional sources. Ratios of propane / ethane and ethene / ethane have been widely used as a measure of atmospheric processing in different air masses (e.g. Nelson and Quigley, 1983; Smyth et al., 1999; So and Wang, 2004). Figure 6.2 (a and b) illustrates the box plots for the two pairs of hydrocarbons at the four sites. As expected, TM has the relatively lowest ratios among the sites, indicating the characteristics of a rural site with more influence of photochemically aged air masses. The average value of propane / ethane at the rural TM site (0.50 pptv/pptv) is close to the value of 0.47 pptv/pptv measured at the rural Linan site in eastern China (Wang et al., 2002). However, such level is much higher than the ratio of 0.1 pptv/pptv for several day-old combustion emissions (Talbot et al., 1996) which may be explained by the use of LPG (major source of propane) by the villagers in TM. In contrast, the highest average ratios were found in YL, suggesting that the site is mainly affected by rather fresh local emissions. The findings reveal the contribution of various sources and indicate a different mix of VOC patterns among the sites.

*Figure 6.2* *Box plots of (a) propane / ethane and (b) ethene / ethane ratios from September 2002 to August 2003 at the four sites in HK. Whiskers indicate the minimum and maximum values and box indicates 25th – 75th percentile range with line for median.*

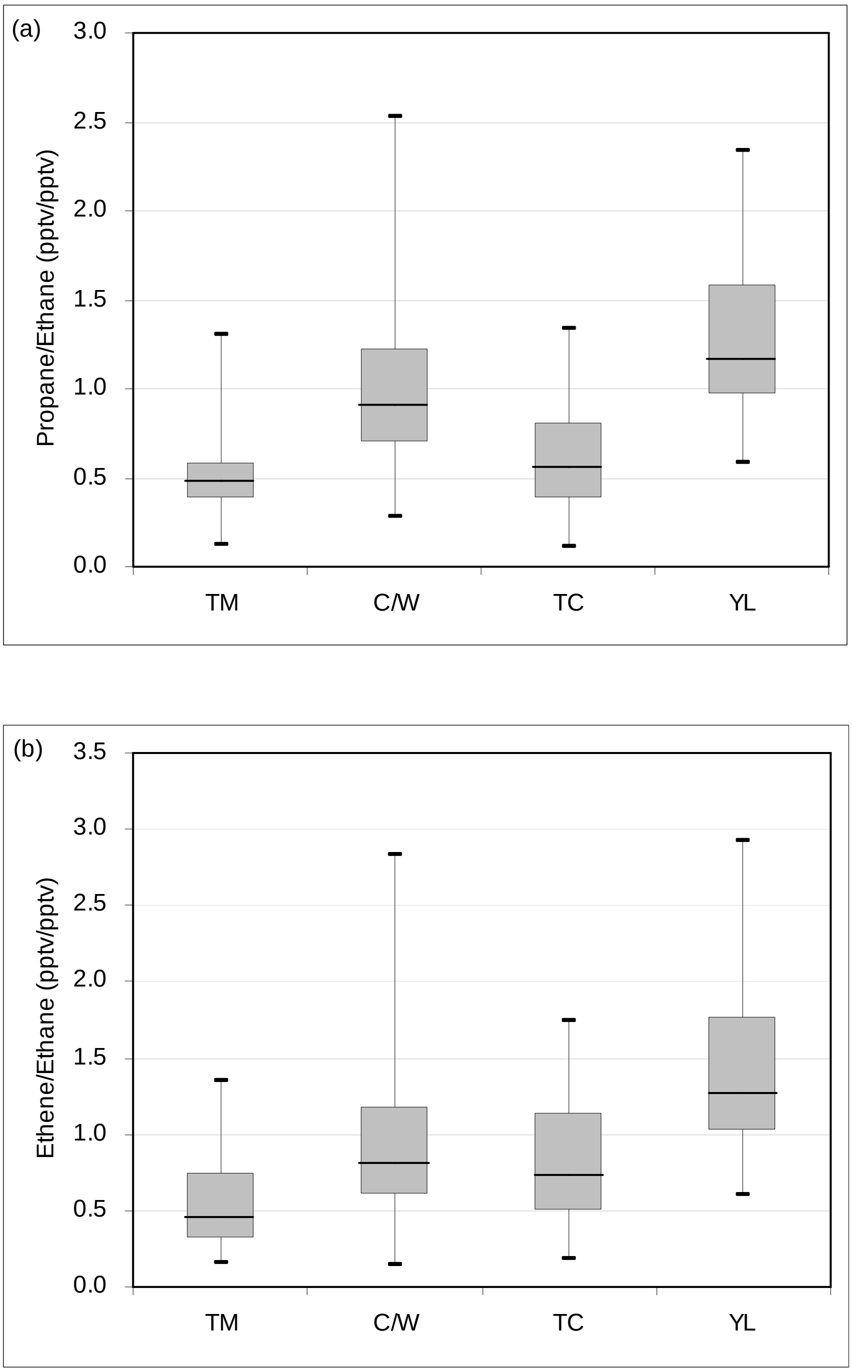

### *6.2.2 Hydrocarbons versus CO*

CO is generally emitted from incomplete combustion of fossil fuel in urban areas. Examining the relationship of CO and hydrocarbons can provide useful information on their sources and emission signatures (Wang et al., 2002; 2003a). Figures 6.3 and 6.4 show the scatter plots of CO versus ethyne and CO versus isoprene for the sites, respectively. The scatter plots show very different emission patterns at the four sites. Among the hydrocarbons measured, ethyne was best correlated with CO ($R^2$ range from 0.91 to 0.93), confirming a common source origin in HK. The ratios range from 5.6 pptv/ppbv of TM to 7.5 pptv/ppbv of YL (see Figure 6.3), indicating a more fresh air mass at YL. The ratio at the rural site is close to that of a remote southeastern coastal site in HK (5.3 pptv/ppbv, $R^2$ =0.93 of Hok Tsui, HT), suggesting a background ratio of 5.3 to 5.6 in HK (Wang et al., 2003a). By comparing the ratio of 2.1 pptv/ppbv based on airborne results during the SOS 1995 Nashville Study (Goldan et al. 2000), this ratio (of 5.6 pptv/ppbv) may represent unprocessed air and show the presence of fresh combustion emissions throughout the HK area.

Isoprene is known to be emitted from biogenic sources (e.g. Jobson et al., 1994) but there are also studies of the contribution of isoprene from vehicular exhausts (e.g. Borbon et al., 2001; Barletta et al., 2002; So and Wang, 2004). Here, the poor correlation between isoprene and CO (see Figure 6.4) suggested that isoprene was emitted from sources other than mobile emissions at the four sites, pointing mainly to a biogenic source. From

Section 6.1, the highest isoprene level at the rural TM site reflects the influence of biogenic isoprene emissions.

*Figure 6.3 Scatter plots of CO with ethyne from September 2002 to August 2003 at the four sites in HK.*

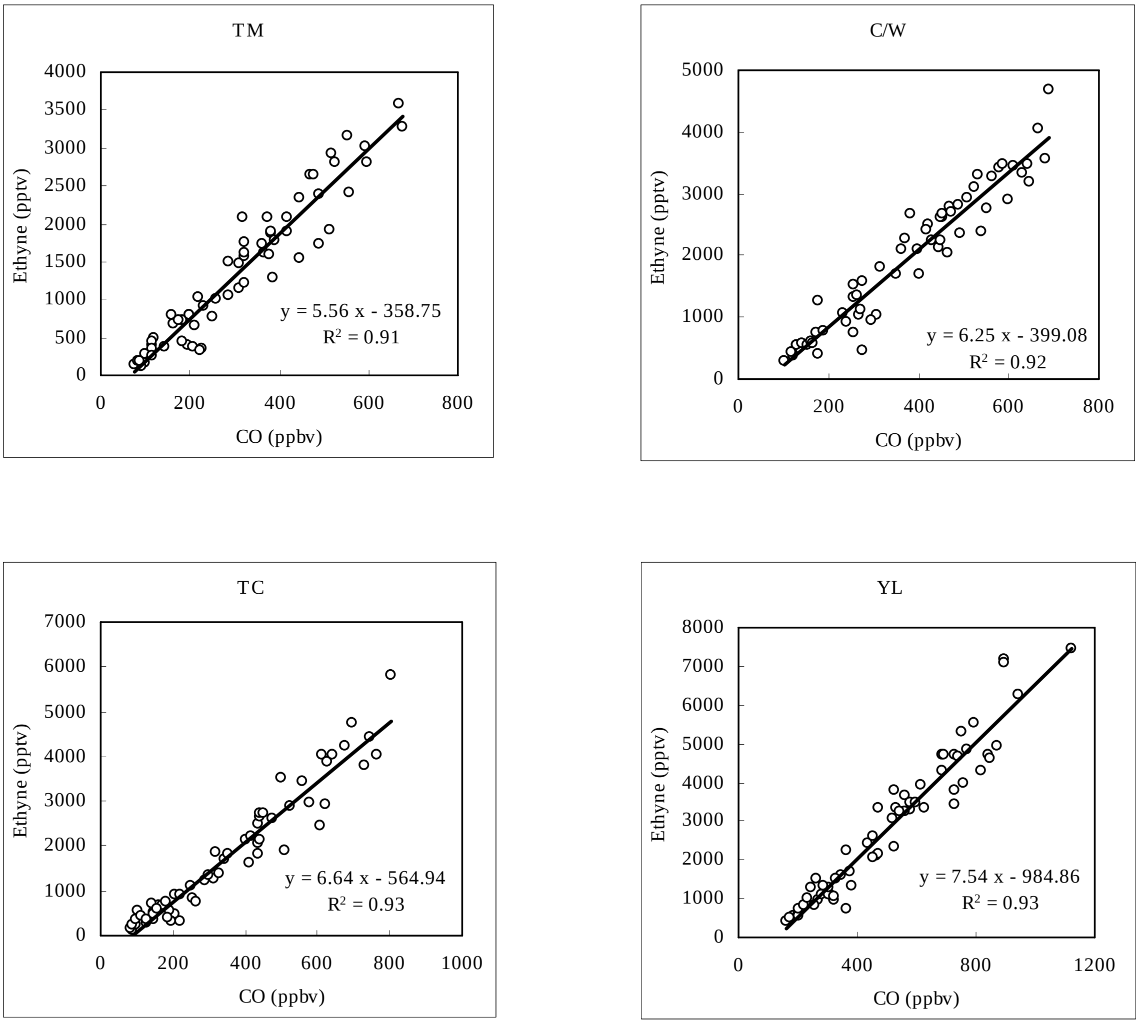

*Figure 6.4 Scatter plots of CO with isoprene from September 2002 to August 2003 at the four sites in HK.*

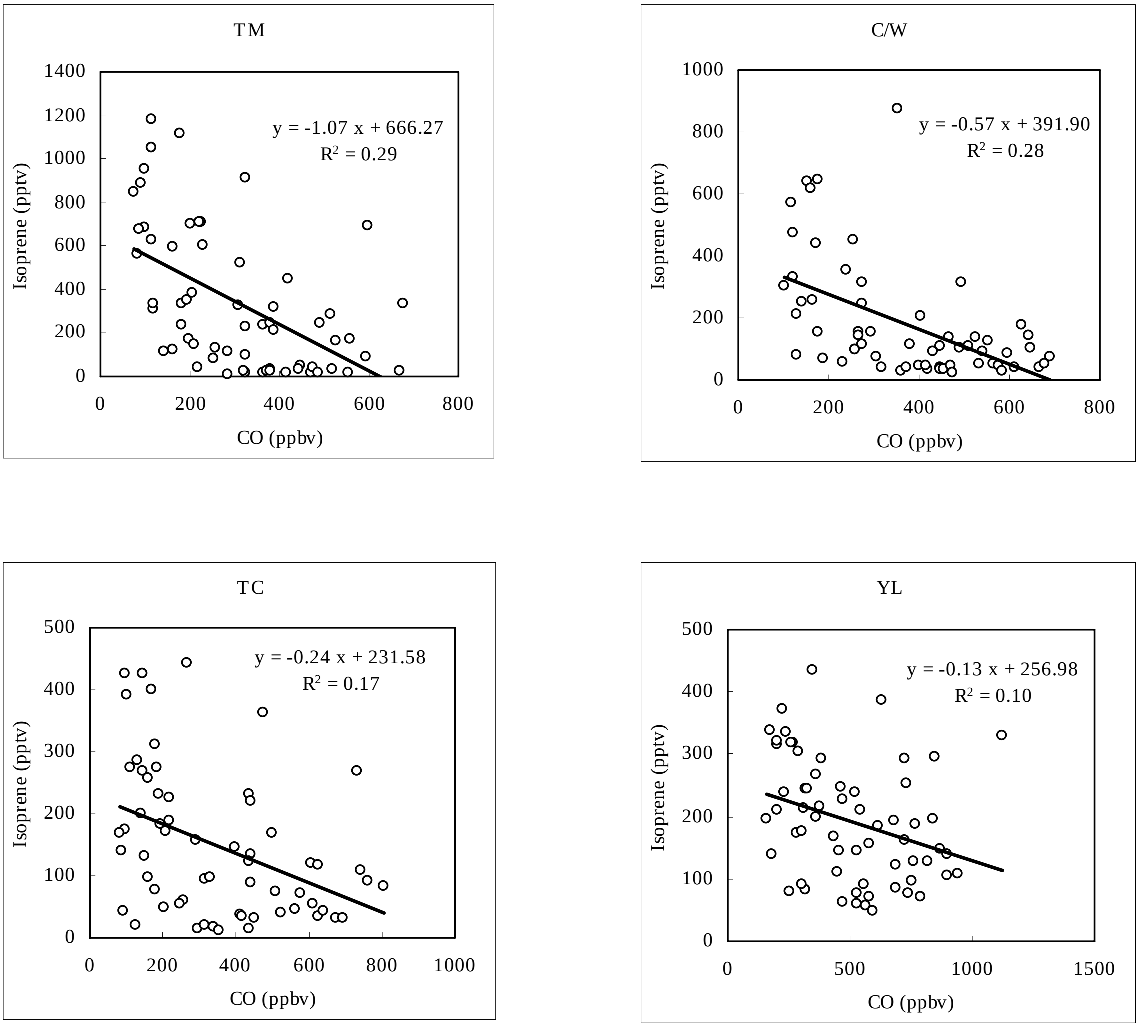

### *6.2.3 Relations to Ethyne / CO and Propane / Ethane*

The ratios of ethyne / CO and propane / ethane have been used as a measure of atmospheric processing within an air mass (Smyth et al., 1999; Wang et al., 2003a). The relationship between certain trace gases ($O_3$, CO, $SO_2$ and $NO_2$) and these two ratios can further provide insights into these pollutants emission sources. Figures 6.5 and 6.6 show the scatter plots of $O_3$, CO, $SO_2$ and $NO_2$ versus the ratios of ethyne / CO and propane / ethane at the rural TM site, respectively. There are no clear relationships (low $R^2$) between these trace gases and ratios, suggesting the influence of mixed local and regional pollutants at the rural site. By comparison, similar results were also reported for another rural coastal site (HT) in HK, with little or no relationships between these ratios and trace gases (Wang et al., 2003a). The two rural sites are respectively located on the northeastern and southeastern parts of HK and the results suggested that the whole territory was influenced by both air pollutants of long-range transport and local emissions.

*Figure 6.5 Scatter plots of $O_3$, CO, $SO_2$ and $NO_2$ with ethyne / CO at the rural TM.*

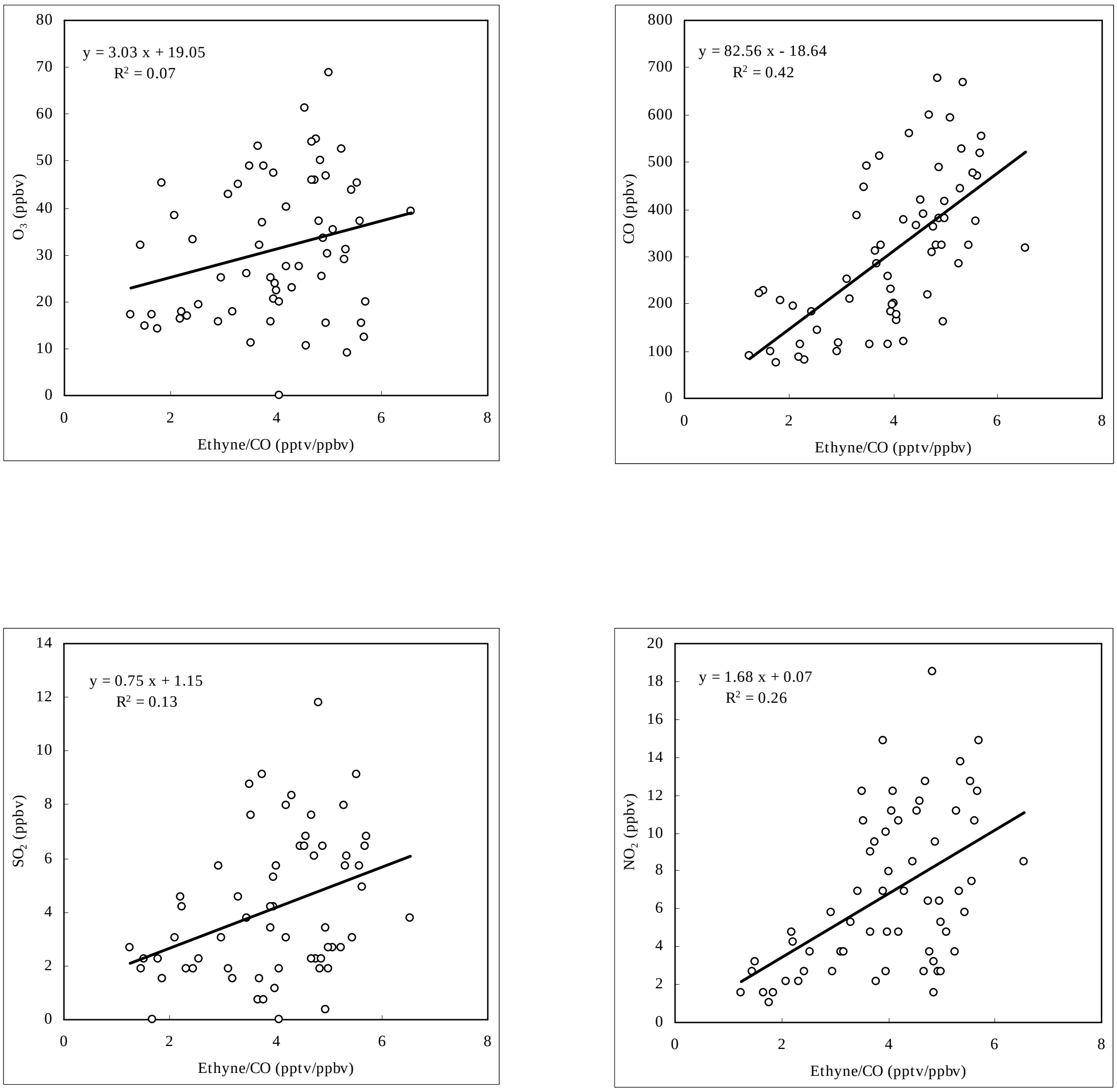

*Figure 6.6 Scatter plots of $O_3$, CO, $SO_2$ and $NO_2$ with propane / ethane at the rural TM.*

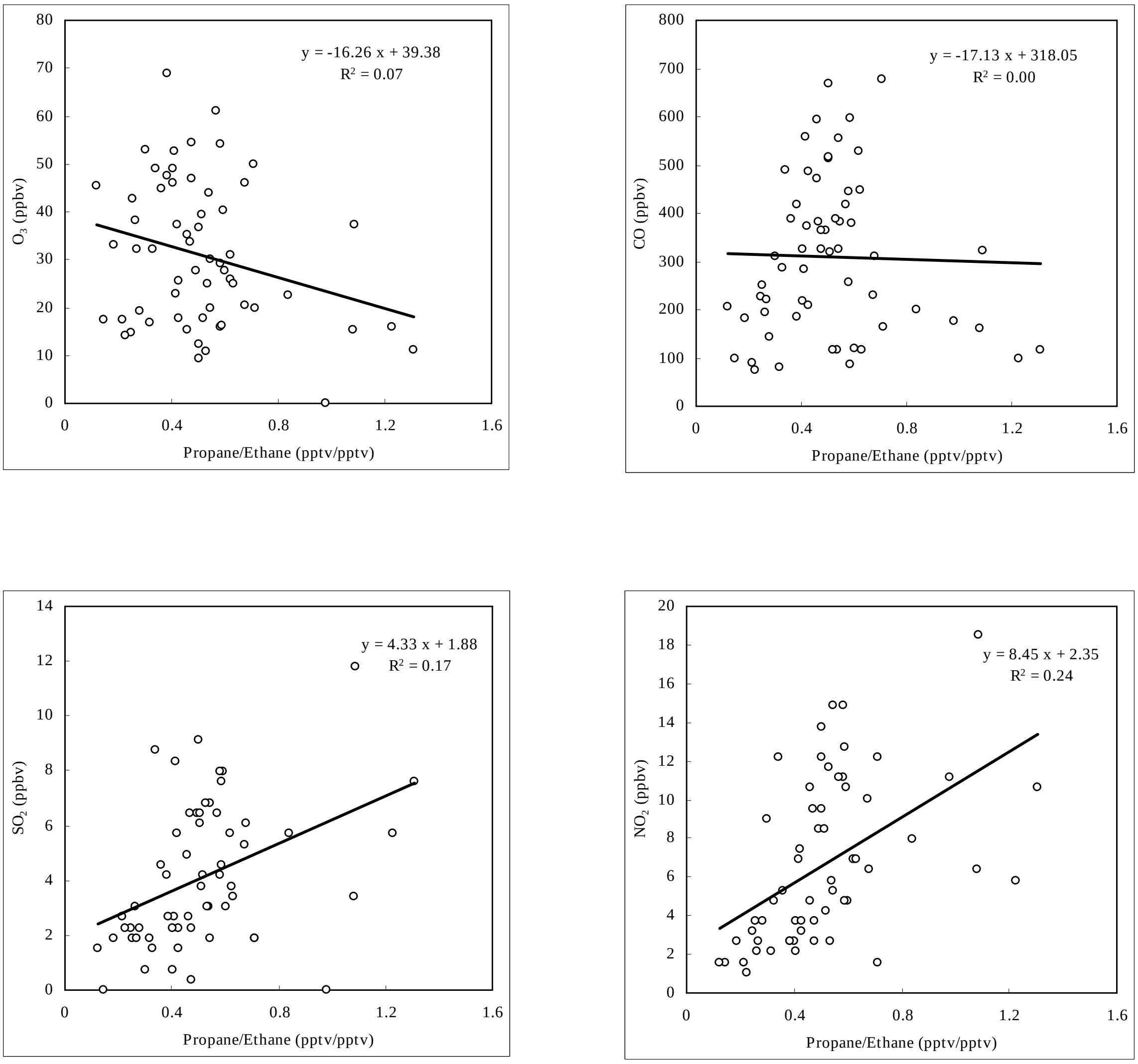

## 6.3 Chapter Summary

Analysis of $C_1$ to $C_8$ hydrocarbons data from September 2002 to August 2003 at four different HK sites provided further information about the variation of VOC patterns in the territory. In a similar way to the seasonal pattern of general air quality, higher VOC levels were observed in wintertime with lower results during summertime, in response to air circulation patterns driven by the Asian monsoons. In contrast, isoprene was an exceptional parameter with a higher level at the rural site in summer because of its sources from biogenic emissions. Negative and poor relationships of isoprene with CO further revealed that isoprene was not largely emitted from combustion sources at the rural TM site.

The concurrent measurement of VOC and other selected trace gases yielded important insights into the interspecies relationships and emission characteristics among the four sites. Ratios between VOC with different photochemical reactivities showed the mix of emission sources and the increase of atmospheric processing from urban to rural areas. Compared to respective results in overseas rural areas, higher ethyne / CO ratio (of 5.6 pptv/ppbv at TM) showed that the subtropical city was influenced by a rather freshly mixed local and regional pollution. In summary, Chapters 5 and 6 display a comprehensive VOC picture of HK which is essential to our understanding of the photochemical $O_3$ production. The next chapter will attempt to further study the roles of VOC in controlling the $O_3$ formation in HK and also the PRD region.

# CHAPTER 7 ROLES OF HYDROCARBONS IN CONTROLLING OZONE FORMATION IN THE PRD

Chapters 5 and 6 presented the overall patterns of VOC in HK. In order to formulate an effective strategy to control regional ground-level $O_3$ pollution, it is essential to understand the roles of VOC in controlling $O_3$ formation in HK. Since $O_3$ pollution is not only generated from local production but also influenced by long-range transport, it is of interest to know the $O_3$–$O_3$ precursors' information at both HK and the PRD sites. Therefore, this chapter will focus on the understanding of the relationship between $O_3$ and its photochemical precursors like $NO_x$ and VOC in the PRD by analyzing the $O_3$ and its precursors measurements obtained at two rural sites (TO and WQS) in the PRD during 2002 and 2004. Tools of photochemical indicators (Sillman, 1995) and an observational-based model (Cardelino and Chameides, 1995) will be used to study the $O_3$-$O_3$ precursors' relationship, aiming at providing useful data on the management of surface $O_3$ pollution in the rapidly developing region. The sensitivity of different VOC in $O_3$ formation will be analyzed in accordance with their sources (stationary, mobile and natural) and photochemical reactivity. The results are significant and summarized on a paper titled "Roles of Volatile Organic Compounds in the Ground-level Photochemical Ozone Production at Two Rural Sites in the Pearl River Delta Region of China" (So et al., manuscript in preparation).

## 7.1 Overview of Measurement Data and Techniques

Trace gases of $O_3$, CO, NO and $NO_y$ in TO and WQS were measured by commercial analyzers with regular calibrations using a NIST traceable standard. Detailed accounts of the respective instruments have been given elsewhere (Wang and Kwok, 2003; Wang et al. 2003b; 2005). The detection limits of $O_3$, CO, NO/$NO_y$ were 2, 30 and 0.05 ppbv for a 2-min average, respectively. In this chapter, hourly averaged values were used for data analysis.

VOC were derived from analyses of whole air samples collected at two sites. Each whole air sample was collected over a one-minute period into a conditioned, evacuated 2-litre stainless steel canister. The samples were then sent to the UCI for chemical analysis including methane ($CH_4$) and $C_2$ to $C_{10}$ NMHC. The detection limits of $CH_4$ and $C_2$ to $C_{10}$ NMHC are 5 ppbv and 3 pptv, respectively, and details of the analytical procedures employed at the UCI laboratory can be referred to elsewhere (Blake et al. 1994; Colman et al., 2001). The VOC sampling strategy emphasized $O_3$ episodes, during which samples were mostly taken every two hours between LST 0700 and 1900 (i.e. seven samples per day).

For TO, measurement data in late summer and autumn (1 September to 30 November 2002) were used in the present study because elevated $O_3$ levels were frequency observed during this period. Within the three months, there were 12 days of 1-hour $O_3$ concentration exceeding 120 ppbv and a maximum value of 203 ppbv was recorded on 7 November 2002. A total of 84 VOC samples were collected at TO.  Measurement data of WQS in late spring / summer (19 April to 28 June 2004) were used and 54 VOC samples were collected for analysis.  During the period, seven days were recorded with elevated $O_3$ levels (1-hour $O_3$ > 120 ppbv) and the highest $O_3$ level of 178 ppbv was measured on 24 May 2004.

The basic statistics of the measured pollutants at the two sites are given in Table 7.1.  Higher averages of $O_3$ were found in TO but WQS had higher averages of CO, NO and $NO_y$.  Among the two sites, higher VOC levels were observed in TO, especially for ethane, propane, butane, toluene and isoprene. By comparison, toluene was the most abundant NMHC at both sites, which is different to other background sites (Lin'an, China and Birmingham, UK) with ethane as the most abundant NMHC (Wang et al, 2004; Hopkins et al., 2005).

Zhang et al. (2004; 2006) also analyzed the TO data set during the autumn period (October to November 2002) and reported their findings on $O_3$ episodes and their precursors' relationship in HK.  They revealed that half of the $O_3$ episodes are indicative of an impact from the PRD.  The following sections will further elucidate the $O_3$-$O_3$ precursors' relationship, study the roles of different $O_3$ precursors and extend the analysis of measurement data to a Guangdong site (WQS).

*Table 7.1 Statistics of trace gases at Tai O (01 September to 30 November 2002) and Wan Qing Sha (19 April to 28 June 2004)*

| Pollutants | Tai O | | Wan Qing Sha | |
|---|---|---|---|---|
| | Average | Standard Deviation | Average | Standard Deviation |
| $O_3$ (ppbv) | 32.0 | 26.1 | 25.6 | 26.0 |
| CO (ppbv) | 424 | 280 | 502 | 414 |
| $NO^a$ (ppbv) | 5.8 | 11.5 | 7.1 | 12.4 |
| $NO_y$ (ppbv) | 26.1 | 22.9 | 31.2 | 26.5 |
| Methane (ppmv) | 2.17 | 0.41 | 2.05 | 0.21 |
| Unit for NMHC: pptv | | | | |
| Ethane | 2672 | 3881 | 1746 | 793 |
| Ethene | 2018 | 2049 | 1720 | 1400 |
| Ethyne | 3237 | 2334 | 2670 | 1809 |
| Propane | 3755 | 8563 | 2268 | 1862 |
| Propene | 282 | 410 | 354 | 359 |

*(to be continued)*

*Table 7.1 continued*

| Pollutants (Unit: pptv) | Tai O | | Wan Qing Sha | |
|---|---|---|---|---|
| | Average | Standard Deviation | Average | Standard Deviation |
| *n*-butane | 3155 | 6658 | 1564 | 1452 |
| *i*-butane | 1584 | 3588 | 793 | 684 |
| *1*-butene | 94 | 148 | 123 | 125 |
| *i*-butene | 170 | 261 | 226 | 376 |
| Benzene | 1112 | 1395 | 1170 | 1080 |
| Toluene | 7880 | 7981 | 5301 | 5547 |
| *o*-xylene | 471 | 778 | 442 | 546 |
| *m*-xylene | 860 | 1735 | 692 | 1080 |
| *p*-xylene | 641 | 1047 | 462 | 624 |
| Ethylbenzene | 1395 | 1761 | 1113 | 1316 |
| 1,2,4-trimethylbenzene | 137 | 225 | 189 | 258 |
| 1,3,5-trimethylbenzene | 50 | 84 | 68 | 60 |
| Isoprene | 364 | 793 | 203 | 189 |

Note: [a] Only data taken between LST 0600 and 1700 were used for the NO statistics here.

## 7.2. Measurement Indicators for $O_3$-$NO_x$-VOC Sensitivity

First, the $O_3$-$NO_x$-VOC sensitivity at the two sites are interpreted by measurement indicators ($NO_y$ and $O_3/NO_y$) as proposed by Sillman (1995) who established the use of measurement indicators to determine the split into VOC-sensitive and $NO_x$-sensitive regimes. Examples are the association of VOC-sensitive chemistry with high afternoon $NO_y$ levels (>20 ppbv) and low ratios of $O_3/NO_y$ (<~6-8 ppbv/ppbv). Table 7.2 shows the mean and median of afternoon (LST 1500 to 1600) $NO_y$ and $O_3/NO_y$ during the measurement period at TO and WQS. The data at LST 1500-1600 is selected because *in-situ* photochemical $O_3$ formation is high in the afternoon period (Sillman and He, 2002). The mean values of $NO_y$ were greater than 20 ppbv and $O_3/NO_y$ were less than 4 ppbv/ppbv, indicating that the $O_3$ formation was VOC-sensitive at both sites. To verify the role of VOC on $O_3$ formation, the relationships with the indicator species for the two sites were further studied with reference to the 3-D simulation results demonstrated by Sillman and He (2002). The principal of their predicted $NO_x$-VOC sensitivity for each location is based on differences between $O_3$ in each model base case and in equivalent scenarios with 25% or 35% reductions in anthropogenic VOC and in $NO_x$. Figure 7.1 presents the scatter plots of $O_3$ versus $NO_y$ and $O_3/NO_y$ versus $O_3$, using the afternoon data (LST 1500 to 1600) collected at the sites, with the $NO_x$-sensitive regimes (elliptic areas) simulated from the 3-D simulation results (Sillman and He, 2002). For both sites, all the points of $O_3$ versus $NO_y$ and $O_3/NO_y$ versus $O_3$ are out of the $NO_x$-sensitive regimes. The correlation between $O_3$ versus $NO_y$ also looks very similar to the $O_3$ versus $NO_y$ in models for VOC-sensitive locations given in Sillman and He (2002). The region of maximum $O_3$, of the $O_3$ versus $NO_y$, is followed by a decrease in $O_3$ as $NO_y$ increases further (see Figures 7.1a and 7.1c). This is evidence that $O_3$ is being inhibited by further $NO_x$ emissions and the $O_3$ formation at the two sites is sensitive to VOC rather than to $NO_x$. Here, the analysis is based on transition values derived from the model results in the US data. The uncertainties of the model and different mix of emissions and meteorological conditions between the PRD and US cities might induce some changes of the transition values. Looking at the results, there can be confidence that $O_3$ formation at the PRD sites is limited by VOC, not $NO_x$.

*Table 7.2 Mean and median of afternoon (LST 1500 to 1600) $NO_y$ and $O_3/NO_y$ at Tai O (01 September to 30 November 2002) and Wan Qing Sha (19 April to 28 June 2004)*

| | Tai O | | Wan Qing Sha | |
|---|---|---|---|---|
| | $NO_y$ (ppbv) | $O_3/NO_y$ (ppbv/ppbv) | $NO_y$ (ppbv) | $O_3/NO_y$ (ppbv/ppbv) |
| Mean | 24.4 | 3.9 | 24.6 | 3.1 |
| Medium | 19.6 | 3.0 | 19.6 | 2.9 |

*Figure 7.1 Plots of $O_3$ versus $NO_y$ and $O_3/NO_y$ versus $O_3$ for afternoon data (LST 1500 to 1600) at Tai O (01 September to 30 November 2002) and at Wan Qing Sha (19 April to 28 June 2004). $NO_x$-sensitive regimes are represented by elliptic circles which are created in accordance with the 3-D simulations given by Sillman and He (2002).*

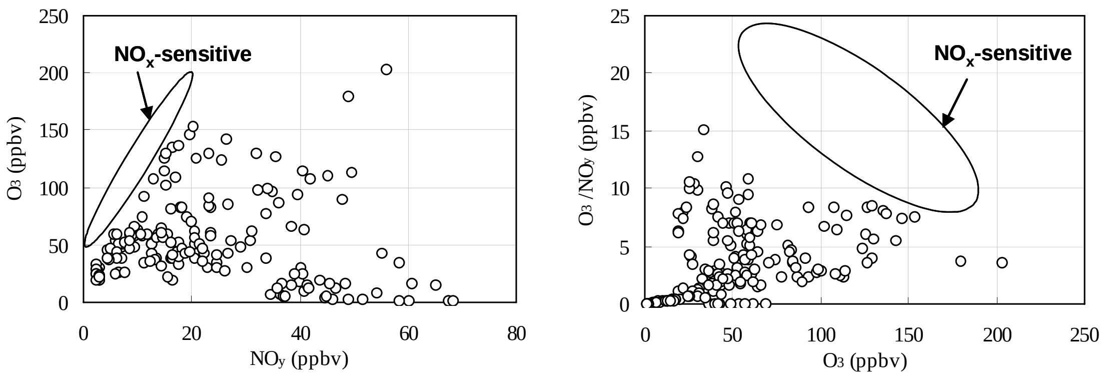

(a) Afternoon O3 versus NOy at Tai O

(b) Afternoon O3/NOy versus O3 at Tai O

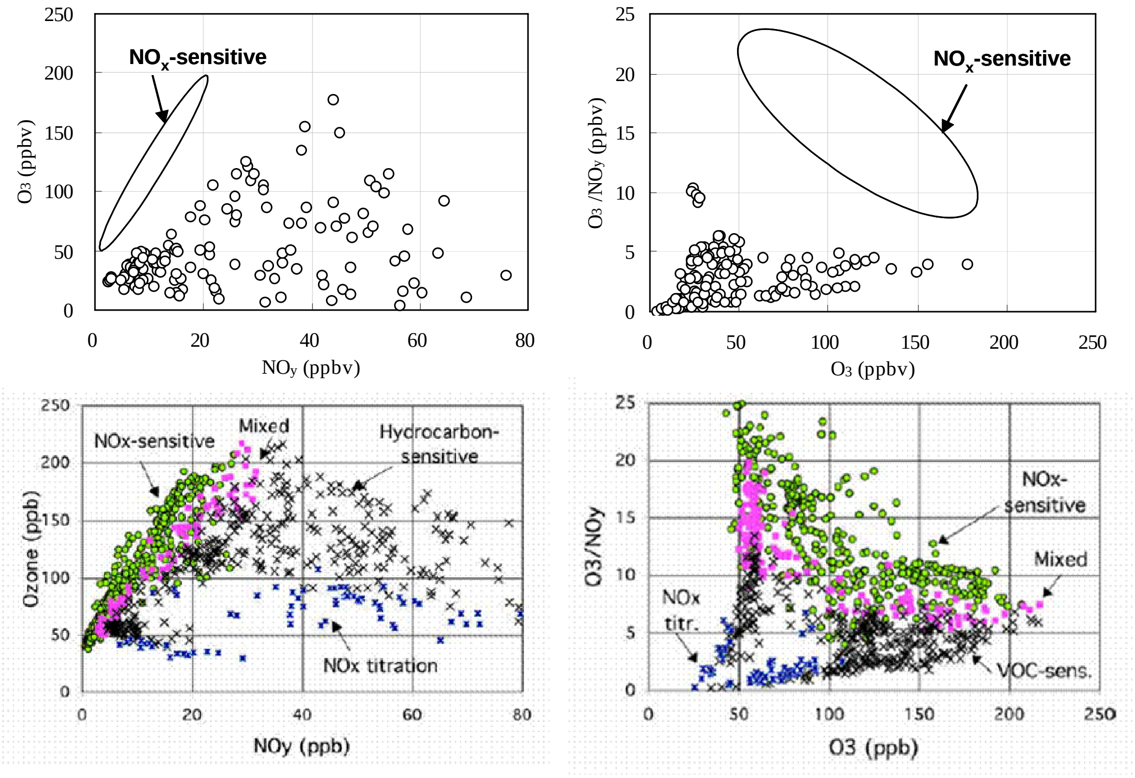

(c) Afternoon O3 versus NOy at Wan Qing Sha

(d) Afternoon O3/NOy versus O3 at Wan Qing Sha

Note: The two coloured figures are extracted from Sillman and He (2002).

## 7.3 Assessment of $O_3$-$NO_x$-VOC Chemistry from OBM Results

Next, the OBM is used to evaluate the $O_3$-$NO_x$-VOC chemistry at the two rural sites. Measurement from eight days at TO and five days at WQS were selected because diurnal VOC samples were collected on those days for OBM analysis. Table 7.3 presents the daytime (LST 0700 to 1900) average RIR values for VOC and NO and maximum 1-hour $O_3$ concentrations of the thirteen days. Positive RIR values for the total hydrocarbons (THC) were found on all days, indicating that the reduction in VOC would reduce the $O_3$ formation. In contrast, negative values of RIR for NO were found on most of the days, suggesting that NO tended to suppress $O_3$ formation. Positive RIR(NO) values were found on a few days, but the values were much smaller than those of RIR(THC), representing the leading role of THC in $O_3$ formation. By comparison, CO should play an insignificant role on $O_3$ formation in view of its very small RIR (CO) magnitude. To summarize, the OBM results revealed that the $O_3$ production at the two rural PRD sites is generally VOC-sensitive, which is similar to those of typical urban sites in HK (So and Wang, 2004). Consistent with our results, Lam et al. (2005) and Huang et al. (2005) also identified the VOC-sensitive regime in HK and Guangdong areas from an $O_3$ episode analyzed by an EBM.

*Table 7.3 OBM-calculated relative incremental reactivities (RIRs) in %/% for CO, NO and THC and daily maximum 1-hour $O_3$ for 13 days at Tai O and Wan Qing Sha*

| **Date and Site** | **RIR(CO) in %/%** | **RIR(NO) in %/%** | **RIR(THC) in %/%** | **Daily Maximum 1-hour $O_3$ in ppbv (Hour: LST)** |
|---|---|---|---|---|
| Tai O (in 2002) | | | | |
| 5 September | 0.00 | 0.29 | 0.73 | 84 (1600) |
| 6 September | 0.01 | 0.17 | 0.75 | 157 (1400) |
| 11 October | 0.03 | -0.21 | 0.83 | 144 (1300) |
| 25 October | 0.14 | -1.23 | 1.21 | 114 (1600) |
| 6 November | 0.15 | -0.71 | 0.80 | 129 (1500) |
| 7 November | 0.07 | -0.36 | 0.91 | 203 (1500) |
| 8 November | 0.08 | -0.65 | 0.95 | 91 (1500) |
| 12 November | 0.10 | -1.54 | 1.37 | 108 (1600) |
| Wan Qing Sha (in 2004) | | | | |
| 20 April | 0.03 | -0.10 | 0.81 | 71 (1200) |
| 17 May | 0.19 | -1.93 | 1.59 | 40 (1300) |
| 18 May | 0.07 | -0.93 | 1.30 | 110 (1600) |
| 23 May | 0.06 | -0.44 | 0.93 | 129 (1600) |
| 24 May | 0.00 | 0.21 | 0.67 | 178 (1500) |

## 7.4 The Relative Importance of VOC Species on Ozone Formation

In this section, the relative importance of different groups of hydrocarbons will be further estimated using the OBM. The THC (46 $C_2$ to $C_{10}$ hydrocarbons) are classified into three groups in terms of their sources, namely stationary hydrocarbons (SHC), mobile hydrocarbons (MHC) and natural hydrocarbons (NHC), in accordance with the apportionment of the VOC given by Zhang et al. (2004) (see Table 7.4). Briefly, the apportionments of the 46 VOC were estimated by using the emission inventories by sector for the year 2000 from a PRD study (CH2M, 2002) and the overseas' speciation profiles. The speciation profiles for each source type were drawn from two major information sources: the USEPA SPECIATE database (USEPA, 2000), and Andreae and Merlet (2001) for open biomass burning. For the first information source, it is assumed that the species profile for a given source type in HK and PRD is identical to the same source type in the West.

Table 7.5 shows the emission inventory of VOC by section for the year 2000 (CH2M, 2002). In view of percentage, a higher anthropogenic emission was estimated from the transport sector in Guangdong Province whereas there was a stronger anthropogenic emission from stationary sectors in HK.

Under the assumption that a given source type in HK and the PRD is identical to the same source type in the West, the speciation profiles for each source type were drawn from two above information sources. Although the assumption may not be reasonable, as there is a complete lack of local VOC emissions test data / profiles for most sources in the HK / PRD's setting, there is no other choice and such an assumption was also used in other PRD's study (Streets et al., 2003). Clearly more measurements of the speciation of VOC sources in China will be needed in the future to solve this issue.

Figure 7.2 lists the detailed RIR results of four days which represents different RIR patterns for various $O_3$ precursors. THC has the highest RIR values, indicating its superior role in controlling $O_3$ production as compared to NO and CO. When we further investigate the roles of different categories of hydrocarbons, quite different pictures are obtained among the four cases. For the case of 5 September 2002 at the coastal site (see Figure 7.2a), RIR (NHC) was much higher than RIR (MHC) and RIR (SHC), demonstrating that NHC (in particular isoprene) was more sensitive than SHC and MHC to $O_3$ production. In contrast, RIR (SHC) and RIR (MHC) accounted for the majority of RIR (THC) on 7 November 2002 (see Figure 7.2b). By comparison, anthropogenic hydrocarbons (AHC=MHC+SHC) played a more important role than NHC in controlling $O_3$ formation at the inland site (see Figures 7.2c and 7.2d). In summary, the above results are quite different to those obtained from the summer data of the US metropolitan areas (Washington DC; Bronx, New York; and Houston, Texas) with similar magnitudes between RIR(AHC) and RIR(NHC) (Cardelino and Chameides, 2000), reflecting the comparable contribution of anthropogenic and natural VOC to the $O_3$ formation in the US cities. It should be borne in mind that the RIR results are controlled by the factors of sampling period (summer versus winter) and locations. The different RIR results for various VOC sources among the local and overseas sites reveal that the relative efficacy of $O_3$ mitigation strategy depends much on the specific chemical characteristics of the areas.

*Figure 7.2 OBM-calculated daytime average RIRs for CO, NO, THC, SHC, MHC and NHC for (a) Tai O on 5 September 2002; (b) Tai O on 7 November 2002; (c) Wan Qing Sha on 17 May 2004; and (d) Wan Qing Sha on 24 May 2004.*

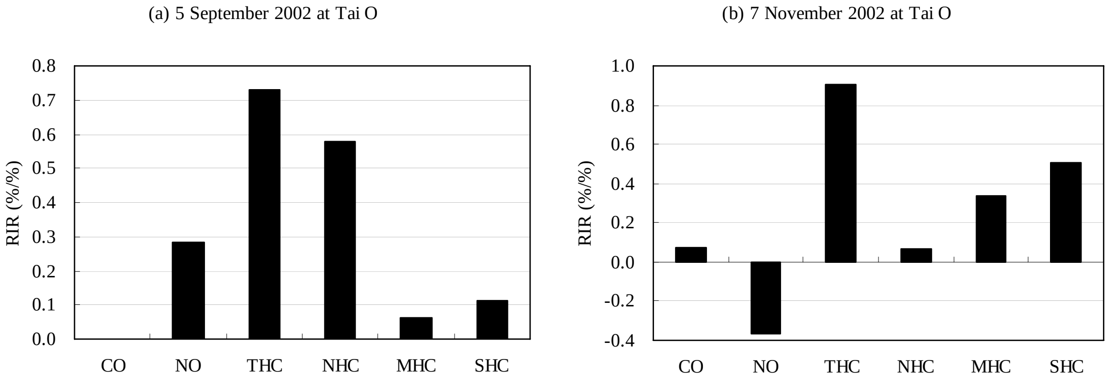
(a) 5 September 2002 at Tai O

(b) 7 November 2002 at Tai O

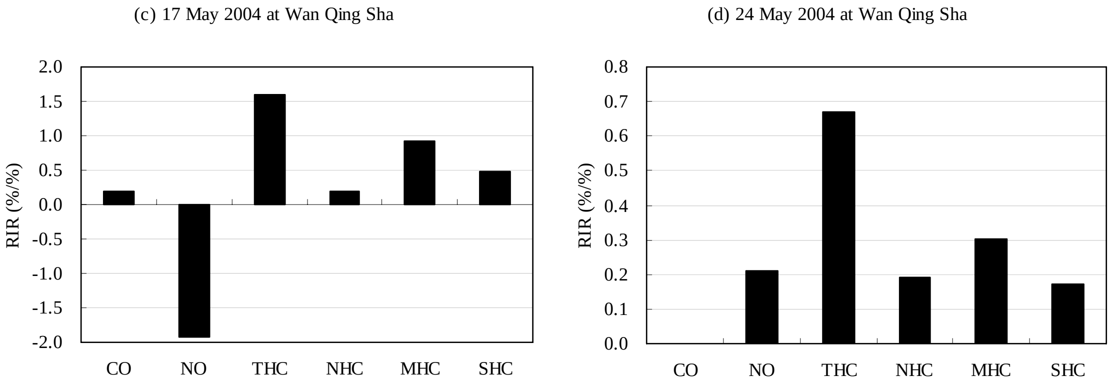
(c) 17 May 2004 at Wan Qing Sha

(d) 24 May 2004 at Wan Qing Sha

*Table 7.4 The apportionment among source categories (mobile, stationary and natural) for 46 $C_2$-$C_{10}$ hydrocarbons*

| Species | Percent Apportionment to Source Category | | | | | |
|---|---|---|---|---|---|---|
| | Hong Kong | | | Guangdong | | |
| | Mobile | Stationary | Natural | Mobile | Stationary | Natural |
| Ethane | 78 | 22 | 0 | 70 | 30 | 0 |
| Propane | 2 | 98 | 0 | 0 | 100 | 0 |
| *n*-butane | 70 | 30 | 0 | 95 | 5 | 0 |
| *i*-butane | 16 | 84 | 0 | 60 | 40 | 0 |
| *n*-pentane | 75 | 25 | 0 | 91 | 9 | 0 |
| *i*-pentane | 74 | 26 | 0 | 96 | 4 | 0 |
| *n*-hexane | 50 | 50 | 0 | 80 | 20 | 0 |
| *n*-heptane | 11 | 89 | 0 | 49 | 51 | 0 |
| *n*-octane | 100 | 0 | 0 | 100 | 0 | 0 |
| *n*-nonane | 97 | 3 | 0 | 100 | 0 | 0 |
| *n*-decane | 98 | 2 | 0 | 99 | 1 | 0 |
| 2,2-dimethylbutane | 91 | 9 | 0 | 100 | 0 | 0 |
| 2,3-dimethylbutane | 68 | 32 | 0 | 94 | 6 | 0 |
| 2-methylpentane | 86 | 14 | 0 | 100 | 0 | 0 |
| 3-methylpentane | 88 | 12 | 0 | 100 | 0 | 0 |
| 2-methylhexane | 0 | 100 | 0 | 0 | 100 | 0 |
| 3-methylhexane | 92 | 8 | 0 | 100 | 0 | 0 |
| 2,2,4-trimethylpentane | 97 | 3 | 0 | 100 | 0 | 0 |
| Methylcyclopentane | 88 | 12 | 0 | 100 | 0 | 0 |
| Cyclohexane | 22 | 78 | 0 | 77 | 23 | 0 |
| Ethene | 100 | 0 | 0 | 96 | 4 | 0 |

*(to be continued)*

*Table 7.4 continued*

| Species | Percent Apportionment to Source Category | | | | | |
|---|---|---|---|---|---|---|
| | Hong Kong | | | Guangdong | | |
| | Mobile | Stationary | Natural | Mobile | Stationary | Natural |
| Propene | 99 | 1 | 0 | 90 | 10 | 0 |
| *i*-butene | 95 | 5 | 0 | 95 | 5 | 0 |
| 1-butene | 64 | 36 | 0 | 78 | 22 | 0 |
| 1-pentene | 77 | 23 | 0 | 100 | 0 | 0 |
| 1,3-butadiene | 100 | 0 | 0 | 23 | 77 | 0 |
| Isoprene | 0 | 0 | 100 | 0 | 0 | 100 |
| *cis*-1-butene | 67 | 33 | 0 | 97 | 3 | 0 |
| *trans*-2-butene | 43 | 57 | 0 | 95 | 5 | 0 |
| Ethyne | 90 | 10 | 0 | 88 | 12 | 0 |
| Benzene | 78 | 22 | 0 | 91 | 9 | 0 |
| Toluene | 7 | 93 | 0 | 39 | 61 | 0 |
| *m*-xylene | 12 | 88 | 0 | 33 | 67 | 0 |
| *p*-xylene | 33 | 67 | 0 | 69 | 31 | 0 |
| *o*-xylene | 16 | 84 | 0 | 52 | 48 | 0 |
| Ethylbenzene | 32 | 68 | 0 | 72 | 28 | 0 |
| *i*-propylbenzene | 0 | 100 | 0 | 0 | 100 | 0 |
| *n*-propylbenzene | 78 | 22 | 0 | 96 | 4 | 0 |
| *m*-ethyltoluene | 79 | 21 | 0 | 96 | 4 | 0 |
| *p*-ethyltoluene | 0 | 100 | 0 | 0 | 100 | 0 |
| *o*-ethyltoluene | 42 | 58 | 0 | 83 | 17 | 0 |
| 1,3,5-trimethylbenzene | 84 | 16 | 0 | 97 | 3 | 0 |
| 1,2,4-trimethylbenzene | 93 | 7 | 0 | 99 | 1 | 0 |
| 1,2,3-trimethylbenzene | 79 | 21 | 0 | 96 | 4 | 0 |
| $\alpha$-pinene | 0 | 0 | 100 | 0 | 0 | 100 |
| $\beta$-pinene | 0 | 0 | 100 | 0 | 0 | 100 |

*(Source: Zhang, et al., 2004)*

Regarding the ratio of RIR (SHC) to RIR (MHC), we found different results between the coastal and inland sites (see Figure 7.2). At the HK coastal site, RIR(SHC) was larger than RIR(MHC), suggesting that a reduction in SHC was more effective than MHC, in terms of percentage, in reducing $O_3$ production. However, opposite results of higher RIR(MHC) values were obtained at the inland site in Guangdong. The results from Figures 7.2c and 7.2d suggested that a reduction in mobile source emissions (in terms of percentage) would be about twice as effective in reducing $O_3$ production than a reduction on stationary sources because RIR(MHC) $\approx 2 \times$ RIR(SHC). By comparison, Cardelino and Chameides (1995) also performed similar RIR calculations on summer data of Atlanta and some of their findings were similar to those of WQS but some were not. On the one hand, Atlanta also had a higher value of RIR(MHC) which was about twice of RIR(SHC). On the other hand, values of RIR(NO) were significant and larger than RIR(AHC) at Atlanta, suggesting the US metropolitan area was somewhat more sensitive to the reduction of $NO_x$ emissions than to the reduction of anthropogenic hydrocarbon emissions.

The above RIR calculations revealed that the $O_3$ production at the two PRD sites (TO and WQS) was strongly VOC-limited and dominated by anthropogenic VOC. Emission controls of both stationary sources and mobile sources of VOC would be effective in controlling $O_3$, with stationary-source controls being somewhat more efficient at TO. By comparison, the $O_3$ mitigation at WQS is more sensitive to the control of VOC from mobile sources. The overall results strongly suggest that different $O_3$ mitigation strategies should be formulated over the PRD subject to the variation of major VOC sources between the coastal and inland areas in the region. Bearing in mind that the estimation is associated with sources apportionment of the VOC, sampling periods and locations, the findings will be more representative for the region if the estimation is based on a large scale of sampling and more accurate sources apportionment of the VOC.

*Table 7.5 Emission inventory of VOC by sector for the year 2000*

| | VOC Emission (Unit in tonnes) | | | |
|---|---|---|---|---|
| Sector | HK | | Guangdong Province | |
| Transportation | 13,560 | (22.3%) | 375,893 | (47.9%) |
| Stationary | | | | |
| *Energy* | *487* | *(0.8%)* | *6,990* | *(0.9%)* |
| *Industry* | *9,508* | *(15.7%)* | *51,597* | *(6.6%)* |
| *VOC-containing products* | *31,368* | *(51.6%)* | *92,464* | *(11.8%)* |
| Sub-total | 41,363 | (68.1%) | 151,051 | (19.3%) |
| Biogenic | 5,833 | (9.6%) | 257,370 | (32.8%) |
| Total | 60,756 | | 784,314 | |

Note: The data in parenthesis are in units of percentage of total emissions.

*(Source: CH2M, 2002)*

## 7.5 Diurnal Variation of Hydrocarbons

Diurnal variation of hydrocarbons gives useful insights into the interplay of emission, chemical and physical processes during a day. It also highlights the relative importance for various hydrocarbons to the $O_3$ peak. Figures 7.3a to 7.3d compare the diurnal profiles of THC on the four days in terms of their mass concentrations and photochemical reactivity, using the PE scale of Chameides et al. (1992) *[Equation 2..1]*. The respective diurnal $O_3$ variations are also provided for comparison. At the coastal site, there was a decreasing diurnal profile of SHC and MHC for both mass concentration and PE on 5 September 2002 (see Figure 7.3a). In contrast, there were peak values at LST 1300 for both mass concentration and PE profiles of NHC which was attributable to the isoprene mixing ratio of 5352 pptv at that time. The fraction of NHC in THC was much higher for PE than for mass concentration, reflecting the strong photochemical reactivity of isoprene. Under such circumstances, NHC would be more sensitive than the AHC to the photochemical $O_3$ production which agrees with our previous OBM result (see Figure 7.2a).

For the case of 7 November 2002 at TO (see Figure 7.3b), the diurnal profile of THC for mass concentration was similar to that for PE, showing a decreasing trend through a day. AHC (sum of SHC and MHC) accounted for a major proportion of THC and their mass concentrations were much higher than the respective PE values. The diurnal plots of the coastal site also showed a larger component of SHC (than MHC) which was consistent with the RIR results given in Figures 7.2a and 7.2b. The overall results suggest that $O_3$ formation at the coastal site is most sensitive to SHC, but under favourable conditions of hot and sunny weather, emissions from biogenic sources could also become a dominant factor.

In contrast to the results at TO, the diurnal profiles of THC at WQS are somewhat different. Two peaks (at LST 0900 and 1900) were observed for the profiles on 17 May 2004 (see Figure 7.3c). The appearance of these peaks seems to be related to the general diurnal traffic pattern, which could be verified by higher MHC (than SHC) levels every hour at the inland site. The diurnal profile of THC for mass concentration was very similar to that of PE, but with much higher values. The results highlighted that the site was mainly affected by AHC (particularly from vehicular emissions) with relatively low photochemical reactivity. For the case of 24 May 2004, the contribution of NHC to $O_3$ formation became apparent, especially in the afternoon (see Figure 7.3d). The enhancement of PE level for NHC revealed the occasional influence of biogenic emission (primarily isoprene) on the photochemical reactivity at the inland site.

*Figure 7.3(a) Diurnal profiles of $O_3$ and THC (SHC, MHC and NHC) in terms of concentrations and PE for Tai O on 5 September 2002.*

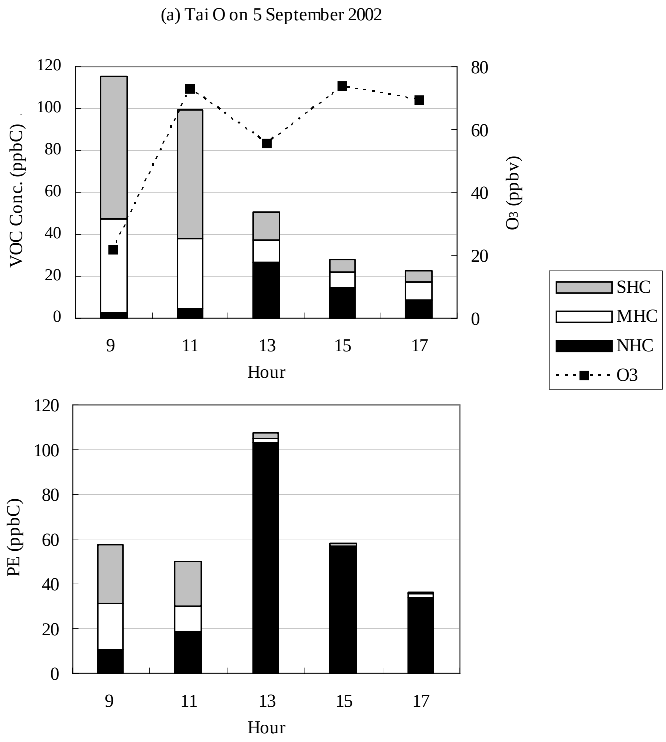
(a) Tai O on 5 September 2002

*Figure 7.3(b)Diurnal profiles of $O_3$ and THC (SHC, MHC and NHC) in terms of concentrations and PE for Tai O on 7 November 2002.*

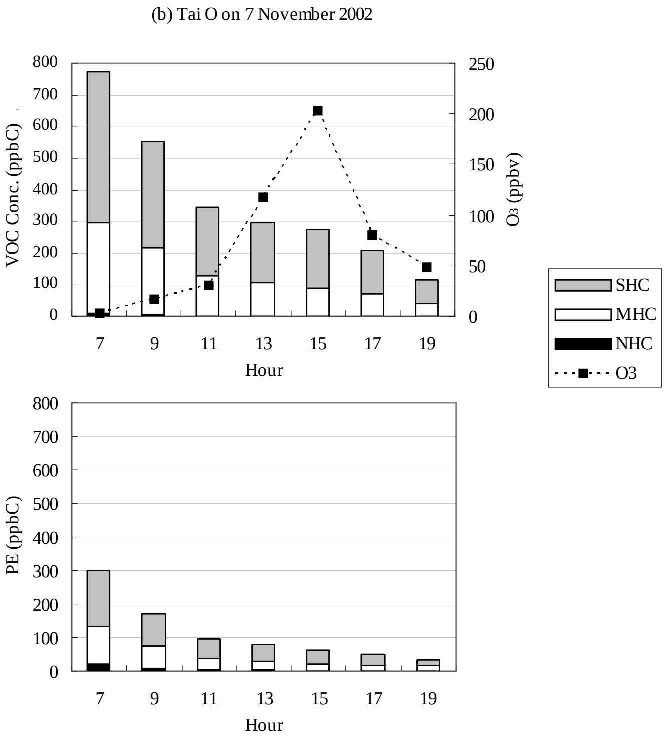
(b) Tai O on 7 November 2002

Figure 7.3(c) Diurnal profiles of $O_3$ and THC (SHC, MHC and NHC) in terms of concentrations and PE for Wan Qing Sha on 17 May 2004.

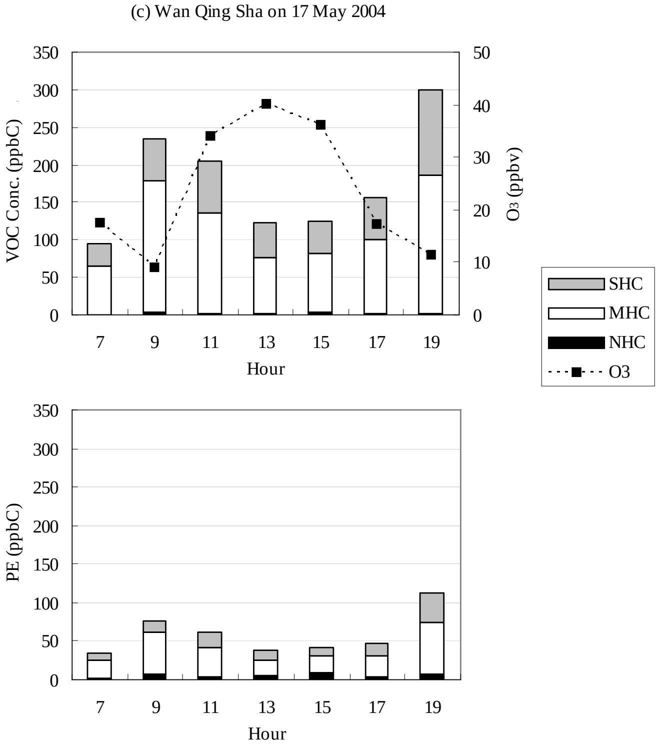

Figure 7.3(d)Diurnal profiles of $O_3$ and THC (SHC, MHC and NHC) in terms of concentrations and PE for Wan Qing Sha on 24 May 2004.

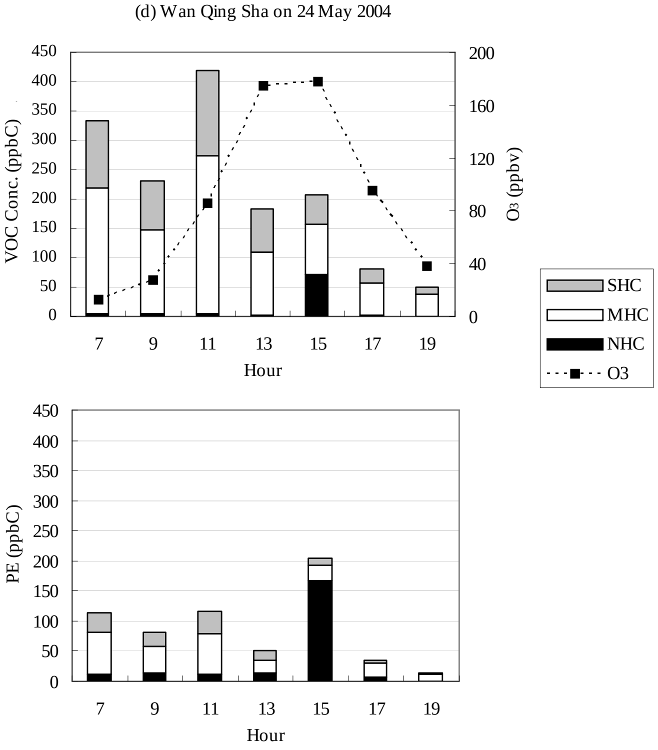

## 7.6 Significance of Aromatic Hydrocarbons on Ozone Formation

It have been revealed that $O_3$ production in the PRD region was generally limited by AHC, whereas SHC and MHC were playing the leading roles at TO and WQS, respectively. To further examine the speciation of AHC at the two sites, the AHC is classified into five sub-groups according to their structure and reactivity in the atmosphere, namely:

(i) low reactivity hydrocarbons (LR) including ethane, propane, ethyne and benzene;

(ii) alkanes with four or more carbons (>=C4);

(iii) ethene (ETH);

(iv) reactive olefins (R-OLE) including all olefins except ethene; and

(v) reactive aromatics (R-AROM) encompassing xylenes, toluene, trimethylbenzenes and ethylbenzene.

Figures 7.4a and 7.4b illustrate the average mass concentrations of NHC and sub-groups of AHC at TO (for eight days) and WQS (for five days), respectively. For both sites, mass concentration of AHC was much higher than that of NHC, and R-AROM had the highest mass concentration among the five sub-groups of AHC. By comparison, aromatic hydrocarbons (toluene and xylenes) also contributed most to the $O_3$ formation in the urban areas of HK and Taiwan (So and Wang, 2004; Chang et al., 2005). When we further compare the PE for different groups of VOC, quite different pictures are obtained (see Figures 7.4c and 7.4d). R-AROM was still the dominant species group but NHC had a relatively higher proportion of the total OH-reactivity in

THC, indicating the significance of NHC regardless of its relatively low mixing ratio. Thus, the results suggest that emission controls of R-AROM would provide the most effective way to reduce $O_3$ in the PRD including HK. Since aromatic hydrocarbons are associated with different sources e.g. vehicular emissions, solvent application, etc., more rigorous studies like sources apportionment on the VOC data is therefore needed to characterize VOC sources over the PRD areas.

*Figure 7.4 Comparison of average composition for NHC and sub-groups of AHC in (a) mass concentration at Tai O; (b) mass concentration at Wan Qing Sha; (c) PE at Tai O; and (d) PE at Wan Qing Sha.*

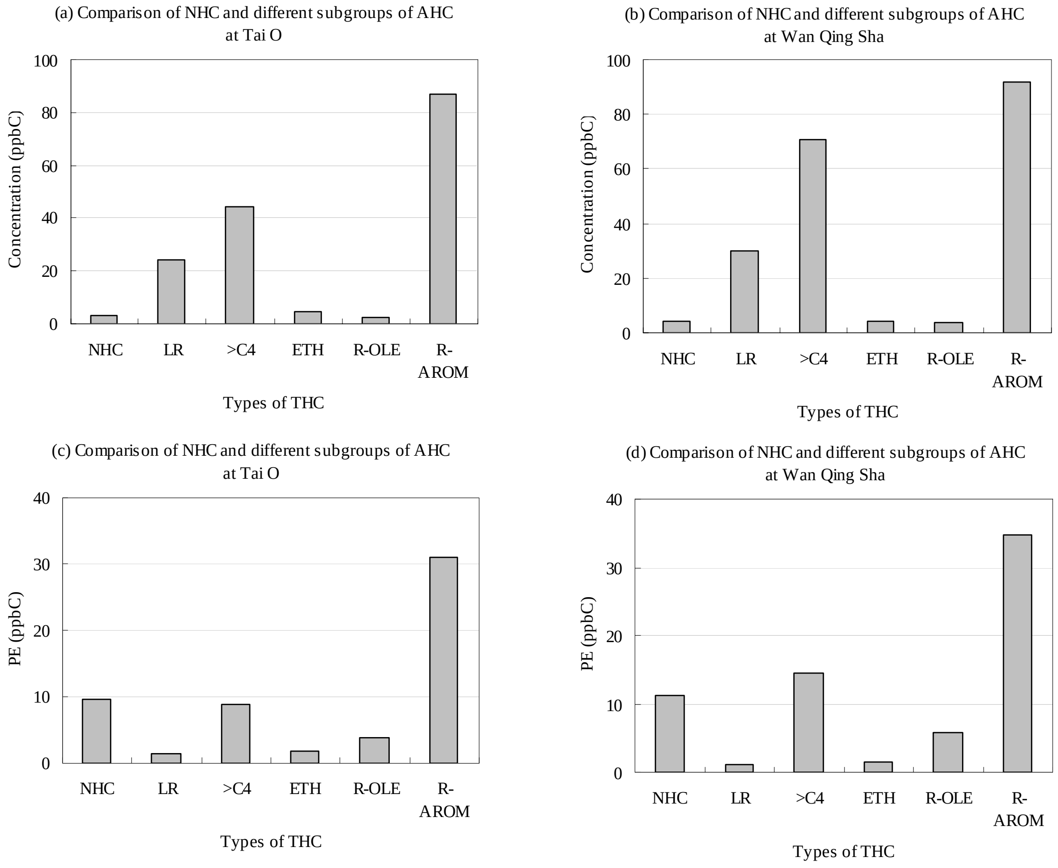

## 7.7 Sensitivity to ΔS in RIR Calculation

Following the practice of Cardelino and Chameides (1995), a value of 10% (of ΔS) as the percent change in the precursor source was adopted to compute the RIR values in this thesis. It had been revealed that there was an insignificant sensitivity to ΔS in RIR calculation (see Figure 2.1) for the dataset in Atlanta. Such an environment was characterized by strong and positive sensitivity of NO and NHC, which is quite different to the cases in the PRD with cases of negative sensitivity of NO (i.e. negative RIR(NO)). To verify the applicability of the assumption to the PRD cases, similar sensitivity tests were conducted for the selected four days as discussed in Section 7.4. Figure 7.5 shows the ΔS reductions in 10, 20 and 50% for different $O_3$ precursor groups on the two days each in TO and WQS. Similar to the results from Cardelino and Chameides (1995), there is some dependence on ΔS for AHC, NHC and NO. It is interesting to note that positive RIR(NO) tends to increase (see Figures 7.5(a) and (d)) but negative RIR(NO) tends to decrease (see Figures 7.5 (a) and (c)) when ΔS becomes more negative. By comparison, the variation of RIR(CO) is insignificant for all the cases. Therefore, the relative importance of each precursor group is not significantly affected by the change in ΔS and the assumption of a hypothetical 10% reduction in ΔS is appropriate and applicable to the PRD cases.

*Figure 7.5 Variation of daytime average RIR as functions of the percent change in precursor group for AHC, NHC, CO and NO for (a) Tai O on September 2002; (b) Tai O on 7 November 2002; (c) Wan Qing Sha on 17 May 2004; and (d) Wan Qing Sha on 24 May 2004.*

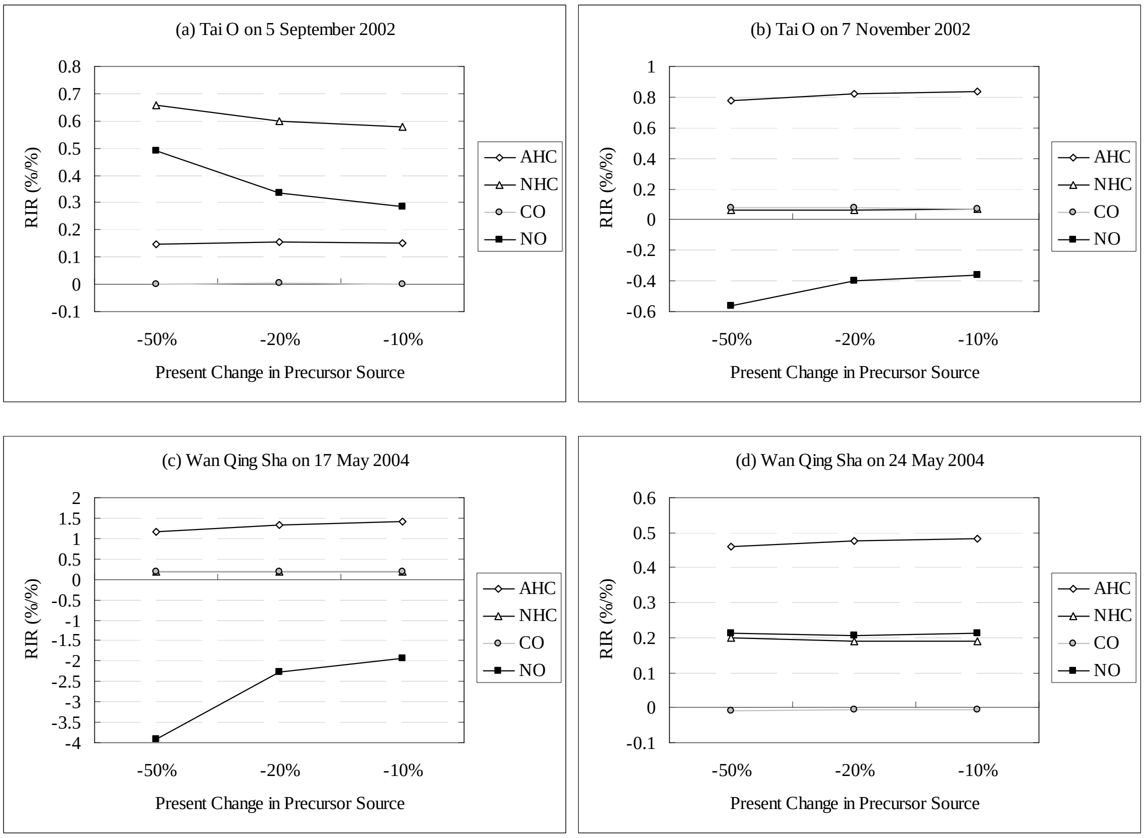

## 7.8 Chapter Summary

This chapter provided a comprehensive picture about the role of VOC in the photochemical $O_3$ production in the PRD. Measurement data and modelling results of a coastal site in HK and an inland site in Guangdong were examined and it was concluded that the photochemical $O_3$ production was generally limited by VOC. Reduction in NO would however enhance the $O_3$ formation and role of CO was found to be negligible. Emission controls in VOC from stationary and mobile sources are both effective in $O_3$ mitigation. Further looking into the VOC sources apportionment, it was revealed that control of SHC was more effective than MHC in reducing $O_3$ at TO, but the opposite result was observed at WQS. Occasional high levels of NHC (primarily isoprene) were observed and the influence of natural emissions of VOC on the $O_3$ production could not be ignored. Furthermore, various sub-groups of VOC were playing different roles in $O_3$ production and aromatic compounds (e.g. toluene and xylenes) were the key VOC controlling photochemical $O_3$ production in the region.

The overall findings identified the similarities and differences of VOC mix between two rural PRD sites, suggesting that a unique $O_3$ migrating strategy might not be fully applicable to the whole region. Instead, depending on the areas characteristics and emission patterns, somewhat different VOC reduction plans should be implemented in different PRD areas in order to attain the largest overall reduction in regional $O_3$ pollution. Subject to the complexity of pollution sources over the PRD, it is highly recommended that comprehensive VOC surveys should be conducted and further studies are needed to address the VOC source apportionment and to better characterize the photochemical $O_3$ pollution.

# CHAPTER 8 CHEMISTRY OF PHOTOCHEMICAL OZONE PRODUCTION OVER THE PRD

The previous chapters described the $O_3$ pattern, and examined the sources and roles of the major $O_3$ precursor (VOC) in the photochemical $O_3$ production in HK. Such information is essential to local authorities to better understand the causes of photochemical $O_3$ pollution and formulate effective $O_3$ migrating strategies. This chapter will assess the contribution of local production and long-range transport to elevated ground-level $O_3$ at TO and WQS. It will further make use of the OBM to infer the $O_3$ production processes and the fast chemistry involved in the photochemical $O_3$ pollution. Attempts will be made to get some insights into the variation of intermediates, the partitioning of reactive nitrogen compounds, and $O_3$ budget and production efficiency during the elevated $O_3$ days. On elevated $O_3$ days, record high hourly $O_3$ mixing ratios of 203 ppbv and 178 ppbv were measured at TO and WQS on 7 November 2002 and 24 May 2004, respectively. The corresponding chemistry involved on these two $O_3$ episodes will be compared to highlight the similarities and differences of photochemical $O_3$ production between the two sites.

## 8.1 *In-situ* Photochemical Production versus Long-range Transport contributing to High Ozone Levels over the PRD

The ground-level $O_3$ at a site is due to local photochemical production plus the transport of $O_3$ that has been produced elsewhere, including downward mixing (entrainment) of $O_3$-rich air above the nocturnal inversion and advection to the site of photochemically aged urban plumes (Kleinman et al., 1994; Frost et al., 1998). Here, the RIR functions calculated by the OBM only pertain to the $O_3$ produced locally but not the $O_3$ that had been transported to the site. If the calculated $O_3$ production represents a significant portion of the total $O_3$ increase (or increment), the $O_3$ episode should be mainly contributed by local production. On the other hand, if the calculated value is much smaller then the $O_3$ increment, it indicates the limited utility of the OBM and suggests an important contribution of regional transport of pollutants to the respective $O_3$ formation. Therefore, by comparing the net photochemical $O_3$ production calculated by the OBM at each site with the actual $O_3$ increment (or increase) observed at each site during the episode day, we can get insights into the relative contributions of local production and long-range transport to the $O_3$ episode at a site.

Figure 8.1 illustrates the OBM-calculated net $O_3$ production and observed $O_3$ increment at TO for the eight days in autumn 2002 (see Table 7.3). The $O_3$ increment represents the maximum increase in $O_3$ on each day and it was calculated from the difference between the maximum afternoon and minimum morning hourly $O_3$ levels. For half of the eight days (25 October, 6, 7 and 12 November 2002), the calculated values were only able to account for a small fraction of the observed $O_3$ increment, suggesting a significant impact from long-range transport on those days. By comparison, the results of the other four days were different and suggested that the $O_3$ levels should be mainly contributed by local production. On 11 October and 8 November 2002, the observed and calculated $O_3$ production values were similar. Furthermore, the other two days (5 and 6 September 2002) were found with higher calculated values than their respective measured results. Since the calculated results could account for all the observed $O_3$ levels, it represented that the local $O_3$ production was strong and responsible for the observed $O_3$ levels at TO on those four days.

There is a large difference between the calculated and observed values on 5 and 6 September 2002. As the model does not account for the horizontal transport of air pollutants (details are given in Chapter 2.5), over-estimation of the $O_3$ production could be interpreted as the boundary layer being a region that exports $O_3$.

*Figure 8.1 Comparison of net $O_3$ photochemical production calculated by the OBM and the observed $O_3$ increment at Tai O on eight days.*

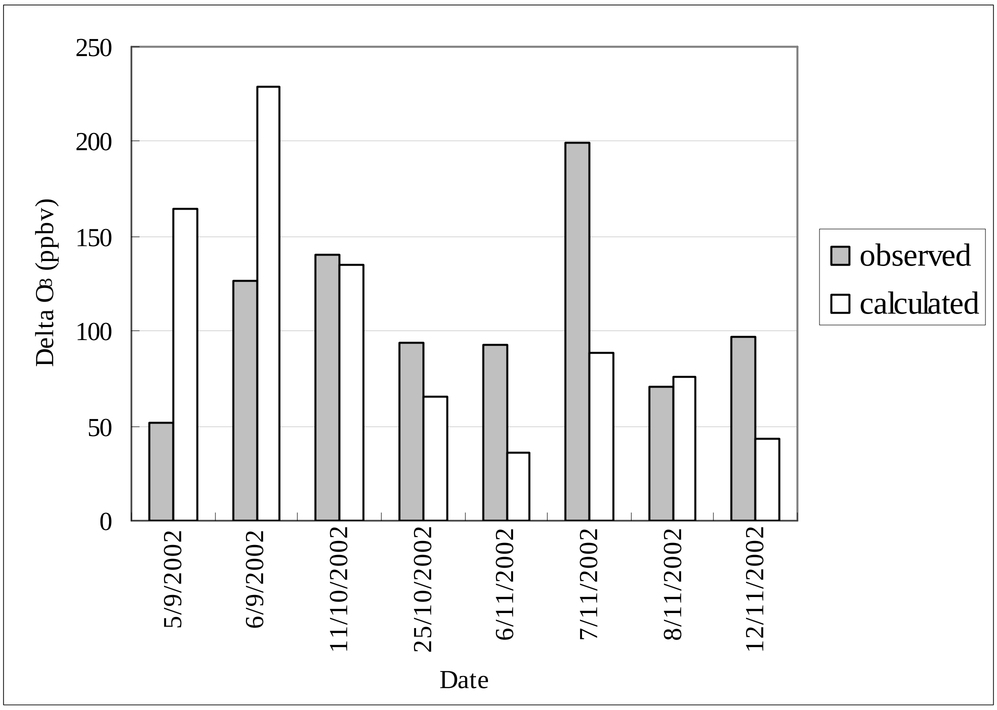

Comparison between the OBM-calculated net $O_3$ production and observed $O_3$ increment at WQS for the five $O_3$ episode days is given in Figure 8.2. In contrast to the TO's results, observed results at WQS were all lower than the corresponding calculated values, demonstrating that the $O_3$ episodes were mainly attributable to local production.

For all the five days, there was a large difference between the observed and calculated $O_3$ production values. As the model does not account for the horizontal transport of air pollutants (details are given in Chapter 2.5), over-estimation of the $O_3$ production could be interpreted as the boundary layer being a region that exports $O_3$.

To summarize, elevated $O_3$ levels at TO in autumn were partly due to local production and regional transport. In contrast, local production was the major source of $O_3$ episodes at WQS in spring. To further understand and compare the sources and chemical process involved in generating elevated $O_3$ levels between TO and WQS, more detailed analyses on the $O_3$ episodes of the two sites are needed and will be given in the following sections.

*Figure 8.2 Comparison of net $O_3$ photochemical production calculated by the OBM and the observed $O_3$ increment at Wan Qing Sha on five days.*

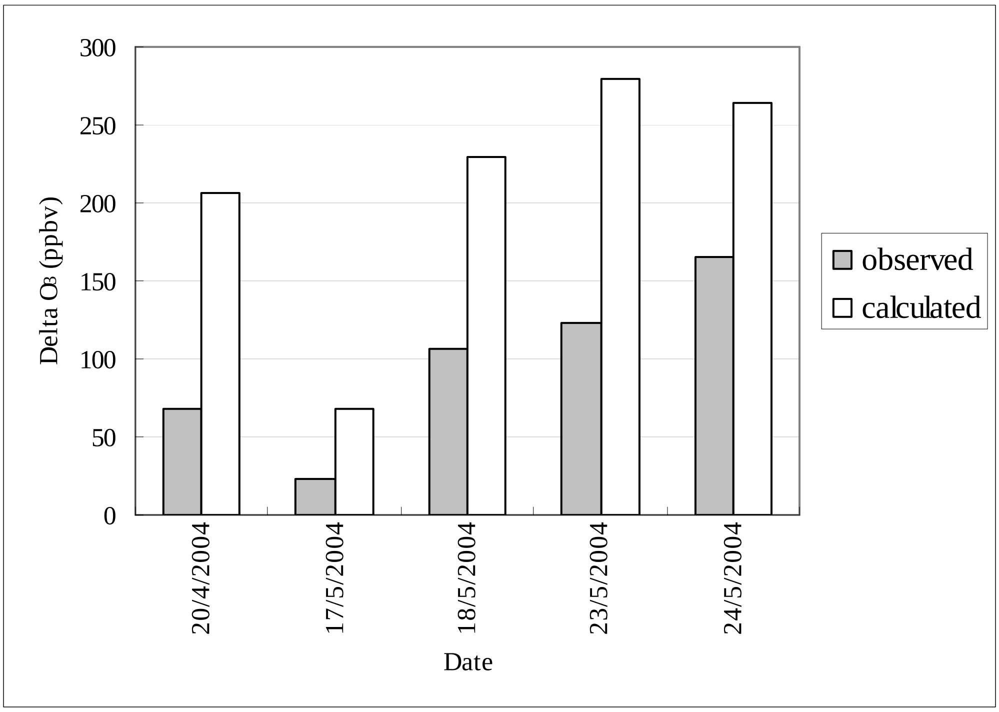

## 8.2 Comparison of Ozone Production at Tai O and Wan Qing Sha

One of the key issues to be addressed in this thesis is to understand the causes and chemical processes contributing to the $O_3$ production. To address this issue, the previous section compared the calculated and observed $O_3$ production values, showing the different sources of elevated $O_3$ levels at the HK and PRD sites, with mixed local production and transport at TO but mainly local production at WQS. To infer the $O_3$ production processes and the fast chemistry involved in the photochemical $O_3$ pollution, this section will further examine the $O_3$ episodes of the two sites in depth and attempt to get some insights into $O_3$ production and chemistry on those elevated $O_3$ days.

The OBM will be applied to study and compare two $O_3$ episodes: 7 November 2002 at TO and 24 May 2004 at WQS. These two days are selected because of their record high 1-hour $O_3$ concentration of 203 ppbv (at TO) and 178 ppbv (at WQS), which is the key to analyzing the causes and details of such high $O_3$ levels. The two episodes will be analyzed and compared with regard to the areas of diurnal variation of measured and non-measured pollutants, $O_3$ budgets, $O_3$ production efficiency as well as observed and calculated $O_3$ changes, aiming to infer the similarities and differences of $O_3$ production processes involved in these two events. As a caveat, it should be noted that the following analysis are based on two cases with data gathered at two sites in different seasons. A more representative picture of the region will be obtained if analysis is performed on a comprehensive data set with regard to sampling sites and period.

### *8.2.1 Time Series of Hourly Data*

Figure 8.3 shows the time series of hourly data of measured trace gases ($O_3$, CO, $SO_2$, NO and $NO_y$) at TO on 7 November 2002. Corresponding 1-hour $O_3$ levels measured at the other two EPD's air quality monitoring stations at TC and TM are also shown in Figure 8.3 for comparison. It can be seen that the $O_3$ levels in the western part of HK (TO and TC) were higher than the eastern part (TM). During the whole day, TO was under the influence of north to northeasterly winds (see Figure 8.3). A large peak of $NO_y$ and / or $SO_2$ (missing morning data) were observed in the morning with a high $NO/NO_y$ ratio. Also, maximum VOC level in PE was found in the morning and its level gradually decreased during the day. Such patterns indicated the arrivals of fresh urban plumes which activated the $O_3$ formation. An increase in $O_3$ level started from LST 1100 and it peaked at LST 1500, subsequent to drops of $SO_2$, CO, NO, $NO_y$, and their ratio ($NO/NO_y$) from LST 1100. In order to further analyze the pollution sources, the ratio of $\Delta CO/\Delta NO_y$ was calculated by using the 1-hour averaged CO and $NO_y$ measurements recorded at TO, subtracting the "background" CO and $NO_y$ concentrations of 211 and 3.37 ppbv, respectively (Wang et al., 2001c). Because of the different emissions characteristics between HK and other cities in the PRD, the ratio of CO to $NO_y$ in HK (3.3 ppbv/ppbv) had been reported to be smaller than those in other PRD cities (e.g. 16 ppbv/ppbv in Shenzhen) (Lind and Kok, 1999). On 7 November 2002, the hourly ratios were found to have consistently high levels (8 to 26) during the late morning and whole afternoon hours (see Figure

8.3), indicating the influence of PRD's emission at TO during the period. As an independent check on the above results, a plot of a back trajectory for air mass at Tai O on 7 November 2002 is given in Figure 8.4 (Zhang et al. 2004), further identifying the long-range transport of air masses from the PRD to TO. The above results, which are consistent with the model findings found in Section 8.1, indicate the significant contribution of regional pollutants to this $O_3$ episode.

The corresponding time series plots of WQS case show a somewhat different picture, suggesting a rather strong contribution of local $O_3$ production. Figure 8.5 presents the diurnal variation of measured trace gases ($O_3$, CO, $SO_2$, NO and $NO_y$), their respective ratios ($NO/NO_y$ and $\Delta CO/\Delta NO_y$), PE of VOC and wind data at WQS on 24 May 2004. Large peaks of CO and $SO_2$ were observed in the morning with high $NO/NO_y$ ratios under northwesterly to northeasterly winds, indicating the arrival of fresh urban plumes from the upwind areas. In the afternoon, the wind shifted to southeasterly and it prevented the further dispersion of air pollutants from the north. Wind speeds were relatively low (less than 5 m/s) during the day, suggesting that the air pollutants were mainly contributed from local sources. Concurrence of the maxima for $O_3$ and PE of VOC at LST 1500 indicated a good correlation between the diurnal variation of $O_3$ and VOC. The overall diurnal results revealed the significant contribution of local pollution to the site. In contrast, for the case of 7 November 2002, VOC at TO was attributable to regional transportation and maximum VOC was found in the morning (see Figure 8.3).

*Figure 8.3* *Diurnal measurement of* $O_3$ *(at Tai O, Tung Chung and Tap Mun), CO,* $SO_2$*,* $NO_y$*, their ratios (*$NO/NO_y$ *and* $\Delta CO/\Delta NO_y$*), PE of VOC and wind at Tai O on 7 November 2002.*

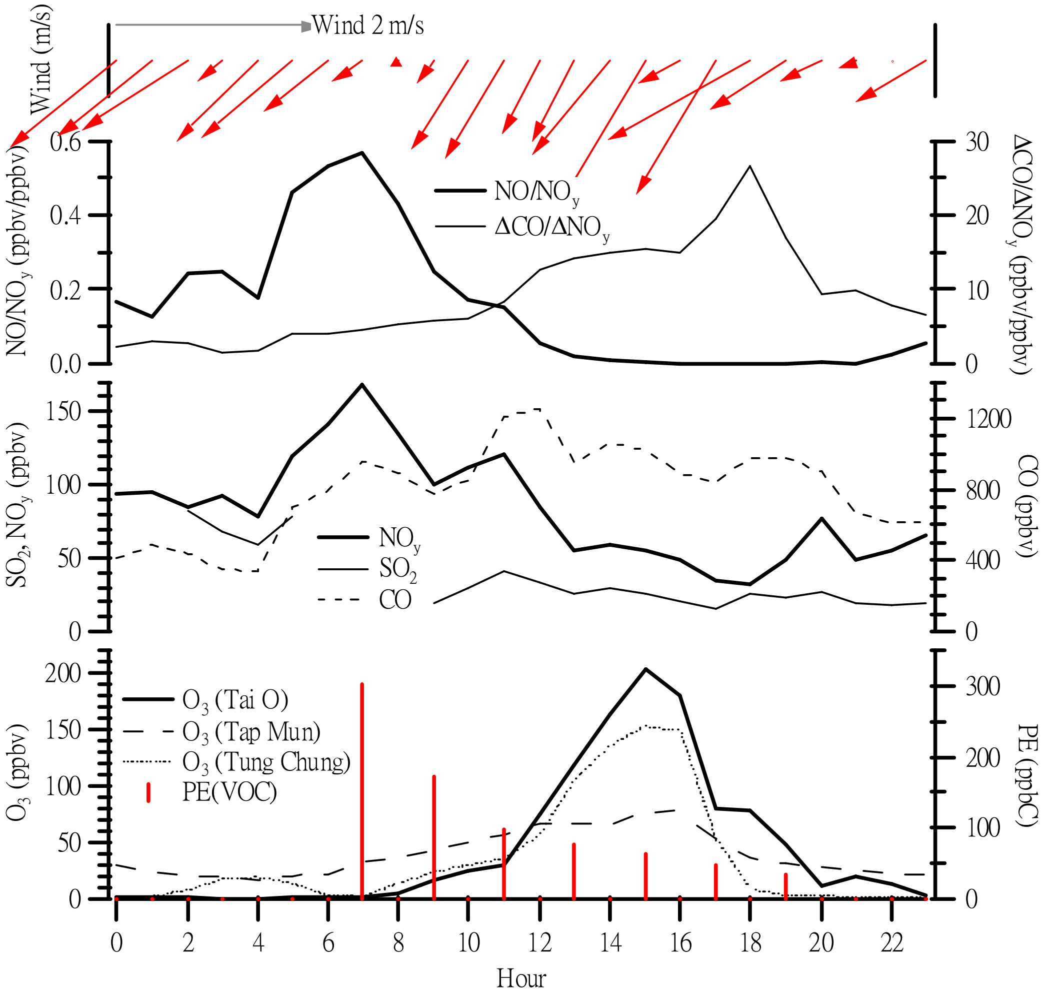

*Figure 8.4 Back trajectory for air mass arriving at Tai O on 7 November 2002.*

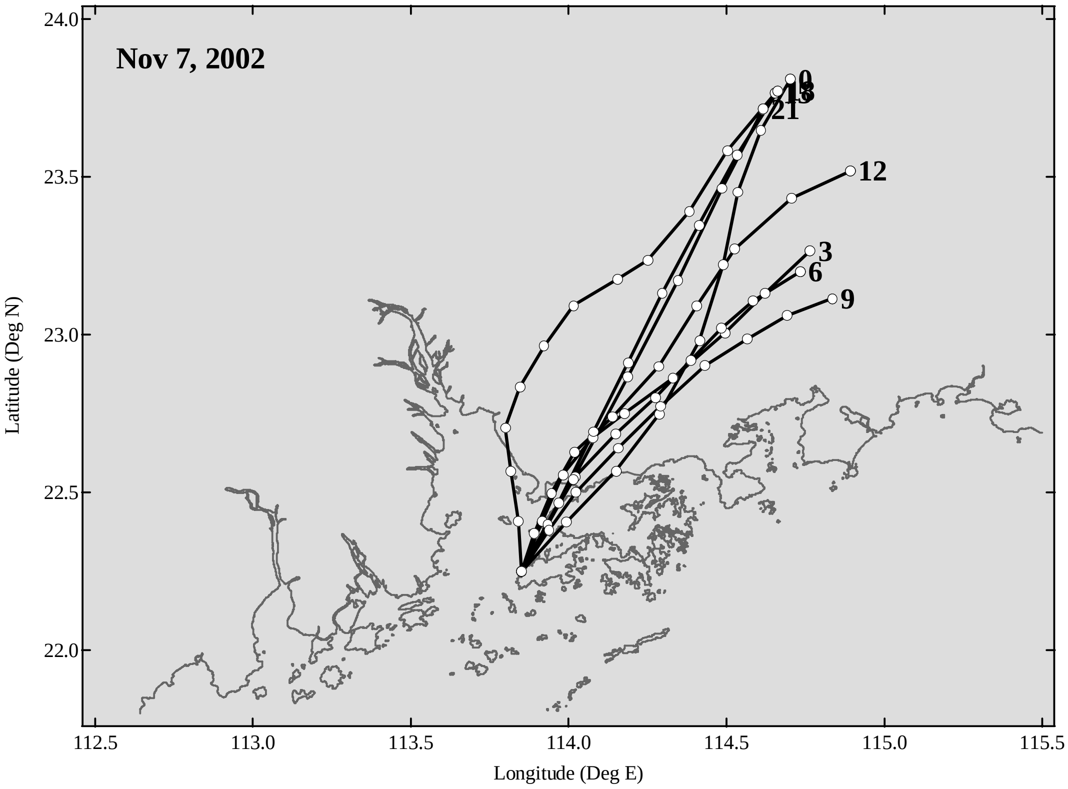

*(Source: Zhang et al. 2004)*

*Figure 8.5 Diurnal measurement of $O_3$, CO, $SO_2$, $NO_y$, their ratios ($NO/NO_y$ and $\Delta CO/\Delta NO_y$), PE of VOC and wind at Wan Qing Sha on 24 May 2004.*

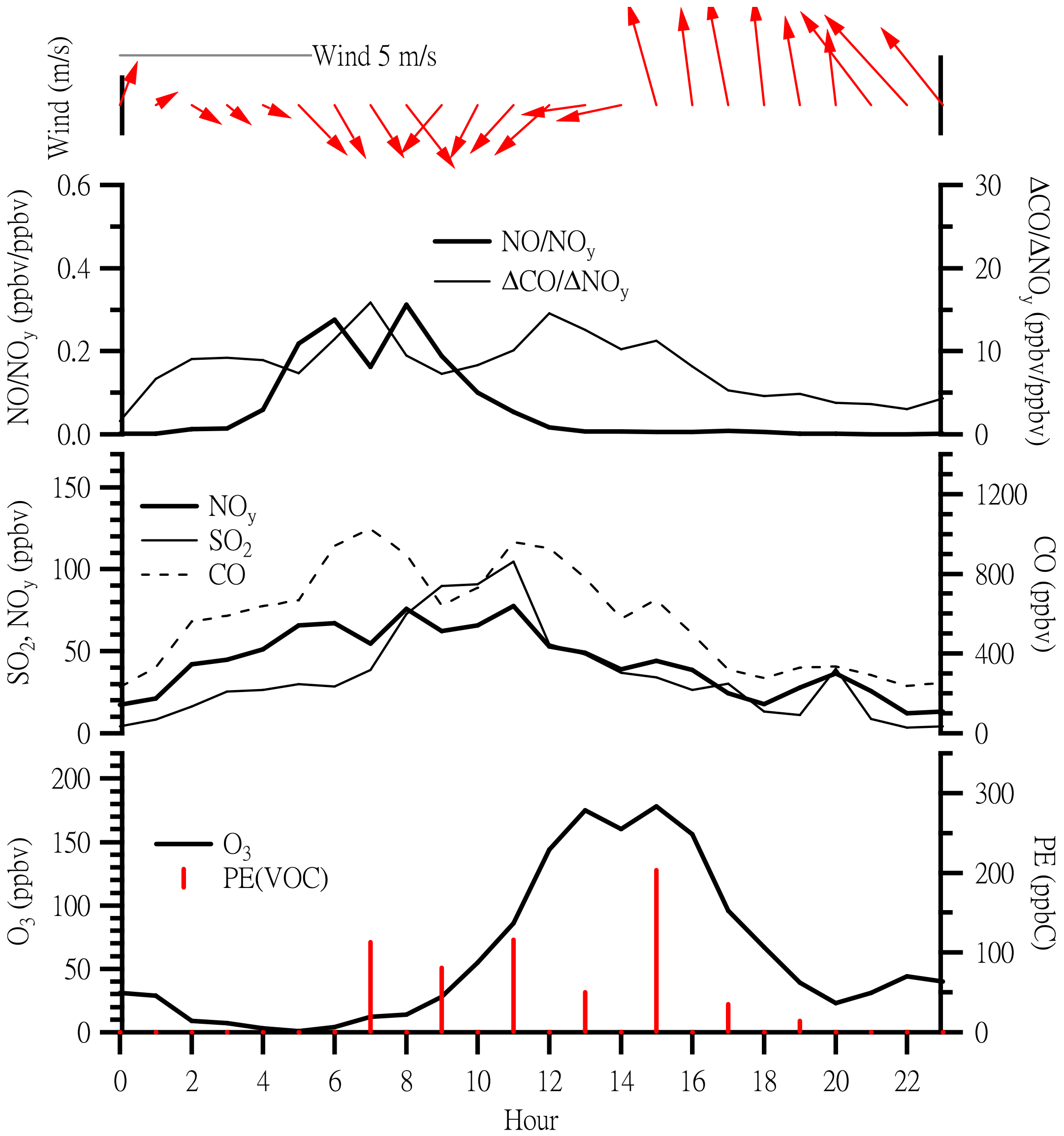

### *8.2.2 Ozone Budget*

The fundamental question with respect to tropospheric $O_3$ is: What are the sources and sinks of $O_3$? Qualitatively, the tropospheric balance of $O_3$ ($O_3$ budget) mainly includes the processes of physical transportation (entrainment and deposition), and *in situ* chemical production and destruction (Seinfeld and Pandis, 1998). Such information is very critical to our understanding of the key reaction(s) in governing the photochemistry in the atmosphere. Briefly, the $O_3$ production and destruction occur primarily by means of the following reactions:

**(a) $O_3$ Production:**

$NO + HO_2 \rightarrow NO_2 + OH$ *[Equation 1.10]*

$NO + CH_3O_2 \rightarrow NO_2 + CH_2O$ *[Equation 8.1]*

$NO + RO_2 \rightarrow NO_2 + RO$ ($RO_2$ refers to organic peroxy radicals other than $CH_3O_2$) *[Equation 1.8]*

**(b) $O_3$ Destruction:**

$O_3 + hv \rightarrow O(^1D) + H_2O \rightarrow 2OH$ *[Equations 1.4 and 1.5]*

$OH + NO_2 \rightarrow HNO_3$ *[Equation 1.12]*

$O_3 + OH \rightarrow HO_2 + O_2$ *[Equation 8.2]*

$O_3 + HO_2 \rightarrow OH + 2O_2$ *[Equation 8.3]*

Without the use of an appropriate model, we could not estimate the $O_3$ budget in an area from the measurement data. This thesis will therefore make use of the OBM to study the *in situ* chemical processes and estimate the relative contribution of different reactions participating in the photochemical $O_3$ production and destruction at TO and WQS. Figure 8.6 compares the daytime average contributions of the major reactions to the photochemical $O_3$ production and destruction at TO on 7 November 2002 and WQS on 24 May 2004. For TO case, the conversion of NO to $NO_2$ by $HO_2$ (P1, see Figure 8.6) contributed to the majority of the $O_3$ production, indicating the key role of $HO_2$ as compared to other organic peroxy radicals ($CH_3O_2$ and $RO_2$). The contribution of $RO_2$ was higher than $CH_3O_2$ and the order of significance was $HO_2$ (91%) > $RO_2$ (6%) > $CH_3O_2$ (3%) for reaction with NO on $O_3$ production. By comparing to the results ($HO_2$ (46%) > $RO_2$ (35%) > $CH_3O_2$ (19%)) at Sable Island, Nova Scotia (Duderstadt et al., 1998), it was found that the order was same but the relative contributions of the radicals were different.

By comparison, the WQS case had a higher daytime average $O_3$ production rate of 15.8 ppbv/hr which was much larger than that of TO (6.0 ppbv/hr), indicating a stronger local contribution at WQS. The conversion of NO to $NO_2$ by $HO_2$ (P1, see Figure 8.11) contributed to the majority of the $O_3$ production, indicating a key role of $HO_2$ as compared to other organic peroxy radicals ($CH_3O_2$ and $RO_2$). The contribution of $RO_2$ was higher than $CH_3O_2$ and the order of significance ($HO_2$ (83%) > $RO_2$ (13%) > $CH_3O_2$ (4%)) on $O_3$ production is similar to the TO case.

For the photochemical $O_3$ loss at TO, the rates were dominated by the reaction of $NO_2$ and OH (57%), followed by the reactions of $O_3$ and $HO_2$ (24%); O1D and $H_2O$ (15%); $O_3$ and OH (4%). The results therefore identified the strong role of $HO_x$ played in the photochemical $O_3$ reaction at TO. In contrast, the $O_3$ photochemical loss rates at WQS were somewhat different to the TO case. The major $O_3$ destruction was contributed by the reaction of $O_3$ and $HO_2$ (38%) (D2, see Figure 8.6) which was different to the dominant reaction of $NO_2$ and OH for the TO case. The difference is obviously due to the relatively higher morning NO concentration at TO than WQS (cf Figure 8.3 to Figure 8.5), which caused a dominant $O_3$ loss through the reaction between $NO_2$ and OH at TO. The contributions of the other two reactions ($NO_2$ and OH (31%); O1D and $H_2O$ (26%)) on $O_3$ destruction at WQS were similar. Reaction between $O_3$ and OH (5%) had the least contribution on $O_3$ destruction.

*Figure 8.6* *Daytime average $O_3$ production (P) and destruction (D) rates at Tai O on 7 November 2002 and Wan Qing Sha on 24 May 2004 calculated by the OBM.*

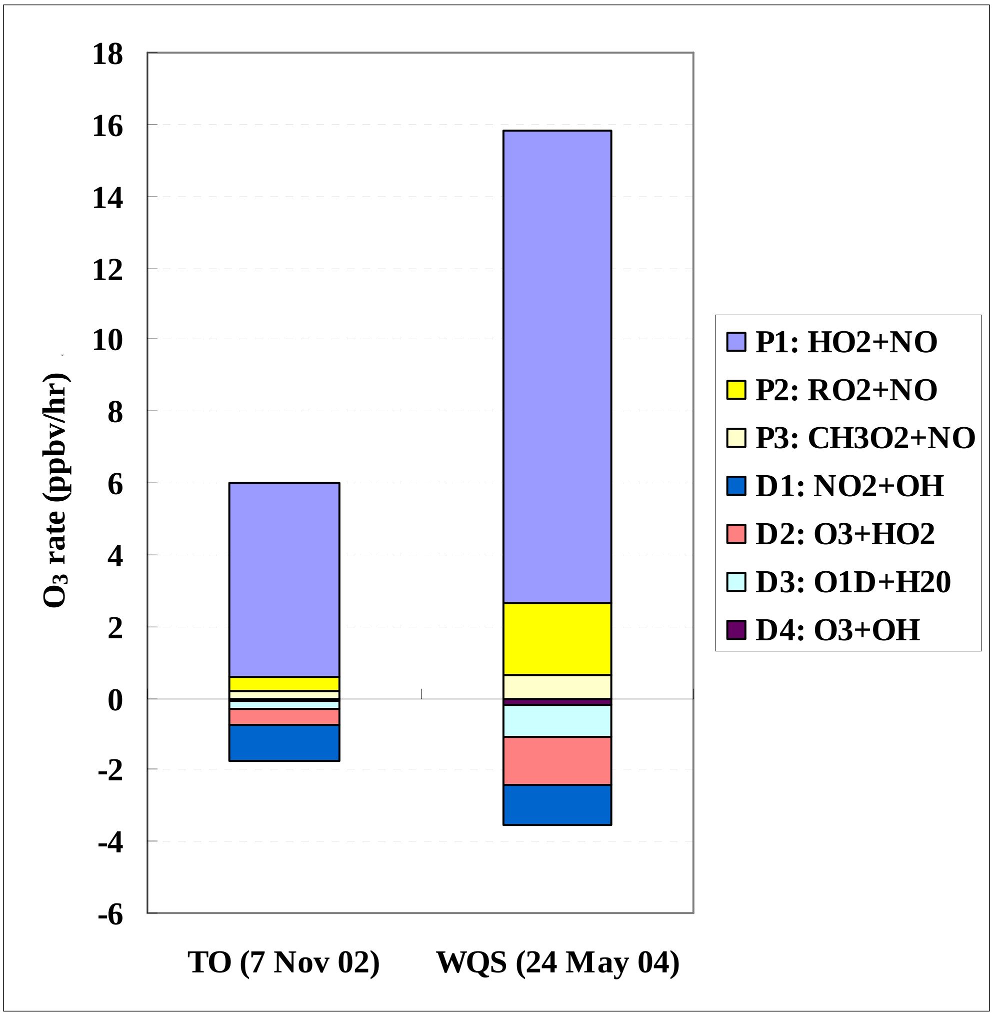

### *8.2.3 Diurnal Variations of OH Radicals*

The OH radicals are important chemicals in the atmosphere because they decompose (scavenge) many gases and play a key role in the photochemical $O_3$ production and destruction as discussed above. Here, the OH concentrations are estimated by the OBM in order to calculate the respective $O_3$ production rate and the respective diurnal cycles of the two cases are analyzed below with the purposes of (1) checking the accuracy of the model results by comparing the estimated OH levels with the documented range and (2) comparing the OH levels between two cases under different features of $O_3$ formation.

In urban air, OH concentrations are in the order of $10^6$ molecules per $cm^3$ (Jacobson, 1999). Table 8.1 lists the OH peak values for the 13 days and they range from $10^6$ to $10^7$ molecules per $cm^3$. By comparing with the results of Section 8.1, elevated $O_3$ days mainly contributed by local production were all found with high OH peak values (OH $>10^7$ molecules per $cm^3$), illustrating the pivotal role of OH in photochemical $O_3$ formation. Figure 8.7 further compares the model calculated diurnal cycles of OH of the two cases with the maximum levels of $7.5\times10^6$ and $1.3\times10^7$ molecules per $cm^3$ at TO and WQS, respectively. By comparison, the values were larger than the average urban levels of $5\times10^6$ molecules per $cm^3$ (Jacobson, 1999). As expected, the two cycles both show maxima at midday because of the strongest solar radiation at that time (Liu et al., 1992). Clearly, WQS had a higher OH levels than TO due to a stronger contribution of local $O_3$ production.

*Table 8.1 OBM-calculated OH peak values and the corresponding comparison between observed and calculated $O_3$ production for 13 days at Tai O and Wan Qing Sha.*

| **Date and Site** | **OH peak level** (molecule per $cm^{-3}$) | **Observed vs Calculated $O_3$ production** *(see Figures 8.1 and 8.2)* | **$O_3$ episode due to** *(Local production (L) vs Mix of local production and long-range transport (L&T))* |
|---|---|---|---|
| Tai O (in 2002) | | | |
| 5 September | $1.90\times10^7$ | Calculated > Observed | L |
| 6 September | $1.56\times10^7$ | Calculated > Observed | L |
| 11 October | $1.13\times10^7$ | Calculated ~ Observed | L |
| 25 October | $4.22\times10^6$ | Calculated < Observed | L&T |
| 6 November | $6.89\times10^6$ | Calculated < Observed | L&T |
| 7 November | $7.45\times10^6$ | Calculated < Observed | L&T |
| 8 November | $8.12\times10^6$ | Calculated ~ Observed | L |
| 12 November | $3.77\times10^6$ | Calculated < Observed | L&T |
| Wan Qing Sha (in 2004) | | | |
| 20 April | $2.26\times10^7$ | Calculated > Observed | L |
| 17 May | $3.53\times10^7$ | Calculated > Observed | L |
| 18 May | $1.00\times10^7$ | Calculated > Observed | L |
| 23 May | $1.38\times10^7$ | Calculated > Observed | L |
| 24 May | $1.29\times10^7$ | Calculated > Observed | L |

*Figure 8.7 Daytime diurnal cycle of hydroxyl (OH) radical concentration (molecules per cm$^3$) at Tai O on 7 November 2002 and Wan Qing Sha on 24 May 2004 calculated by the OBM.*

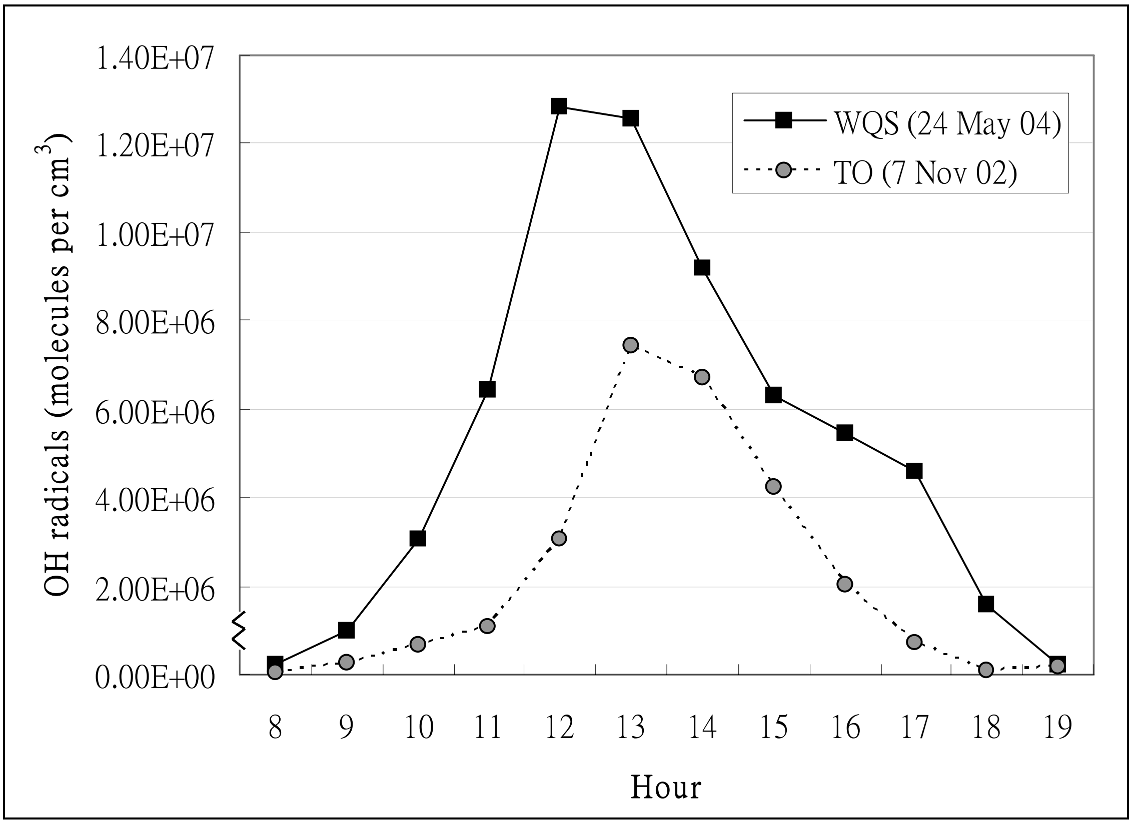

### *8.2.4 Ozone Production Efficiency*

The $O_3$ production efficiency (OPE) is defined as the number of molecules of $O_3$ produced chemically by each molecule of $NO_x$ oxidized. It conveys information about the condition under which $O_3$ is formed and is an important parameter to consider when evaluating impacts from $NO_x$ emission sources (Trainer et al., 1993; Roberts et al., 1996; Griffin et al., 2004). The OPE depends on ambient conditions such as UV radiation, VOC mixture, $NO_x$ concentrations as well as the VOC/$NO_x$ ratios. Kleinman et al.(2002) reported that a $NO_x$ molecule could be more effective in forming $O_3$ in clean remote regions (high OPE, ~10) as compared with a polluted region (low OPE, ~2 to 4). In this regard, the OPE (ratio of $O_3$ to $NO_z$) has been used by Sillman (1995) as an indicator of whether $O_3$ was formed under $NO_x$ limited (high OPE ratio) or VOC limited (low OPE ratio) condition.

The OPE can be estimated by calculating the ratio of $O_3$ to $NO_z$ (product of $NO_x$ oxidation). Here, the plots of $O_3$ versus $NO_z$ for the two $O_3$ episodes are prepared in order to estimate the respective OPE. The $NO_z$ values can be obtained either by measurement data ($NO_y$ – $NO_x$) or model results. It has been reported that there is uncertainty of the $NO_2$ measurement from the $NO_x$ analyzer employing surface catalytic conversion. This is because it suffers from problems including a high limit of detection and the non-specific conversion of $NO_2$, with instrument responding to PAN, alkyl nitrates and $HNO_3$ (Logan, 1989; Wang et al., 2001a). A negative bias of $NO_z$ levels would exists because measurements of NO and $NO_x$ may include not only the $NO_2$ level but also the sum of PAN and alkyl nitrates and $HNO_3$. In our case, since no field measurement of $NO_2$ was conducted at TO, the hourly $NO_2$ data was calculated by the OBM with respect to the relevant photochemical mechanisms in order to get the respective hourly $NO_z$ data (i.e. calculated $NO_z$ = measured $NO_y$ – measured NO – calculated $NO_2$).

Figure 8.8 shows the measured $O_3$ levels at TO as a function of calculated $NO_z$ ($NO_y$ – $NO_2$ - NO) during the afternoon period (LST 1300 to 1700) of 7 November 2002. Afternoon data is generally selected for the analysis because of the occurrence of strong oxidation and photochemical reactions within the period (Trainer et al., 1993). The slope of the regression line of Figure 8.8 was 3.04 ($R^2$=0.76), illustrating that about three $O_3$ molecules were formed per $NO_x$ molecule oxidized. By comparing with values of the OPE between 3 and 6 in the urban plumes of Nashville (St. John et al., 1998), the OPE value (of 3) at TO indicated a strong sensitivity of VOC on the $O_3$ production on 7 November 2002.

The background $O_3$ level at the site could be interpreted from the y-intercept of the regression between $O_3$ and $NO_z$ (Griffin et al., 2004). A background $O_3$ level of 16 ppbv was estimated from the TO data on 7 November 2002 (see the y-intercept of Figure 8.8). The result was comparable to the mean morning (LST 0100 to 0500) $O_3$ level of 23 ppbv between September and November 2002.

*Figure 8.8 Ozone Production Efficiency at Tai O on 7 November 2002 estimated from the plot of measured $O_3$ versus calculated $NO_z$ for afternoon data (LST 1300 to 1700).*

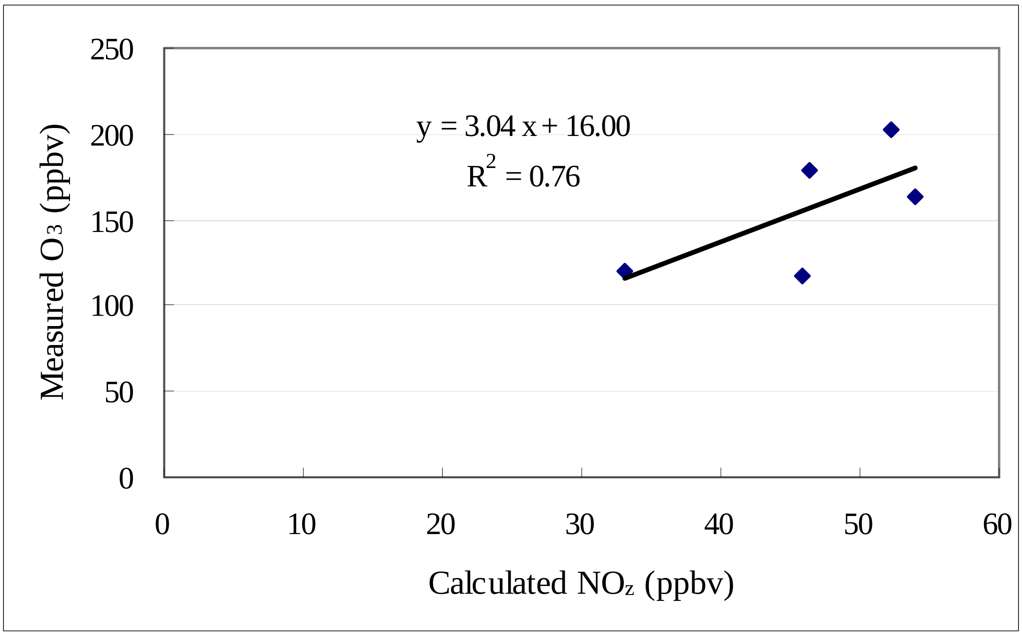

The OPE for the WQS case is illustrated in Figure 8.9 which shows the measured $O_3$ levels at WQS as a function of calculated $NO_z$ during the afternoon period (LST 1300 to 1700) of 24 May 2004. The slope of the regression line was 3.66 ($R^2$=0.94), illustrating about four $O_3$ molecules were produced per $NO_x$ molecule oxidized and this result was slightly higher than the TO case (of 3). The intercept of the regression indicates a background $O_3$ level of about 23 ppbv at the inland site which is higher than the mean morning (LST 0100 to 0500) $O_3$ level of 12 ppbv during the period from 19 April to 28 June 2004, suggesting a strong local contribution to the $O_3$ episode at WQS on 24 May 2004. From the low OPE values, the results highlighted a strong sensitivity of VOC to the $O_3$ formation for the two cases.

*Figure 8.9 Ozone Production Efficiency at Wan Qing Sha on 24 May 2004 estimated from the plot of measured $O_3$ versus calculated $NO_z$ for afternoon data (LST 1300 to 1700).*

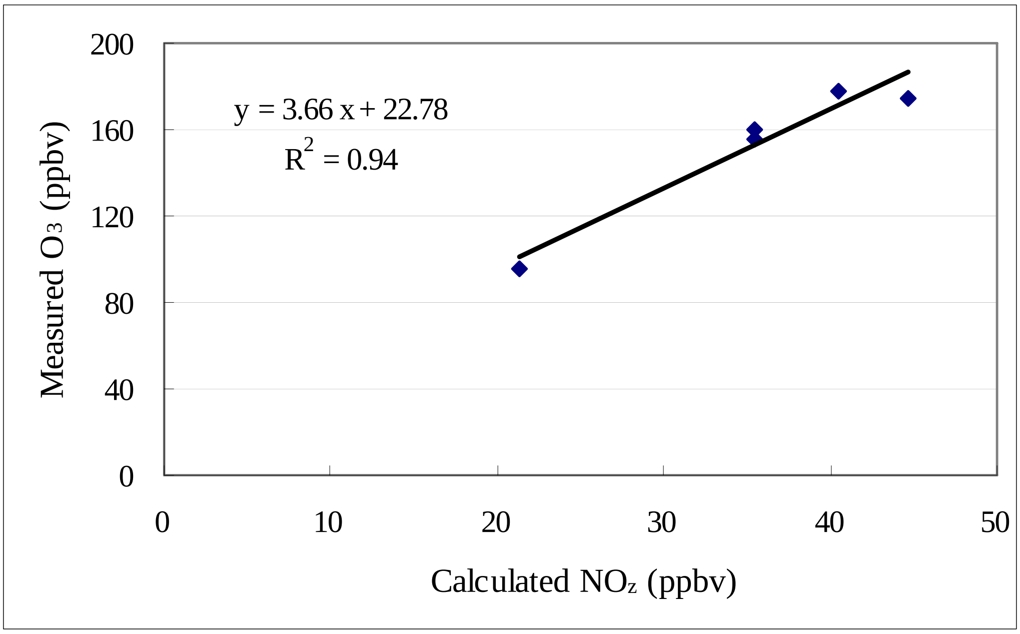

To learn more about the OPE information of the two sites during the study period, we further estimated the OPE values from the plots ($O_3$ versus $NO_z$) with data sets of (a) the eight days at TO, (b) the five days at WQS and (c) the 13 days at the two sites (see Table 7.1). Results (slopes with $R^2$) of the three data sets (a), (b) and (c) were 1.4 ($R^2$=0.21), 1.1 ($R^2$=0.15) and 1.2 ($R^2$=0.16), respectively. The correlations of the plots were fair and the uncertainties of the estimated OPE values could not be ignored. Nevertheless, the general low OPE values strongly implied that there was a high degree of $O_3$ production under VOC-limited condition at the two sites.

### *8.2.5 Partition of Reactive Nitrogen Compounds*

The importance of reactive nitrogen compounds has been identified for its controlling role in $O_3$ production. It is therefore essential to understand the budget and partitioning of the reactive nitrogen species in the atmosphere. The relative contribution of individual $NO_y$ species to the total has been an important subject of research in the past few years (Roberts, 1995). Previous studies indicated that major components of $NO_y$ are $NO_x$, total inorganic nitrate ($HNO_3$+$NO_3^-$) and PAN which accounted for 50 to 70% of the total reactive nitrogen compounds (Roberts, 1995; Warneck, 2000).

Field measurements of total inorganic nitrate and PAN were often reported with high levels of difficulty in measurement and data uncertainty due to interference (Roberts, 1995). This thesis will estimate the levels of these reactive nitrogen compounds using the OBM.

The relative proportions of daytime average OBM-calculated species (of $NO_x$, $HNO_3$+$NO_3^-$ and PAN) at the two $O_3$ episodes of TO and WQS are presented in Figure 8.10. The sum of four major $NO_y$ species ($NO_x$, $HNO_3$+$NO_3^-$ and PAN) was calculated to be accounted for 46% and 76% of the measured $NO_y$ data, which was comparable to those reported at other sites. This shortfall in $NO_y$ should be attributed to the presence of organic nitrates (Roberts, 1995). By comparing the two data sets, a higher proportion of total inorganic nitrates and PAN at WQS revealed the corresponding stronger contribution of *in-situ* local production (see Figure 8.10).

*Figure 8.10 Relative proportion of daytime average calculated $NO_y$ species (nitrogen oxides ($NO_x$), total inorganic nitrate ($HNO_3$+$NO_3^-$) and PAN) at Tai O on 7 November 2002 and Wan Qing Sha on 24 May 2004.*

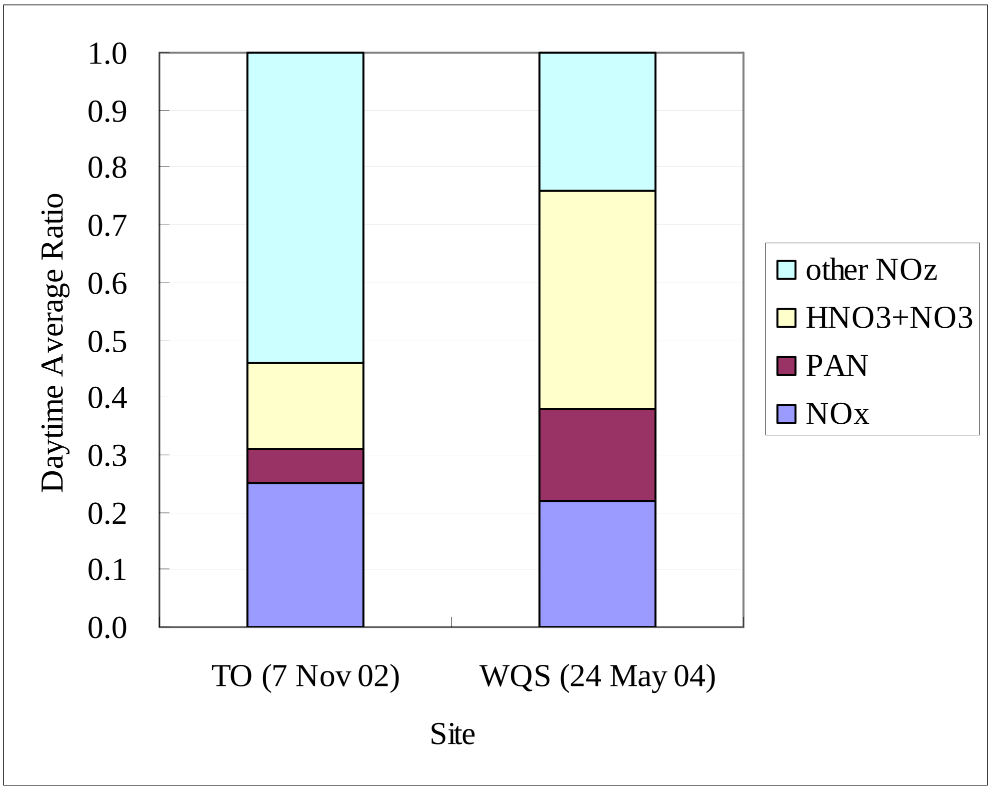

### *8.2.6 Comparison of Observed and Calculated Ozone Changes*

As a caveat, the OBM only calculates the $O_3$ produced locally in accordance with the simulated chemical reactions that happened at the site. As chemistry is one of several factors that vary $O_3$ concentration, the model results do not account for the change of $O_3$ level due to horizontal advections. It is therefore not surprising to see the difference between the calculated and observed rates. Figure 8.1 showed that the OBM-calculated $O_3$ production only accounted for about 50% of the observed $O_3$ increment at TO on 7 November 2002. Figure 8.11 further compares the diurnal variation of calculated and observed $O_3$ rates. The calculated hourly $O_3$ production is based on the hourly difference (production – loss) of $O_3$ production (Cardelino and Chameides, 1995) while the observed rate of change of $O_3$ ($dO_3/dt$) is calculated in accordance with *[Equation 2.6]*. From Figure 8.11, it can be seen that the observed rate was higher than the calculated rate from the early morning to the early afternoon. In the morning, $O_3$ concentration increased faster than calculated, which could be caused by the entrainment of air from aloft by the growing convective boundary layer. Such a finding was also reported by Kleinman et al. (1994, 1995) at a rural site of Atlanta, US. From the late morning to early afternoon, the observed rates were still higher than the calculated values, with larger difference as compared to those of early morning. Considering the above analyses of chemical tracers ($\Delta CO/\Delta NO_y$) and the back trajectory, the observed high $O_3$ concentrations should be attributable to the long-range transport of air pollutants to TO. In the late afternoon, a sharp drop of observed $dO_3/dt$ was observed which had also been reported by different studies (e.g. Kleinman et al., 1995; Frost et al., 1998). The sharp drop, similar to other cases, was mainly attributable to the dilution of high $O_3$ concentration near surface air due to the surface deposition and continued growth of the boundary layer.

*Figure 8.11 Daytime diurnal cycles of observed and calculated $O_3$ production rates at Tai O on 7 November 2002.*

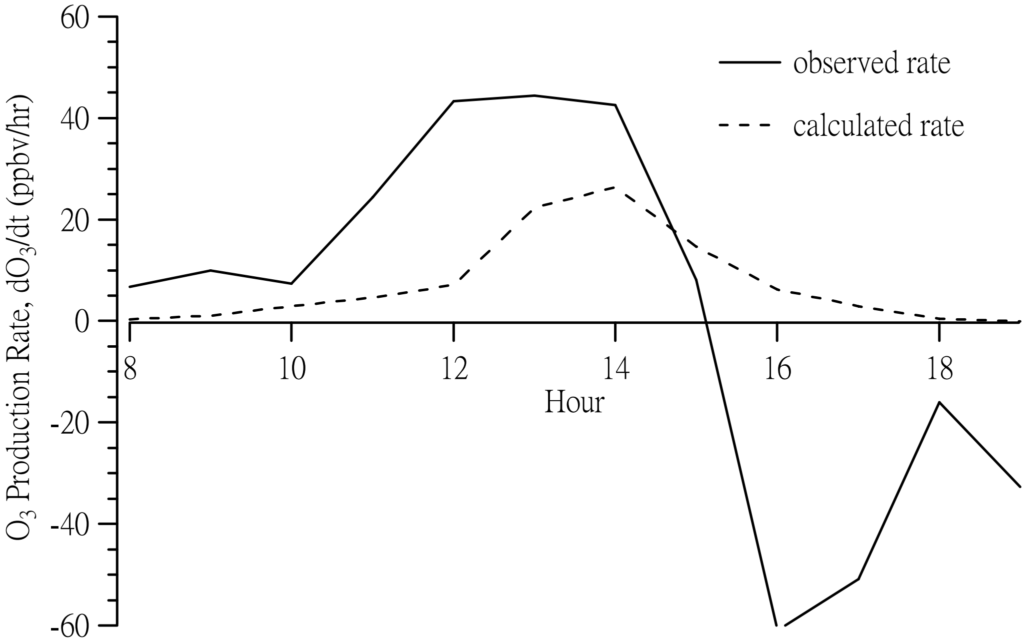

The observed and calculated hourly change of $O_3$ at WQS on 24 May 2004 is also compared and given in Figure 8.12. Similar to the TO case, observed rate was higher than the calculated rate from the early morning to noon, which might be related to the entrainment of air from aloft by the growing convective boundary layer. In contrast, the peak rate at LST 1200 was estimated as 52 ppbv/hr which was close to the observed value of 45 ppbv/hr. The result further indicated the high $O_3$ level was mainly caused by the local production, rather than transportation as in the TO case. There was a sharp drop of observed $dO_3/dt$ in the afternoon, suggesting a strong dilution of high $O_3$ concentration near surface air due to the surface deposition and continued growth of the boundary layer.

*Figure 8.12 Daytime diurnal cycles of observed and calculated $O_3$ production rates at Wan Qing Sha on 24 May 2004.*

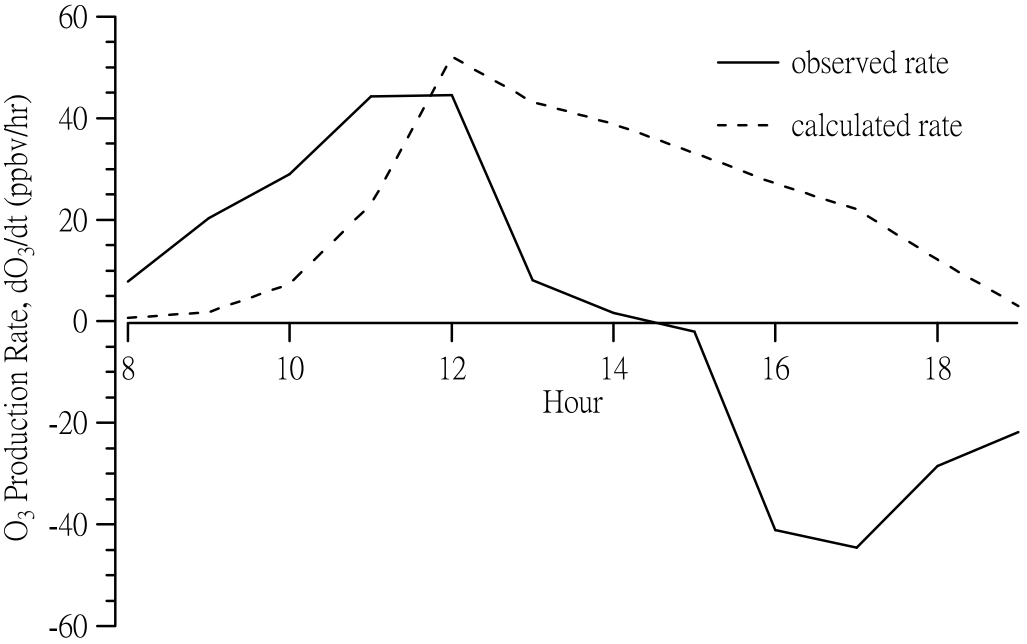

## 8.3 Chapter Summary

Chapter 7 explained how the OBM estimated the efficacy of various $O_3$ precursors like NO, CO and VOC in the reduction of $O_3$ production. This chapter further illustrated how the model evaluated the relative contribution of $O_3$ episodes from *in-situ* local production versus regional transport of air pollutants. It also estimated the variation of non-measured intermediates and species which were difficult to measure. Using the measured and modelled data, the OBM identified the key chemical processes participating in the tropospheric sources and sinks of $O_3$, giving the $O_3$ budget information at two PRD sites.

At TO, half of the $O_3$ episodes were attributable to regional transport of pollutants while local production contributed to the other episodes. By comparison, $O_3$ episodes at WQS were mainly due to the local production. Two elevated $O_3$ events at TO (7 November 2002) and WQS (24 May 2004) were further studied with regard to the areas of diurnal variation of species, $O_3$ budget, OPE, partition of reactive nitrogen compounds and $O_3$ production rates. The two cases both revealed a strong sensitivity of VOC on photochemical $O_3$ production at the sites. For the TO case, elevated $O_3$ peak was contributed by the long-range transport of air pollutants whereas local sources of air pollutants contributed most to the $O_3$ episode at WQS. In both cases, conversion of NO to $NO_2$ by $HO_2$ was the major reaction for photochemical $O_3$ production. The photochemical $O_3$ loss rate was dominated by the reaction between $NO_2$ and OH at TO whereas the reaction of $O_3$ and

$HO_2$ was the major $O_3$ destruction pathway at WQS. The $O_3$ production efficiency and partition of reactive nitrogen compounds were also estimated from the calculated concentrations of $NO_2$, PAN, $HNO_3$ and measured values of NO and $NO_y$ during the two $O_3$ episodes. The results showed that three to four $O_3$ molecules were formed per $NO_x$ molecule oxidized while PAN and $HNO_3$ were the most significant reactive nitrogen compounds in the afternoon. The above conclusions were drawn from the analysis of a limited data set and additional studies using a more comprehensive data set are needed to better characterize the photochemical $O_3$ production in this region.

# CHAPTER 9 CONCLUSIONS AND RECOMMENDATIONS

## 9.1 Summary of Major Findings

This thesis is aimed at filling our knowledge gap on the sources and formation of ground-level $O_3$ in HK, through the understanding of the $O_3$-$NO_x$-VOC chemistry and the sensitivity for different $O_3$ precursors in controlling $O_3$ formation. Since photochemical $O_3$ pollution is a regional problem, the relevant information of the PRD should also be considered. In this connection, measurement data of $O_3$ and related pollutants of HK and PRD sites are presented and analyzed in this thesis, with the following key findings:

**Seasonal and spatial $O_3$ Patterns:** Monthly averaged $O_3$ concentration in HK reached a maximum in autumn and a minimum in summer owing to the influence of Asian monsoon circulation. Average $O_3$ level was highest in the northeastern rural site of HK, which were mainly attributable to the influences of regional air masses from the inland region. By comparison, the southwestern suburban site was impacted by both local and regional pollution, giving occasional elevated $O_3$ episodes coupled with stagnant meteorological conditions.

**Distribution and Reactivity of VOC:** VOC measurements from the rural, urban and roadside sites in HK were examined for their spatial distribution, seasonal variation, source-receptor relationships and photochemical reactivity. In general, the highest VOC level was found at the roadside site because of the vehicular emissions while the rural site was characterized by the aged air mass with the lowest VOC level. Isoprene, a photochemical reactive VOC, was confirmed to be generated from vehicular sources at the roadside site and from biogenic sources in the rural area. Ratios between VOC with different photochemical reactivities showed the mix of emission sources and the increase of atmospheric processing from urban to rural areas.

**Roles of VOC on $O_3$ production:** Photochemical $O_3$ production was controlled by VOC in HK which was indicated by the low ratios of VOC/$NO_x$, low afternoon ratios of $O_3$/$NO_y$, and respective high RIR(THC) results. In contrast, $NO_x$ tended to suppress $O_3$ formation, and CO was found to have played a negligible role. Overall, anthropogenic hydrocarbons were more important than those from natural origins. From the regional point of view, stationary VOC played a more important role than mobile VOC in controlling $O_3$ at the coastal site in HK whereas the opposite is true for the inland site in Guangdong. Among the various anthropogenic hydrocarbons, reactive aromatic compounds (e.g. toluene, xylenes, etc.) contributed most to the $O_3$ formation.

**Local production versus regional transport contributing to $O_3$ production:** Apart from the sensitivities of various $O_3$ precursors in controlling $O_3$, the OBM was also used to estimate the relative contribution of local production and regional transport to $O_3$ production. Results indicated that elevated $O_3$ levels at TO were contributed by both factors whereas local production was the major contributor to the $O_3$ production at WQS.

**Analysis of $O_3$ episodes:** Photochemical $O_3$ production was limited by VOC over the PRD. However, causes for the $O_3$ episodes were different among various conditions. By comparing the two elevated $O_3$ cases, the record high $O_3$ episode of 203 ppbv at TO on 7 November 2002 was found to be impacted by regional air pollutants, while local contributions were the major component for the elevated $O_3$ level (of 178 ppbv) at WQS on 24 May 2005. With the use of the OBM, an in-depth analysis was conducted to investigate the photochemical $O_3$ reactions, non-measured intermediates for the $O_3$ budget, OPE and partition of reactive nitrogen compounds involved in the two $O_3$ episodes. Conversion of NO to $NO_2$ by $HO_2$ was the major reaction for photochemical $O_3$ production at both sites. The photochemical $O_3$ loss rate was dominated by the reaction between $NO_2$ and OH at TO whereas the reaction of $O_3$ and $HO_2$ was the major $O_3$ destruction pathway at WQS. Three to four $O_3$ molecules were formed per $NO_x$ molecule oxidized while PAN and $HNO_3$ were the most significant reactive nitrogen compounds in the afternoon.

**Sensitivity of different VOC to $O_3$ production over the PRD:** Results from this thesis suggested that SHC was more sensitive than MHC to $O_3$ production in HK but the opposite was true for Guangdong. Subject to the change of emission patterns and site characteristics over the PRD, various sources of VOC are found to be playing different roles of $O_3$ formation in the region and somewhat different VOC reduction plans should be implemented in different PRD areas in order to attain the largest overall reduction in regional $O_3$ pollution.

## 9.2 Significance of this Thesis

This thesis makes use of a high quality database of $O_3$, $O_3$ precursors, and related pollutants measured by HKPU and EPD in the different locations over the PRD. Findings of this thesis are significant to our understanding of the photochemical $O_3$ pollution in the region.

Different kinds of mathematical, statistical and modelling techniques were used for the data analysis. This thesis provides a good example to illustrate how to analyze the data set in a systematic and effective approach.

Previous studies only focused on the analysis of the measurement of trace gases in assessing the sources and formation of $O_3$ episodes. This thesis made use of the OBM to evaluate the sensitivity of different $O_3$ precursors. It also estimated the values of various non-measured intermediate species which helped understand the photochemical reactions participating in the $O_3$ formation.

In the light of the continuing economic expansion in the PRD, it is anticipated that the emissions of air pollutants in the region could become more significant in the coming years. Through the detailed analysis of the distribution, sources and chemistry of photochemical pollutants over the region, the findings of this thesis provide the local authorities with essential information for their formulation of effective control measures in tackling the regional air pollution problems.

## 9.3 Suggestions for Further Work

The conclusions drawn from this thesis clearly indicate that the level of photochemical smog pollution is deteriorating in HK, and that it is not only contributed by the local emissions, but also attributed to regional pollutants from the PRD. To address the photochemical smog problem, further work are needed for the following areas:

**Comprehensive measurement of $O_3$, VOC and other air pollutants over the PRD:** VOC is concluded as the major $O_3$ precursors in HK and WQS. To further understand the contribution of different sources of VOC in the PRD, extensive measurement of $O_3$, VOC and other air pollutants should be conducted at different PRD sites, including upwind, inland and downwind areas. With the assistance of relevant meteorological data, concurrent measurement results can provide us with more concrete information about the production and transport of $O_3$ over the region. Also, area-averaged RIR for different precursors can then be calculated to give a more robust indication about their sensitivities to $O_3$ formation over the PRD.

**Sources apportionment of VOC:** Aromatic hydrocarbons (e.g. toluene and xylenes) are the major VOC contributing to the $O_3$ production. As they are associated with different sources e.g. vehicular emissions, solvent application, etc., more rigorous studies like sources apportionment on the

VOC data is needed to characterize VOC sources in HK and over the PRD areas. Although the mass concentration is lower than other key VOC, isoprene also plays an important role in photochemical $O_3$ production because of its high reactivity. It is therefore of interest to understand the relative contribution of isoprene between biogenic and anthropogenic sources at different sites in various seasons.

**Availability of accurate emission data:** Accurate emission data of the PRD is essential to address the regional air pollution issues. Source measurements should be carried out on selected industrial types and facilities/processes to typify the emission profiles associated with the operation of the major industrial facilities and processes. The information can help us to investigate the relative benefits of various emissions control strategies [VOC controls versus $NO_x$ controls] for reducing the severity of photochemical $O_3$ pollution and to make recommendations of the more feasible control options.

**Application of models in $O_3$ analysis:** The OBM, rather than EBM, is used in this study because the OBM does not require the use of challenging China emission inventories and simulation of boundary layer dynamics as in the EBM. However, there are limitations of the OBM; it is diagnostic rather than prognostic and should be used in conjunction with the other EBM in the future study of $O_3$ precursor relationship.

**Quantification of non-measured intermediates:** The OBM is mainly used to estimate the sensitivities of $O_3$ precursors in this thesis. In fact, the model can also provide the concentrations of various intermediates which are difficult to measure. Having obtained the accurate values of the intermediates, we can realize the contributions of different photochemical reactions involved, and confirm and quantify the roles of the intermediates participating in the $O_3$ chemistry. The tropospheric $O_3$ budget, OPE and partition of reactive nitrogen compounds can then be calculated. Such information is useful to our understanding of the controlling species and reactions on $O_3$ production. Preliminary results of the two $O_3$ episode cases were produced from this thesis and more comprehensive studies in this direction should be conducted. In addition, measurement of reactive nitrogen compounds (including PAN, total inorganic nitrate, etc) may be required to verify the model results and understand the partitioning of $NO_y$.

**Estimation of the local and regional contribution to $O_3$ pollution:** Calculation from the OBM adopts a number of assumptions, focusing on the *in-situ* $O_3$ production but neglecting the horizontal transport in solving the concentrations of intermediates. Further study on the comparison between the calculated and observed $O_3$ change will help estimate the physical processes like entrainment of air from aloft, deposition as well as transportation. Therefore, accuracy of the modelled results can be further improved by modifying the model in consideration of the above physical factors. With the help of other information from back trajectory and ratios of air pollutants, we can obtain a better picture about the proportion of $O_3$ generated from local production versus regional transportation.

## REFERENCES

Andreae, M. O. and Merlet, P., 2001. Emissions of trace gases and aerosols from biomass burning, Global Biogeochemical Cycles, 15, 955-966.

Angle, R. P. and Sandhu, H. S., 1989. Urban and rural ozone concentrations in Alberta, Canada. Atmospheric Environment 23, 215-221.

Apel, E. C., Calvert, J. G., Gilpin, T. M., Fehsenfeld, F., Lonneman, W. A., 2003. Nonmethane hydrocarbon intercomparison experiment (NOMHICE): Task 4, ambient air, Journal of Geophysical Research 108 (D9), 4300, doi:10.1029/2002JD002936.

Aronian, P.F., Scheff, P.A., Wadden, R.A., 1989. Wintertime source-reconciliation of ambient organics. Atmospheric Environment 23, 911-920.

Atkinson, R. 1994. Gas-phase tropospheric chemistry of organic compounds. Journal of Physical and Chemical Reference Data, 1994; Monograph 2.

Barletta, B., Meinardi, S., Simpson, I. J., Khwaja, H. A., Blake, D. R., Rowland, F. S., 2002. Mixing ratios of volatile organic compounds (VOC) in the atmosphere of Karachi, Pakistan. Atmospheric Environment 36, 3429-3443.

Blake, D.R., Smith Jr., W.J., Chen, T.-Y., Whipple, W.J., Rowland, F.S. 1994. Effects of biomass burning on summertime non-methane hydrocarbon concentrations in the Canadian wetlands. Journal of Geophysical Research 99, 1699-1719.

Blake, D. R. and Rowland, F. S., 1995. Urban leakage of liquefied petroleum gas and its impact on Mexico City air quality. Science 269, 953-956.

Borbon, A., Fontaine, H., Veillerot, M., Locoge, N., Galloo, J. C., Guillermo, R., 2001. An investigation into the traffic-related fraction of isoprene at an urban location. Atmospheric Environment 35, 3749-3760.

Borbon, A., Locoge, N., Veillerot, M., Galloo, J. C. and Guillermo, R., 2002. Characterization of NMHCs in a French urban atmosphere: overview of the main sources. The Science of the Total Environment 292, 177-191.

Boudries, H., Toupance, G. and Dutot, A. L., 1994. Seasonal variation of atmospheric nonmethane hydrocarbons on the western coast of Brittany, France. Atmospheric Environment 28, 1095-1112.

Bower, J. S., Stevenson, K. J., Broughton, G. F. J., Lampert, J. E., Sweeney, B. P. and Wilken J., 1994. Assessing recent surface ozone concentrations in the U.K. Atmospheric Environment 28, 115-128.

Bruckmann, P., Kerstem, W., Funcke, W., Balfanz, E., Konig, J., Theisen, J., 1988. The occurrence of chlorinated and other organic trace compounds in urban area. Chemosphere 17, 2363-2380.

Buhr, M., Parrish, D., Elliot, J., Holloway, J., Carpenter, J., Goldan, P., Kuster, W., Trainer, M., Montzka, S., Mckeen, S. and Fehsenfeld, F., 1995. Evaluation of ozone precursor source types using principal component analysis of ambient air measurements in rural Alabama. Journal of Geophysical Research 100 No. D11, 22853-22860.

CAPMoN (Canadian Air and Precipitation Network), 2003. Environment Canada, Climate and Atmospheric Research Directorate, 4905 Dufferin Street, Downsview, Ont., M3H 5T4; http://www.msc-smc.ec.gc.ca/natchem/particles/n_capmon_e.html.

Cardelino, C. A. and Chameides, W. L., 1995. An observation-based model for analyzing ozone precursor relationships in the urban atmosphere. Journal of the Air & Waste Management Association 45, 161-180.

Cardelino, C. A. and Chameides, W. L., 2000. The application of data from photochemical assessment monitoring stations to the observation-based model. Atmospheric Environment 34, 2325-2332.

Carter, W. L., Atkinson, R., 1989. Computer modelling study of incremental hydrocarbon reactivity. Environmental Science and Technology 23, 864.

Carter, W. P. L., 1994. Development of ozone reactivity scales for volatile organic compounds. Journal of Air and Waste Management Association 44, 881-899.

CASTNet (Clean Air Status and Trends Network), 2004. http://www.epa.gov/castnet/.

Census and Statistics Department, The Government of the Hong Kong Special Administrative Region, 1999. Hong Kong Energy Statistic Annual Report 1999 Edition.

CH2M Hill (China) Limited. 2002. Study of air quality in the Pearl River Delta Region, Environmental Protection Department, Hong Kong Special Administrative Region, Agreement No. CH106/98. (http://www.epd.gov.hk/epd/english/environmentinhk/air/studyrpts/study_pearl.html)

Chameides, W.L., Lindsay, R.W., Richardson, J., and Kiang, C.S. 1988. The Role of biogenic hydrocarbons in urban photochemical smog: Atlanta as a case study, Science, 241. 1473-1475.

Chameides, W. L., Fehsenfeld, F., Rodgers, M. O., Cardeling, C., Martinez, J., Parrish, D., Lonneman, W., Lawson, D. R., Rasmussen, R. A., Zimmerman, P., Greenberg, J., Middleton, P. and Wang, T., 1992. Ozone precursor relationship in the ambient atmosphere. Journal of Geophysical Research 97 No. D5, 6037-6055.

Chan, C. Y. and Chan, L. Y., 2000. Effect of meteorology and air pollutant transport on ozone episodes at a subtropical coastal Asian city, Hong Kong. Journal of Geophysical Research 105, D16, 20707-20724.

Chan, L. Y., Chan, C. Y. and Qin, Y., 1998. Surface ozone pattern in Hong Kong. Journal of Applied Meteorology 37, 1153-1165.

Chan, C. Y., Chan, L. Y., Wang, X. M., Liu, Y. M., Lee, S. C., Zou, S. C., Sheng, G. Y. and Fu, J. M., 2002. Volatile organic compounds in roadside microenvironments of metropolitan Hong Kong. Atmospheric Environment 36, 2039-2047.

Chang, C.C., Chen, T.Y., Lin, C.Y., Yuan, C.S., Liu, S.C. 2005. Effects of reactive hydrocarbons on ozone formation in southern Taiwan, Atmospheric Environment 39, 2867-2878.

Chen, T. Y., Simpson, I. J., Blake, D. R., Rowland, F. S., 2001. Impact of the leakage of liquefied petroleum gas (LPG) on Santiago air quality. Geophysical Research Letter 28, 2193-2196.

Cheng, L., Fu, L., Angle, R. P., Sandhu, H. S., 1997. Seasonal variations of volatile organic compounds in Edmonton, Alberta. Atmospheric Environment 31, 239-246.

Cheng, W. L., 2001. Synoptic weather patterns and their relationship to high ozone concentrations in the Taichung Basin. Atmospheric Environment 35, 4971-4994.

Cheung, V. T. F. and Wang, T., 2001. Observational study of ozone pollution at a rural site in the Yangtze Delta of China. Atmospheric Environment 35, 4947-4958.

Chiu, T. and So, C. L., 1986. A geography of Hong Kong, 2nd Edition, University Press, Oxford.

Clapp, L. J. and Jenkin, M. E., 2001. Analysis of the relationship between ambient levels of $O_3$, $NO_2$ and NO as a function of $NO_x$ in the UK. Atmospheric Environment 35, 6391-6405.

CMDL (Climate Monitoring and Diagnostics Laboratory), 2004. CMDL Summary Report #26. Climate Monitoring and Diagnostics

Laboratory, 325 Broadway R/CMDL, Boulder, Colorado, 80305; http://www.cmdl.noaa.gov/publications/annrpt26/4_1_4.pdf.

Colman, J.J., Swanson, A.L., Meinardi, S., Sive, B.C., Blake, D.R., Rowland, F.S., 2001. Description of the analysis of a wide range of volatile organic compounds in whole air samples collected during PEM-Tropics A and B. Analytical Chemistry 73, 3723-3731.

Combrink, J., Diab, R. D., Sokolic, F., Brunke, E. G.,1995. Relationship between surface, free tropospheric and total column ozone in two contrasting areas in South Africa. Atmospheric Environment 29, 685-691.

Darnall, K. R., Lloyd, A. C., Winer, A. M., Pitts, J. N., 1976. Reactivity scale for atmospheric hydrocarbons based on reaction with hydroxyl radical. Environment Science and Technology 10, 692-696.

Derwent, R. G., Davies, T. J., Delaney, M., Dollard, G. J., Field, R. A., Dumitrean, P., Nason, P. D., Jones, B. M. R., Pepler, S. A., 2000. Analysis and interpretation of the continuous hourly monitoring data for 26 $C_2$-$C_8$ hydrocarbons at 12 United Kingdom sites during 1996. Atmospheric Environment 34, 297-312.

De Muer, D., Heylen, R., Van Loey, M., De Sadelaer, G., 1997. Photochemical ozone production in the convective mixed layer, studied with a tethered balloon sounding system. Journal of Geophysical Research 102 (15), 933-947.

Ding, A. J., Wang, T., Zhao, M., Wang, T. J., Li, Z. K., 2004. Simulation of sea-land breezes and a discussion of their implications on the transport of air pollution during a multi-day ozone episode in the Pearl River Delta of China. Atmospheric Environment 38, 6737-6750.

Ding, W. H. and Wang, J. L., 1998. Spatial concentration profiles of $C_2$-$C_6$ hydrocarbons in the atmosphere of Taipei metropolitan area. Chemosphere 37, 1187-1195.

Duderstadt, K.A., Carroll, M.A., Sillman, S., Wang, T., Albercook, G.M., Feng, L., Parrish, D.D., Holloway, J.S., Fehsenfeld, F.C., Blake, D.R., Blake, N.J., Forbes, G. 1998. Photochemical production and loss rate of ozone at Sable Island, Nova Scotia during the North Atlantic Regional Experiment (NARE) 1993 summer intensive. Journal of Geophysical Research 103, D11, 13531–13555.

Environmental Protection Department (EPD), 2000. Air quality in Hong Kong 1999, Air Services Group, Environmental Protection Department, The Government of the Hong Kong Special Administrative Region.

Environmental Protection Department (EPD), 2001. Air quality in Hong Kong 2000, Air Services Group, Environmental Protection Department, The Government of the Hong Kong Special Administrative Region.

Field, R. A., Goldstone, M. E., Lester, J. N., Perry, R., 1994. The variation of volatile organic compound concentrations in Central London during the period of July 1991 to September 1992. Environmental Technology 15, 931-944.

Finlayson, B. J., Pitts, J. N., 1976. Photochemistry of the polluted troposphere. Science 192, 111-119.

Folinsbee, L. J., McDonnell, W. F. and Horstman, D. H., 1998. Pulmonary function and symptom responses after 6.6-hour exposure to 0.12 ppm ozone with moderate exercise. Journal of Air Pollution Control Association 38, 28-35.

Frost, G.J., Trainer, M., Allwine, G.., Buhr, M.P., Calvert, J.G., Cantrell, C.A., Fehsenfeld, F.C., Goldan, P.D., Herwehe, J., Hubler, G., Kuster, W.C., Martin, R., McMillen, R.T., Montzka, S.A., Norton, R.B., Parrish, D.D., Ridley, B.A., Shetter, R.E., Walega, J.G., Watkins, B.A., Westberg, H.H., Williams, E.J. 1998. Peroxy radical concentration and ozone formation rate at a rural site in the southeastern United States. Journal of Geophysical Research 103, D17, 22491–22508.

Gee, I. L. and Sollars, C. J., 1998. Ambient air levels of volatile organic compounds in Latin American and Asian cities. Chemosphere 36, 2497-2506.

Gery, M. W., Whitten, G. Z., Killus, J. P., Dodge, M. C., 1989. A photochemical kinetics mechanism for urban and regional computer modelling. Journal of Geophysical Research, 94, 12925.

Ghim, Y. S. and Chang, Y. S., 2000. Characteristics of ground-level ozone distribution in Korea in the period of 1990-1995. Journal of Geophysical Research, 105, D7, 8877-8890.

Goldan, P. D., Parrish, D. D., Kuster, W. C., Trainer, M., McKeen, S. A., Holloway, J., Jobson, B. T., Sueper, D. T., Fehsenfeld, F. C., 2000. Airborne measurements of isoprene, CO and anthropogenic hydrocarbons and their implications, Journal of Geophysical Research 105, 9091 - 9105.

Griffin, R. J., Johnson, C. A., Talbot, R. W., Mao H., Russo, R. S., Zhou, Y., Sive, B. C., 2004. Quantification of ozone formation metrics at Thompson Farm during the New England Air Quality Study (NEAQS) 2002, Journal of Geophysical Research 109, D24302, doi:10.1029/2004JD005344.

Grosjean, E., Rasmussen, R. A., Grosjean, D., 1998. Ambient levels of gas phase pollutants in Porto Alegre, Brazil. Atmospheric Environment 32, 3371-3379.

Grosjean, E., Rasmussen, R. A., Grosjean, D., 1999. Toxic air contaminants in Porto Alegre, Brazil. Environmental Science and Technology 33, 1970-1978.

Guo, H., Wang, T., Louie, P. K. K., 2004. Source apportionment of ambient non-methane hydrocarbons in Hong Kong: Application of an absolute principal component scores (APCS) receptor model. Environment Pollution 129, 489-498.

Guo, H., So, K. L., Simpson, I. J., Barletta, B., Meinardi, S., Blake, D.R., 2007. $C_1$ to $C_8$ volatile organic compounds in the atmosphere of Hong

Kong: Overview of atmospheric processing and source apportionment. Atmospheric Environment 41, in press.

Hansen, A. B., Palmgren, F., 1996. VOC air pollutants in Copenhagen. Science of the Total Environment 1996, 189/190: 451-457.

Hidy, G. M., 2000. Ozone process insights from field experiments. Atmospheric Environment 34, 2001-2022.

Ho, K. F., Lee, S. C., Chiu, G. M. Y., 2002. Characterization of selected volatile organic compounds, polycyclic aromatic hydrocarbons and carbonyl compounds at a roadside monitoring station. Atmospheric Environment 36, 57-65.

Hogo, H. and Gery, M. W., 1988. User's Guide for Executing OZIPM4 with CBM-IV or optional mechanism. US Environmental Protection Agency: Research Triangle Park, NC, USA; EPA/600/8-88/082.

Holzworth, G.C., 1967. Mixing depths, wind speeds and air pollution potential for selected locations in the United States, Journal of Applied Meteorology 6, 1039-1044.

Hopkins, J. R., Lewis, A. C., Seakins, P. W. 2005. Analysis and applications of measurements of source dominated hydrocarbon concentrations from the PUMA campaigns in June/July 1999 and January/February 2000 at an urban background site in Birmingham, UK, Atmospheric Environment 39, 535-548.

Horvath, S. M. and McKee, D. J., 1993. Acute and Chronic Health Effects of Ozone, Troposheric Ozone: Human Health and Agricultural Impacts. Lewis Publishers, Ann Arbor.

Huang, J.P., Fung, J. C. H., Lau, A. K. H., Qin, Y., 2005. Numerical simulation and process analysis of typhoon-related ozone episodes in Hong Kong. Journal of Geophysical Research 110, D05301, doi:10.1029/2004JD004914.

Jacobson, M.Z. 1999. Fundamentals of Atmospheric Modelling. Cambridge University Press, United Kingdom.

Jaffe, D.A., Hornrath, R.E., Zhang, L., Akimoto, H., Shimizu, A., Mukai, H., Murano, K., Hatakeyama, S., Merrill, J.,1996. Measurements of NO, $NO_y$, CO and $O_3$ and estimation of the ozone production rate at Oki Island, Japan, during PEM-West. Journal of Geophysical Research 101, 2037–2048.

Jeffries, H.E. and Crouse, R., 1990. Scientific and technical issues related to the application of incremental reactivity. Department of Environmental Sciences and Engineering, University of North Carolina, Chapel Hill, NC.

Jobson, B. T., Wu, Z., Niki, H. and Barrie, L. A., 1994. Seasonal trends of isoprene, $C_2$-$C_5$ alkanes, and acetylene at a remote boreal site in Canada. Journal of Geophysical Research 99, 1589-1599.

Jonnalagadda, S. B., Bwila, J., Kosmus, W., 2001. Surface ozone concentrations in Eastern Highlands of Zimbabwe. Atmospheric Environment 35, 4341-4346.

Kasibhatla, P., Chameides, W. L., Saylor, R.D., and Olerud, D., 1998. Relationships between regional ozone pollution and emissions of nitrogen oxides in the Eastern United States. Journal of Geophysical Research, 103, 22663-22669.

King, W.J. and Vukovich, F. M., 1982. Some dynamic aspects of extended air pollution episodes. Atmospheric Environment 16, 1171-1181.

Kleinman, L., Lee, Y.N., Springston, S.R., Nummermacker, L., Zhou, X., Brown, R., Hallock, K., Klotz, P., Leahy, D., Lee, J.H., Newman, L. 1994. Ozone formation at a rural site in the southeastern United States. Journal of Geophysical Research 99, D2, 3469 – 3482.

Kleinman, L., Lee, Y. N., Springston, S. R., Lee, J. H., Nummermacker, L., Weinstein-Lloyd, J., Zhou, X. 1995. Peroxy radical concentration and ozone formation rate at a rural site in the southeastern United States. Journal of Geophysical Research 100, D4, 7263–7273.

Kleinman, L., Lee, Daum, P. H., Lee, Y. N., Nummermacker, L., Springston, S. R., Weinstein-Lloyd, J., Rudolph, J. 2002. Ozone production efficiency in an urban area. Journal of Geophysical Research 107, D23, 4733, doi:10.1029/2002JD002529.

Kok, G.L., Lind, J.A. and Fang, M., 1997. An airborne study of air quality around the Hong Kong territory. Journal of Geophysical Research 102, 19,043-19,057.

Lacaux, J. P., Cachier, H., Delmas, R., 1993. Biomass burning in Africa: an overview of its impact on atmospheric chemistry. In: Crutzen, P. J., Goldammer, J. G. (Eds.), Fire in the Environment: The Ecological Atmospheric and Climatic Importance of Vegetation Fires pp. 163-191 (Chapter 10), Wiley, New York.

Lal, S., Naja, M. and Subbaraya, B. H., 2000. Seasonal variations in surface ozone and its precursors over an urban site in India. Atmospheric Environment 34, 2713-2724.

Lam, K. S., Wang, T. J., Chan, L. Y., Wang, T. and Harris, J., 2001. Flow patterns influencing the seasonal behaviour of surface ozone and carbon monoxide at a coastal site near Hong Kong. Atmospheric Environment 35, 3121-3135.

Lam, K.S., Wang, T.J., Wu, C.L., Li, Y.S. 2005. Study on an ozone episode in hot season in Hong Kong and transboundary air pollution over Pearl River Delta region of China, Atmospheric Environment 39, 1967-1977.

Laurila, T. and Hakola, H., 1996. Seasonal cycle of $C_2$-$C_5$ hydrocarbons over the Baltic Sea and Northern Finland. Atmospheric Environment 30, 1597-1607.

Lee, S. C., Chiu, M. Y., Ho, K. F., Zou, S. C. and Wang, X, 2002. Volatile organic compounds in urban atmosphere of Hong Kong. Chemosphere 48, 375-382.

Lee, Y. L. and Sequeira, R, 2001. Visibility degradation across Hong Kong: its components and their relative contributions. Atmospheric Environment 35, 5861-5872.

Lin, C. Y. C., Jacob, D. J., Munger, J. W. and Fiore, A. M., 2000. Increasing background ozone in surface air over the United States. Geophysical Research Letters 27, No. 21, 3465-3468.

Lin, C. Y. C., Jacob, D. J. and Fiore, A. M., 2001. Trends in exceedances of the ozone air quality standard in the continental United States, 1980-1998. Atmospheric Environment 35, 3217-3228.

Lind, J. A. and Kok, G. L., 1999. Emission strengths for primary pollutants as estimated from an aircraft study of Hong Kong air quality. Atmospheric Environment 33, 825-831.

Liu, C, Xu Z, Du, Y, Guo, H., 2000. Analysis of volatile organic compounds concentrations and variation trends in the air of Changchun, the northeast of China. Atmospheric Environment, 34, 4459-4466.

Liu, C. M., Liu, S. C. and Shen, S. H., 1990. A study of Taipei ozone problem. Atmospheric Environment 24A, 1461-1472.

Liu, C. M., Huang, C. Y., Shieh, S. L. and Wu, C. C., 1994. Important meteorological parameters for ozone episodes experienced in the Taipei basin. Atmospheric Environment 28, 159-173.

Liu, S. C., McFarland, M., Kley, D., Zafiriou, O. and Huebert, B., 1983. Tropospheric $NO_x$ and $O_3$ budgets in the equatorial Pacific, Journal of Geophysical Research, 88, 1360-1368.

Liu, S. C., Trainer, M., Carroll, M. A., Hubler, G., Montzka, D. D., Norton, R. B., Ridley, B. A., Walfga, J. G., Atlas, E. L., Heikes, B. G., Huebert, B. J., and Warren, W., 1992. A study of the photochemistry and ozone budget during the Mauna Loa observatory photochemistry experiment, Journal of Geophysical Research, 97, D10, 10,463-10,471.

Liu, X., Gao, N., Hopke, P. K., Cohen, D., Bailey, G. and Crisp, P., 1996. Evaluation of spatial patterns of fine particle sulphur and lead concentrations in New South Wales, Australia. Atmospheric Environment, 30, 9-24.

Logan, J. A., Prather, M. J., Wofsy, S. C. and McElroy, M. B., 1981. Tropospheric chemistry: a global perspective. Journal of Geophysical Research, 86, 7210-7254.

Logan, J. A., 1989. Ozone in rural areas of the United States. Journal of Geophysical Research 94, 8511-8532.

Luo, C., St. John, J. C., Zhou, X. J., Lam, K. S., Wang, T. and Chameides, W. L., 2000. A nonurban ozone air pollution episode over eastern China: observations and model simulations. Journal of Geophysical Research 105, 1889-1908.

Mayrsohn, D., Crabtree, J. H., 1976. Source reconciliation of atmospheric hydrocarbons. Atmospheric Environment 10, 137-143.

McKendry, I. G., 1993. Ground-level ozone in Montreal, Canada. Atmospheric Environment, 27B, 93-103.

Millan, M. M., Artinano, B., Alonso, L. A., Navazo, M., Castro, M., 1991. The effects of meso-scale flows on the regional and long-range atmospheric transporting the western Mediterranean area. Atmospheric Environment A 25, 949-963.

Monks, P. S., 2000. A review of the observations and origins of the spring ozone maximum. Atmospheric Environment 34, 3545-3561.

Moschonas, N. and Glavas, S., 1996. $C_3$-$C_{10}$ hydrocarbons in the atmosphere of Athens, Greece. Atmospheric Environment 30, 2769-2772.

Na, K. and Kim, Y. P., 2001. Seasonal characteristics of ambient volatile organic compounds in Seoul, Korea. Atmospheric Environment 35, 2603-2614.

Na, K., Kim, Y. P., Moon, K. C., 2003. Diurnal characteristics of volatile organic compounds in the Seoul atmosphere. Atmospheric Environment 37, 733-742.

Naja, M., Lal, S., Chand, D., 2003. Diurnal and seasonal variabilities in surface ozone at a high altitude site Mt Abu (24.6$^{o}$N, 72.7$^{o}$E, 1680m asl) in India. Atmospheric Environment 37, 4205-4215.

National Research Council (NRC), 1991. Rethinking the ozone problem in urban and regional air pollution. Committee on Tropospheric Ozone Formation and Measurement, National Academy Press, Washington, DC.

Nelson, P.F., Quigley, S.M., Smith, M.Y., 1983. Sources of atmospheric hydrocarbons in Sydney: a quantitative determination using a source reconciliation technique. Atmospheric Environment, 17, 439-449.

Nelson, P. F. and Quigley, S. M., 1983. The m, p-xylenes: ethylbenzene ratio, a technique for estimating hydrocarbon age in ambient atmospheres. Atmospheric Environment, 17, 659-662.

Olszyna, K. J., Luria, M. and Meagher, J. F., 1997. The correlation of temperature and rural ozone levels in Southeastern U.S.A. Atmospheric Environment 31, 3011-3022.

Parrish, D. D., Holloway, J. S., Trainer, M., Murphy, P. C., Forbes, G. L. and Fehsenfeld, F. C., 1993. Export of North American ozone pollution to the North Atlantic Ocean. Science 259, 1436-1439.

Pochanart, P., Kreasuwun, J., Sukasem, P., Geeratithadaniyom, W., Tabucanon, M. S., Hirokawa, J., Kajii, Y., Akimoto, H., 2001a. Tropical tropospheric ozone observed in Thailand. Atmospheric Environment 35, 2657-2668.

Pochanart, P, Akimoto, H., Maksyutov S., Staehelin, J., 2001b. Surface ozone at the Swiss Alpine Site Arosa: the hemispheric background and the influence of large-scale anthropogenic emissions. Atmospheric Environment 35, 5553-5566.

Pochanart, P, Akimoto, H., Yoshikatzu, K., Tanimoto, H., 2002. Surface ozone at four remote island sites and the preliminary assessment of the exceedances of its critical level in Japan. Atmospheric Environment 36, 4235-4250.

Rappenglück, B. and Fabian, P., 1999. Non-methane hydrocarbons in the Greater Munich Area / Germany. Atmospheric Environment 33, 3843-3857.

Roberts, J. M., 1995. Reactive odd-nitrogen ($NO_y$) in the atmosphere, in Composition, Chemistry, Climate of the Atmosphere, edited by Singh, H. B., Van Nostrand Reinhold, New York, pp. 176-215.

Roberts, J. M., Parrish, D. D, Norton, R. B., Bertman, S. B., Holloway, J. S, Trainer, M., Fehsenfeld, F. C., Carroll, M. A., Albercook, G. M., Wang, T., Forbes, G., 1996. Episodic removal of $NO_y$ species from the marine boundary layer over the North Atlantic. Journal of Geophysical Research 101, D22, 28947-28960.

Roberts, J. M., Williams, J., Baumann, K., Buhr, M. P., Goldan, P. D., Holloway, J., Hubler, G., Kuster, W. C., McKeen, S. A., Ryerson, T. B., Trainer, M., Williams, E. J., Fehsenfeld, F. C., Bertman, S. B., Nouaime, G., Seaver, C., Grodzinsky, G., Rodgers, M. Young, V. L., 1998. Measurements of PAN, PPN, and MPAN made during the 1994 and 1995 Nashville Intensives of the Southern Oxidant Study: Implications for regional ozone production from biogenic hydrocarbons. Journal of Geophysical Research 103, D17, 22473-22490.

Rodriguez, S and Guerra, J. C., 2001. Monitoring of ozone in a marine environment in Tenerife (Canary Islands). Atmospheric Environment 35, 1829-1841.

Ryan, W. F., Doddridge, B. G., Dickerson, R. R., Morales, R. M., Hallock, K. A., Roberts, R. T., Blumenthal, D. L., Anderson, J. A., Civerolo, K. L., 1998. Pollutant transport during a regional $O_3$ episode in the mid-Atlantic States. Journal of Air and Waste Management Association 48, 786-797.

Schmitt, R., Schreiber, B., Levi, I., 1988. Effects of long-range transport on atmospheric trace constituents at the Baseline Station Tenerife (Canary Islands). Journal of Atmospheric Chemistry 7, 335-351.

Schmitt, R. and Carretero, M., 1995. Ozone in the free troposphere over North Atlantic: production and long-range transport. In: Proceeding of EUROTRAC Symposium.

Seinfeld, J. H., 1989. Urban air pollution: state of the science. Science 243, 745-752.

Seinfeld, J. H. and Pandis, S. N., 1998. Atmospheric Chemistry and Physics: From Air Pollution to Climate Change, Wiley-Interscience, New York.

Sharma, U. K., Kajii, Y., Akimoto, H. 2000. Characterization of NMHCs in downtown urban center Kathmandu and rural site in Nagarkot in Nepal. Atmospheric Environment 34, 3297-3307.

Sillman, S., Samson, P. J. and Master, J. M., 1993. Ozone production in urban plumes transported over water: Photochemical model and case studies in the northeastern and Midwestern United States. Journal of Geophysical Research 98, D7, 12687–12669.

Sillman, S., 1995. The use of $NO_y$, $H_2O_2$, and $HNO_3$ as indicators for ozone-$NO_x$-hydrocarbon sensitivity in urban locations. Journal of Geophysical Research 100, D7, 14,175–14,188.

Sillman S., 1999. The relation between ozone, $NO_x$ and hydrocarbons in urban and polluted rural environments. Atmospheric Environment 33, 1821-1845.

Sillman, S. and He, D., 2002. Some theoretical results concerning $O_3$-$NO_x$-VOC chemistry and $NO_x$-VOC indicators. Journal of Geophysical Research 107, D22, 4659, doi:10.1029/2001JD001123.

Sin, D. W. M., Wong, Y. C., Louie, P. K. K., 2000. Monitoring of ambient volatile organic compounds at two urban sites in Hong Kong from 1997 to 1998. Indoor Built Environment 9, 216-227.

Sin, D. W. M., Wong, Y. C., Sham, W. C., Wang, D., 2001. Development of an analytical technique and stability evaluation of 143 $C_3$-$C_{12}$ volatile organic compounds in Summa$^{®}$ canisters by gas chromatography-mass spectrometry. Analyst 126, 310-321.

Skarby, L. and Sellden, G., 1984. The effect of ozone on crops and forests. Ambio 13, 68-72.

Smyth, S., Sandholm, S., Shumaker, B., Mitch, W., Kanvinde, A., Bradshaw, J., Liu, S., Mckeen, S., Gregory, G., Anderson, B., Talbot, R., Blake, D., Rowland, S., Browell, E., Fenn, M., Merrill, J., Bachmeier, S., Sachse, G. and Collins, J., 1999. Characterization of the chemical signatures of air masses observed during the PEM Experiments over the Western Pacific. Journal of Geophysical Research 104, 16243-16254.

So, K. L. and Wang, T., 2003. On the local and regional influence on ground-level ozone concentration in Hong Kong. Environmental Pollution 123, 307-317.

So, K. L. and Wang, T., 2004. $C_3$-$C_{12}$ Non-methane Hydrocarbons in Subtropical Hong Kong: Spatial-temporal Variations, Source-receptor Relationships and Photochemical Reactivity. Science of Total Environment 328, 161-174.

Solomon, P., Cowling, E., Hidy, George and Furiness, C., 2000. Comparison of scientific findings from major ozone field studies in North America and Europe. Atmospheric Environment 34, 1885-1920.

Southern Oxidants Study (SOS), 1995. http://www2.ncsu.edu/ncsu/CIL/southern_oxidants/

St. John, J. C., Chameides, W. L., Saylor, R., 1998. Role of anthropogenic NOx and VOC as ozone precursors: A case study from the SOS Nashville/Middle Tennessee Ozone Study. Journal of Geophysical Research 103, 22, 22,415-22,423.

St. John, J. C., Chameides, W. L., 1997. Climatology of $O_3$ exceedances in the Atlanta Metropolitan Area: 1-hour vs 8-hour standard and the role of plume recirculation air pollution episodes. Environmental Science and Technology 31, 2797-2804.

Streets, D. G. and Waldhoff, S. T., 2000. Present and future emissions of air pollutants in China: $SO_2$, $NO_x$ and CO. Atmospheric Environment 34, 363-374.

Streets, D. G., Bond, T. C., Carmichael, G. R., Fernandes, S. D., Fu, Q., He, D., Klimont, Z., Nelson, S. M., Tsai, N. Y., Wang, M. Q., Woo, J.-H., and Yarber, K. F., 2003. An inventory of gaseous and primary aerosol emissions in Asia in the year 2000, Journal of Geophysical Research, 108, doi:10.1029/2002JD003093.

Sunwoo, Y., Carmichael, G. R. and Ueda, H., 1994. Characteristics of Background Surface Ozone in Japan. Atmospheric Environment 28, 25-37.

Talbot, R. W., Dibb, J. E., Klemm, K. I., Bradshaw, J. D., Sandholm, S. T., Blake, D. R., Sachse, G. W., Collins, J., Heikes, B. G., Gregory, G. L., Anderson, B. E., Singh, H. B., Thornton, D. C., Merrill, J. T., 1996. Chemical characteristics of continental outflow from Asia to the troposphere over the western Pacific Ocean during September-October 1991: Results from PEM-West A. Journal of Geophysical Research 101, D1, 1713-1725.

Trainer, M., Parrish, D. D., Buhr, M. P., Norton, R. B., Fehsenfeld, F. C., Anlauf, K. G., Bottenheim, J. W., Tang, Y. Z., Wiebe, H. A., Robert, J. M., Tanner, R. L., Newman, L., Bowersox, V. C., Meagher, J. F., Olzyna, K. J., Rodgers, M. O., Wang, T., Berresheim, H., Demerjiam, K. L., Roychowdhury, U. K., 1993. Correlation of ozone with $NO_y$ in photochemcially aged air. Journal of Geophysical Research 98, 2917-2925.

Tsujino, Y. and Kuwata, K., 1993. Sensitive flame ionization detector for the determination of traces of atmospheric hydrocarbons by capillary column gas chromatography. Journal of Chromatography 642, 383-388.

US Environmental Protection Agency (USEPA), 2000. SPECIATE data base V. 3.1, http://www.epa.gov/ttn/chief/software/speciate, Washington, DC.

Varotsos, C., Kondratyev, K. Y. and Efstathiou, M., 2001. On the seasonal variation of the surface ozone in Athens, Greece. Atmospheric Environment 35, 315-520.

Vingarzan, R., 2004, A review of surface ozone background levels and trends. Atmospheric Environment 38, 3431-3442.

Vukovich, F. M., Bach, W. D., Crissman, B.W. and King, W. J., 1977. On the relationship between high ozone in the rural boundary layer and high pressure systems. Atmospheric Environment 11, 967-983.

Vukovich, F.M., 1979. A note on air quality in high pressure systems. Atmospheric Environment 13, 255-265.

Vukovich, F.M., 1995. Regional-scale boundary layer ozone variations in the eastern United States and their association with meteorological variations. Atmospheric Environment 29, 2259-2273.

Wang, T., Lam, K. S., Chan, L. Y., Lee, A. S. Y., Carroll, M. A., 1997. Trace gas measurements in coastal Hong Kong during the PEM-West B. Journal of Geophysical Research, 102, 28575-28588, 1997.

Wang, T., Lam, K. S., Lee, A. S. Y., Pang, S. W., Tsui, W. S., 1998. Meteorological and chemical characteristics of the photochemical ozone episodes observed at Cape' Aguilar in Hong Kong. Journal of Applied Meteorology 37, 1167-1178.

Wang, T., Cheung, V. T. C., Anson, M. and Li, Y. S., 2001a. Ozone and related gaseous pollutants in the boundary layer of eastern China: Overview of the recent measurements at a rural site. Geophysical Research Letters 28, 2373-2376.

Wang, T., Wu, Y. Y., Cheung, T. F. and Lam, K. S., 2001b. A Study of surface ozone and the relation to complex wind flow in Hong Kong. Atmospheric Environment 35, 3203-3215.

Wang, T., Cheung, V. T. F., Lam, K. S., Kok, G. L. and Harris, J. M., 2001c. The characteristics of ozone and related compounds in the boundary layer of the South China Coast: Temporal and vertical variations during autumn season. Atmospheric Environment 35, 2735-2746.

Wang, T., Cheung, T. F., Li, Y. S., Yu, X. M., Blake, D. R., 2002. Emission characteristics of CO, $NO_x$, $SO_2$ and indications of biomass burning observed at a rural site in eastern China. Journal of Geophysical Research, 107, D12, 10.1029/2001JD000724.

Wang, T, 2003. Study of Visibility Reduction and its Causes in Hong Kong, Tender Reference AS01-286, September 2003. Final Report to the Environmental Protection Department of HKSAR.

Wang, T. and Kwok, J. Y. H., 2003. Measurement and analysis of a multi-day photochemical smog episode in Pearl River Delta of China. Journal of Applied Meteorology 42, 404-416.

Wang, T., Ding, A. J., Blake, D. R., Zakorowski, W., Poon, C. N., Li, Y. S., 2003a. Chemical characterization of the boundary layer outflow of air pollution to Hong Kong during February-April 2001. Journal of Geophysical Research 108, D20, 8787, doi:10.1029/ 2002JD003272.

Wang, T., Poon, C. N., Kwok, Y. H., Li, Y. S., 2003b. Characterizing the temporal variability and emission patterns of pollution plumes in the Pearl River Delta of China. Atmospheric Environment 37, 3539-3550.

Wang, T., Wong, C. H., Cheung, T. F., Blake, D. R., Arimoto, R., Baumann, K., Tang, J., Ding, G. A., Yu, X. M., Li, Y. S., Streets, D. G., Simpson, I. J., 2004. Relationships of trace gases and aerosols and the emission characteristics at Lin'an, a rural site in eastern China, during spring 2001. Journal of Geophysical Research 109, D19S05, doi:10.1029/ 2003JD004119.

Wang, T., Guo, H., Blake, D. R., Kwok, Y. H., Simpson, I. J., Li, Y. S., 2005. Measurements of Trace Gases in the Inflow of South China Sea

Background Air and Outflow of Regional Pollution at Tai O, Southern China. Journal of Atmospheric Chemistry 52, 295-317.

Warneck, P., 2000. Chemistry of the Natural Atmosphere, Second Edition, Academic Press, UK.

Watson, J. G., Chow, J. C., Fujita, E. M., 2001. Review of volatile organic compounds source apportionment by chemical mass balance. Atmospheric Environment 35, 1567-1584.

Xu, J. L., Zhu, Y. X. and Li, J. L., 1999. Case studies on the processes of surface ozone pollution in Shanghai. Journal of Air & Waste Management Association 49, 716-724.

Zhang, Y. H., Shao, K. S., Tang, X. Y., Li, J. L., 1998. The study of urban photochemical smog pollution in China. Acta Scientiarum Naturaliun Universitiatis Pekinensis 34, 393-399.

Zhang, J., Chameides, W.L., Wang, T., Kiang, C.S., 2004. Final report of Hong Kong and the Pearl River Delta pilot air monitoring project: pilot study on the use of atmospheric measurements to manage air quality in Hong Kong and the Pearl River Delta: Project 1 Ground-level ozone pollution in Hong Kong. Civic Exchange.

Zhang, J., Wang, T., Chameides, W.L., Cardelino, C., Kwok, J., Blake, D. R., Ding, A., So, K. L., 2006. Ozone production and hydrocarbon reactivity in Hong Kong, Southern China. Atmospheric Chemistry and Physics Discussion 6, 8961-9002.